UNIVERSITA' DEGLI STUDI DI VERONA

DEPARTMENT OF BIOTECHNOLOGY

GRADUATE SCHOOL OF NATURAL AND ENGINEERING SCIENCES

DOCTORAL PROGRAM IN BIOTECHNOLOGY

XXXIII cycle/ 2017

A multi-omics approach identifies the pivotal role of cardiolipin remodelling, alpha subunit of the mitochondrial trifunctional protein and long chain fatty acids in stem cells of pancreatic cancer

S.S.D. CHIM/01

Coordinator:
Prof. Matteo Ballottari

Signature _____

Tutor:
Prof.ssa Daniela Cecconi

Signature _____

Doctoral Student:
Dott.ssa Claudia Di Carlo

Signature _____

Summary

L'adenocarcinoma duttale pancreatico (PDAC) costituisce la settima causa di morte per cancro al mondo. Negli stadi iniziali, questa patologia è asintomatica e non presenta sintomi specifici, di conseguenza la diagnosi nei pazienti avviene prettamente quando il tumore non è resecabile per la presenza di metastasi. L'elevato tasso di mortalità associato al PDAC è in parte attribuito ad una sottopopolazione di cellule molto aggressive, note come cellule staminali tumorali del pancreas (PCSC). Sebbene sia noto che le PCSC siano associate a scarsi risultati nel trattamento chemioterapico dei pazienti, è ancora poco nota la regolazione sia delle vie di trasduzione del segnale che di quelle metaboliche. Una caratterizzazione molecolare completa della biologia delle PCSC è di fondamentale importanza per colpire il PDAC.

Pertanto, l'obbiettivo principale di questa tesi di dottorato è stato caratterizzare approfonditamente queste cellule da un punto di vista molecolare per identificare disfunzioni cellulari, metaboliche e di segnalazione correlate alla fisiopatologia del PDAC, al fine di suggerire nuovi bersagli terapeutici.

Il mio progetto di dottorato si è svolto presso il laboratorio di "Proteomica e spettrometria di massa" afferente al Dipartimento di Biotecnologie dell'Università degli studi di Verona sotto la guida della Prof.ssa Daniela Cecconi, ma anche in altri laboratori grazie alla consolidata rete di collaborazioni instaurate. La coltura delle linee cellulari PDAC è stata svolta presso il laboratorio diretto dalla Prof.ssa Marta Palimeri (presso il Dipartimento di Neuroscienze, Biomedicina e Movimento dell'Università degli studi di Verona); l'analisi proteomica è stata effettuata in collaborazione con il gruppo di ricerca del Prof. Emilio Marengo (presso il Dipartimento di Scienze e Innovazione Tecnologica, dell'Università degli studi del Piemonte Orientale); e l'analisi lipidomica è stata realizzata in collaborazione con il gruppo di ricerca del Prof. Michael Wakelam e della Dr.ssa Andrea F. Lopez-Clavijo presso l'istituto di ricerca Babraham di Cambridge (Regno Unito), dove ho svolto il mio tirocinio estero della durata di tre mesi.

Durante questo progetto, sono state analizzate e confrontate tra loro le PCSC di quattro linee PDAC (ossia, PaCa3, PaCa44, MiaPaCa2 e PC1J) e le rispettive cellule pancreatiche tumorali, dette parentali (P).

Le cellule P sono state coltivate in un apposito terreno di coltura per l'ottenimento di PCSC. La morfologia delle cellule P e degli sferoidi tumorali PCSCs è stata esaminata tramite microscopia. Successivamente, è stata valutata l'espressione di geni e proteine correlate alla staminalità e alla quiescenza mediante analisi qPCR e di immunoblotting.

In seguito, le possibili alterazioni nel proteoma e nel lipidoma delle PCSC sono state investigate con analisi proteomiche e lipidomiche. I dati "omici" sono stati poi approfonditi sia tramite analisi bioinformatiche, che con ulteriori saggi, tra i quali: il Western blot, la microscopia confocale a fluorescenza per rilevare le goccioline lipidiche, e un saggio enzimatico colorimetrico per valutare il contenuto di acidi grassi liberi.

Dall'integrazione dei dati di proteomica e lipidomica sono emerse modulazioni comuni tra le PCSC e anche significative differenze rispetto alle cellule P.

Tutte e quattro le PCSC hanno mostrato in comune la sottoregolazione sia della L-lattato deidrogenasi A (LDHA) che della sua forma fosforilata (p-LDHA), e la sovraregolazione della subunità alpha dell'enzima trifunzionale mitocondriale (HADHA), che è coinvolta nel rimodellamento della cardiolipina (CL). Inoltre, l'analisi bioinformatica ha evidenziato il coinvolgimento delle proteine sovraspresse nelle PCSC in alcune vie del metabolismo lipidico, quali ad esempio l'allungamento degli acidi grassi (FA) e la biosintesi degli FA insaturi.

A supporto di questi risultati, l'analisi lipidomica ha indicato un aumento nei livelli di FA a catena lunga e molto lunga, prodotti dall'attività dell'elongasi-5 che è stato predetto come gene in comune delle PCSC delle linee PaCa3, PaCa44, MiaPaCa2 e PC1J. In accordo con la sovra-regolazione di HADHA, nelle PCSC è stata determinata l'induzione di specie molecolari di CL derivanti da incorporamento di catene aciliche 16:0, 18:1 e 18:2 miste. Inoltre, l'analisi

lipidomica ha anche suggerito l'induzione del pathway degli fosfoinositidi nelle PCSC.

Per concludere, i risultati ottenuti in questa tesi di dottorato evidenziano innanzitutto la potenzialità di un approccio multi-omico, e contribuiscono a migliorare la comprensione del metabolismo lipidico nelle PCSC.

I dati ottenuti hanno suggerito l'importanza dell'allungamento degli FA, e per la prima volta hanno messo in rilievo il ruolo del rimodellamento della CL nelle PCSC. Complessivamente, questo studio potrà fornire preziose informazioni per lo sviluppo di nuove promettenti terapie contro il PDAC.

Abstract

Pancreatic ductal adenocarcinoma (PDAC) is the seventh leading cause of cancer-related deaths worldwide. This pathology is asymptomatic at early stages and there are no specific symptoms, so patients are typically diagnosed when an unresectable tumour caused by the presence of metastases is shown. The high mortality rate of PDAC has also been attributable to the presence of a small subset of cells with very aggressive features called pancreatic cancer stem cells (PCSCs). Although PCSCs play a key role in driving patient poor outcomes and resistance to targeted therapies, little is known about the regulation of their signalling and metabolic pathways. A complete molecular characterization of PCSC biology is fundamental to make an impact on PDAC.

Therefore, the aim of this PhD thesis was to obtain an in-depth characterization of PCSCs from a molecular point of view to detect cellular, metabolic and signalling dysfunctions implicated in pathophysiology of PDAC, possibly suggesting new therapeutic targets.

My PhD project was carried out in the Proteomic and Mass Spectrometry Laboratory of Biotechnology Department at University of Verona under the guidance of Prof. Daniela Cecconi and in other laboratories thanks to established collaborations. PCSCs and PDAC cell cultures were obtained in collaboration with the research group of Prof. Marta Palmieri (Dept. of Neuroscience, Biomedicine and Movement of the University of Verona); proteomic analysis was done in collaboration with the research group of Prof. Emiliano Marengo (Dept. of Sciences and Technological Innovation, University of Eastern Piedmont); and lipidomic analysis was performed in collaboration with Prof. Michael J.O. Wakelam and Dr Andrea F. Lopez-Clavijo during my three-months placement abroad at the Lipidomics facility of the Babraham Institute in Cambridge (UK).

During my PhD project, four PCSC lines (*i.e.*, PaCa3, PaCa44, MiaPaCa2, and PC1J) and relative pancreatic tumour cells, called parental (P), were analysed and compared. The four P cell lines were cultured and used to obtain PCSCs.

Morphological evaluation by microscopy of PCSC tumour spheres and their relative P cells was performed. Then, the expression of stem and quiescence related markers were investigated in PaCa3, PaCa44, MiaPaCa2, and PC1J CSCs by qPCR and immunoblotting analyses.

Subsequently, proteomics and lipidomics analyses were performed to evaluate possible alterations in proteome and lipidome of PCSCs. Omics data were subjected to bioinformatic analysis and evaluated further in-depth by western blotting to confirm protein modulation, confocal fluorescence microscopy to detect lipid droplets, and colorimetric enzymatic kit to assess free fatty acid levels.

The integration of proteomics and lipidomics data suggested that PCSCs displayed common modulations, while significant differences were detected compared to their counterpart. The downregulation of L-lactate dehydrogenase A chain (LDHA) and its phosphorylated form (p-LDHA), and the upregulation of the trifunctional enzyme subunit alpha (HADHA) involved in cardiolipin remodelling were in common among all four PCSC lines. Bioinformatic analysis also revealed that upregulated proteins of PCSCs were mainly involved in lipid-related pathways, such as fatty acid (FA) elongation and biosynthesis of unsaturated FAs.

Lipidomics analysis supported these results, indicating an increase of long and very long FAs, which are products of fatty acid elongase-5 predicted as an active gene of PaCa3, PaCa44, MiaPaCa2, and PC1J CSCs. In accordance with HADHA upregulation, PCSCs were also characterized by the induction of molecular species of cardiolipin with mixed incorporation of 16:0, 18:1, and 18:2 acyl chains. In addition, lipidomic analysis also suggested the induction of phosphoinositide pathway in PCSCs.

In conclusion, the results obtained in the present PhD thesis support the potential of a multi-omics approach and provide a better understanding of lipid metabolism in PCSCs. The findings obtained indicated the importance of FA elongation and highlight for the first time the involvement of cardiolipin remodelling in PCSCs. Altogether this study provides novel information for the development of promising new therapies against PDAC.

Table of contents

List of abbreviations

ALDH	Aldehyde dehydrogenase
CE	Cholesterol esters
CEPT1	Choline/ethanolamine phosphotransferase 1
Cer	Ceramides
CH	Cholesterol
CHPT1	Choline phosphotransferase 1
CL	Cardiolipin
CSCs	Cancer stem cells
DG	Diacylglycerol
dhCer	Dihydroceramides
dhSG	Dihydrosphingosine
dhSM	Dihydrosphingomyelin
DMEM	Dulbecco's modified eagle's medium
ELOVL5	Fatty acid elongase-5
ELOVL6	Fatty acid elongase 6
FA	Fatty acid
FBS	Fetal Bovine Serum
FLT1	Vascular endothelial growth factor receptor 1
FZD	Frizzled
GEM	Gemcitabine
GO	Gene ontology
HADHA	Trifunctional enzyme subunit alpha
HNRNPAB	Heterogeneous nuclear ribonucleoprotein A/B Isoform 2
Ig	Immunoglobulin
IGF1R	Insulin-like growth factor 1
IPA	Ingenuity pathway analysis
IPMNs	Intraductal papillary mucinous neoplasms
ITPNs	Intraductal tubulopapillary neoplasms
KEGG	Kyoto encyclopedia of genes and genomes
LC-MS/MS	Liquid chromatography tandem mass spectrometry
LDHA	L-lactate dehydrogenase A chain
LDs	Lipid droplets
LPA	Lysophosphatidic acid
LPC	Lysophosphatidylcholine
LPE	Lysophosphatidylethanolamine
LPG	Lysophosphatidylglycerol
LPI	Lysophosphatidylinositol
LPS	Lysophosphatidylserine
mTOR	Mammalian target of rapamycin
Oct	Octamer-binding transcription factor

O-DG	Alkyl−acylglycerol
O-LPA	Alkyl−lysophosphatidic acid
O-LPC	Alkyl−lysolysophosphatidylcholine
O-LPE	Alkyl−lysophosphatidylethanolamine
O-PC	Alkyl−acylphosphatidylcholine
O-PE	Alkyl−acylphosphatidylethanolamine
O-TG	Alkyl−triacylglycerol
OXPHOS	Oxidative phosphorylation
P	Parental
PA	Phosphatidic acid
PC	Phosphatidylcholine
PCSCs	Pancreatic cancer stem cells
PDAC	Pancreatic ductal adenocarcinoma
PE	Phosphatidylethanolamine
PG	Phosphatidylglycerol
PI	Phosphatidylinositol
PI3K	Phosphatidylinositol 3kinase
PIP	Phosphatidylinositolmonophosphate
PIP2	Phosphatidylinositoldiphosphate
PL	Phospholipid
P-LPA	Alkenyl−lysophosphatidic acid
P-LPC	Alkenyl−lysophosphatidylcholine
P-PC	Alkenyl−acylphosphatidylcholine
P-PE	Alkenyl−acylphosphatidylethanolamine
PS	Phosphatidylserine
PTEN	Phosphatase and tensin homolog
PVDF	Polyvinylidene fluoride
Q-TOF	Quadrupole- time of flight
qPCR	Quantitative polimerase chain reaction
RICTOR	Rapamycin-insensitive companion of mTOR
RPN2	Dolichyl-diphosphooligosaccharide-protein glycosyltransferase subunit 2 Isoform 2
SG	Sphingosine
SGMS	Ceramide choline phospho-transferase
SL	Sphingolipid
SM	Sphingomyelin
Sox2	Sex-determining region Y-box 2
SsM	Stem-selective medium
TG	Triacylglycerol
VDAC2	Voltage-dependent anion-selective channel protein 2
XBP1	X-box binding protein 1

SECTION 1

Chapter 1

Introduction

1. Pancreatic cancer

1.1. Epidemiology and risk factors

Pancreatic cancer is an aggressive disease of the pancreas, a glandular organ behind the stomach, in which cells arise to proliferate out of control and to form a mass [1]. This pathology represents a lethal condition with high mortality and poor clinical outcomes. Indeed, it is the seventh leading cause of global cancer-related deaths in industrialized countries, including Italy. Its incidence rate continues to increase, and therefore pancreatic cancer is expected to become the second cause of cancer-related deaths within the next decade [1, 2].

There are different types of pancreatic cancer, classified in two general groups based on clinical characteristics: pancreatic neuroendocrine tumours (PanNETs) which constitute the small minority percentage, and exocrine cancer (adenocarcinoma) which represents 95% of pancreas malignancies. PanNETs arise in the hormone-producing (endocrine) tissue of the pancreas, while the exocrine tumour most commonly occurs in the pancreatic ducts; hence it is referred to as pancreatic ductal adenocarcinoma (PDAC).

As shown in Figure 1, the pancreatic duct carries secretions away from the pancreas and it is divided into three sections: head, body, and tail [3]. 60–70% of PDAC cases take place in the pancreatic duct head and give infiltration into surrounding tissues, including lymphatics, spleen, and peritoneal cavity, causing metastasis formation to the liver and lungs [3], whilst 20-25% of PDAC cases involve the duct's body/tail part, and the remainder involves the whole organ [4]. PDAC is usually asymptomatic at early stages, so the disease is typically not diagnosed until the advanced stages, when it has spread to the pancreas and beyond [5]. This tumour is unmanageable with conventional treatments (*i.e.*, chemo- and radio- therapy); therefore, it is almost always fatal. Indeed, PDAC is characterized

by the lowest five-year survival rate (< 8%) compared to other major cancer types, including prostate, breast, and lung cancer, characterized by a survival rate of 100%, 90%, and 16% respectively [6].

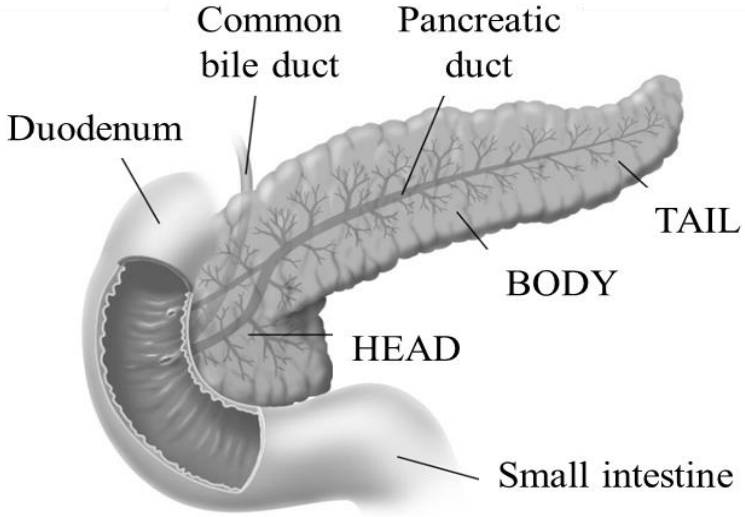

Figure 1. Anatomy of the Pancreas. Anatomically, the pancreas is divided into a head, body, and tail. Pancreatic ducts connect the pancreas with the duodenum and small intestine.

The advanced symptoms of PDAC vary according to the tumour location. Reported symptoms include mid-back pain, upper abdominal pain, jaundice and unexplained weight loss, caused either by loss of appetite or loss of exocrine function, which consequently result in poor digestion and pale and smelly stools [3]. Moreover, at the time of diagnosis at least 50% of patients with PDAC manifest diabetes, and 10-20% of cases depression. Diabetes is caused by the destruction of cells secreting insulin (the so called β-cells), while depression is associated with hormonal imbalance [3].

PDAC clinical screening only begins after the patient has developed the most common symptoms, including blood clots in veins with large diameter, middle back pain, weight loss and jaundice. These manifestations are believed to occur by the pressure of the tumour mass on the bile duct. It is accepted that middle back pain may indicate the spreading of PDAC to the nerves surrounding the pancreas.

Moreover, PDAC tumour pressing on the far end of the stomach can be associated with nausea, vomiting and satiety, and consequently weight loss. Some PDAC patients present liver enlargement, if the cancer has spread to this organ [4].

Risk factors for PDAC development include ageing, sex, ethnicity, smoking, obesity, genetic factors, pancreatitis and alcohol consumption (Fig. 2) [7]. Ageing is considered the main PDAC risk factor, indeed most reported cases belong to patients aged 65 or older, whereas patients below 40 years of age are uncommon. PDAC tends to affect men more severely than it does in women [7]. Regarding ethnicity, it has been reported that in United Stated PDAC is over 1.5 times more common in African-Americans than Caucasians, while in Africa its incidence is quite low [7]. Smoking is an avoidable risk factor for PDAC. Long-term smokers show a two times higher risk incidence of developing PDAC than non-smokers, and this incidence rate can be reduced after the patient has stopped smoking.

Reported results indicate that the risk of developing PDAC can be reduced after around 20 years without tobacco use [8]. Obesity is another fundamental risk factor for developing PDAC: a body mass index-BMI > 35 kg/m^2 is related to an increase compared to individuals with a BMI between 18.9 and 24.9. Excessive alcohol consumption (≥ 6 drinks per day) can also increase the risk of developing PDAC, while chronic pancreatitis almost tripled the risk of developing PDAC [3, 9]. Several studies suggested hereditary pancreatitis, nonpolyposis colorectal carcinoma, breast and ovarian cancer, familial adenomatous polyposis, Peutz-Jeghers or familial atypical multiple mole melanoma syndrome [10] and certain genetic disorders as other risk factors for pancreatic cancer [11], due to mutations on genes related to Fanconi anaemia pathway (*i.e. FANC-C* and *FANC-G*), DNA mismatch repair (*i.e.*, *PALB2* or *ATM*, *MLH1*, *MSH2*, *MSH6* and *PMS2*) [3, 12] and in germline (*i.e.*, *BRCA1*, *BRCA2*, *PRSS1* and *SPINK1*) [3, 12].

Studies on the genetic factors within the same family showed that 5-10 % of PDAC patients have an inherited component. Genetic predisposition cannot be changed, even if it is possible to reduce the risk of developing PDAC by conducting an healthy life, including performing physical activity, having a balanced diet, with a reduced alcohol consumption and without smoking [13].

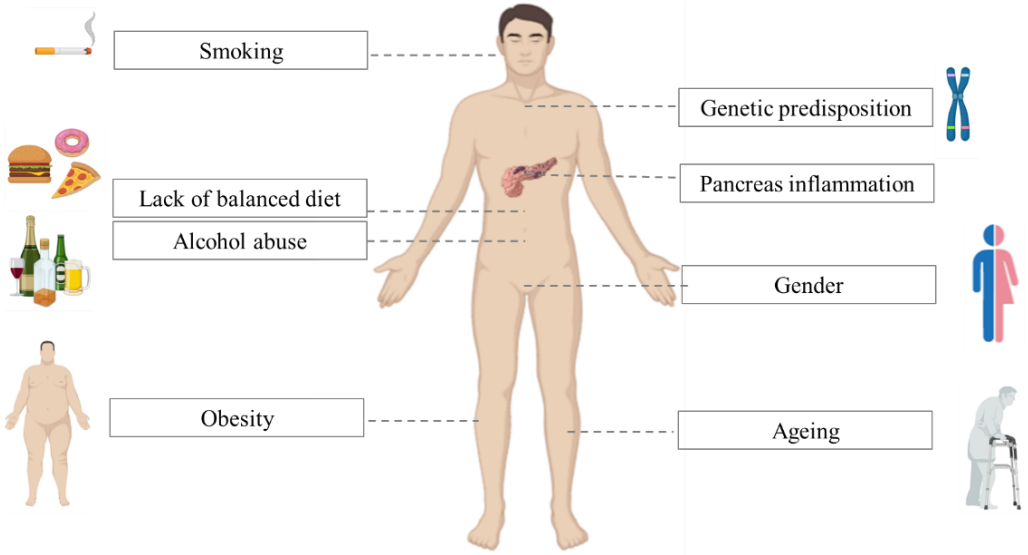

Figure 2. Risk factors of pancreatic cancer

1.2. Biology and genetics of pancreatic ductal adenocarcinoma

Carcinogenesis is a complex process characterized by a gradual modification of cell identity and function. Several clinical and histopathologic studies have demonstrated that PDAC is characterized by common mutations of genes involved in tumorigenesis [5]. The most important and frequent mutations are on *p16*, *p53*, *KRAS* and *SMAD4* genes [5, 10]. 95% of patients with PDAC present mutation on *p16* and *KRAS* genes, followed by the mutation on *p53* (75%) and *SMAD4* (55%) genes.

These genes are encoded for different proteins that play a pivotal role in several cell pathways able to influence PDAC progression. Specifically, the encoded p16 protein is a cell cycle regulator (involved in G1-S transition) and can modulate senescence and ageing. It is usually mutated in different human cancers [14]. Another cell cycle regulator (involved in G2-M transition) is p53 that orchestrates both DNA damage pathway and TGF-β signalling pathway. Several mutations on p53, including C176S, R248W, R175H and R273H, can determine protein gain-of-function (GOF) [15], favouring cell proliferation and the formation of metastasis *in vitro* [16].

However, PDAC cell viability and proliferation may also be regulated by the Kras activity [17, 18]. This GTPase is an upstream regulator of the Mitogen-activated protein kinase (MAPK) and Phosphoinositol-3-kinase (PI3K) pathways that promote cell proliferation and the activation of several signalling pathways [19]. Finally, the tumour suppressor Smad4 is downstream effector in the TGF-β signalling [20], that influences G1 cycle cell arrest and senescence of PDAC cells, due to its interaction with cyclin-dependent kinase inhibitor 1A [21]. In 2018, Wang F. *et al*. demonstrated that Smad4 modulates reactive oxygen species (ROS) scavenging, favouring radioresistance in pancreatic cancer cells [22].

Alternatively, PDAC can be also classified by five distinct precursor lesions: pancreatic intraepithelial neoplasias (PanINs), intraductal papillary mucinous neoplasms (IPMNs), intraductal tubulopapillary neoplasms (ITPNs), intraductal oncocytic papillary neoplasms (IOPNs) and mucinous cystic neoplasms (MCNs), summarized in Table 1 [23].

The most common and extensively studied precursor lesion is PanIN, which is a non-invasive neoplasia confined within pancreatic ducts [24]. Due its small size, this lesion does not allow radiological identification. However, two different conditions can be detected: low- and high- grade PanINs. The first one displays mutation on *KRAS* and *p16* genes, while the second one frequently also presents alteration on *p53* and *SMAD4* gene expression.

IPMNs present an observing size (with a diameter from 0.5 to 1 cm) [23], which can be distinguished in low-, high- and mixed- grade (based on their atypia in main, branch or both ducts, respectively) or in gastric, intestinal, or pancreatobiliary ones (based on histological structure) [23]. IPMNs are characterized by *KRAS* mutation (30-80% of cases), even if in high-grade IPMNs the allelic loses of *p16, p53* and *SMAD4* are significantly increased (see Tab. 2).

Another epithelial rare precursor lesion is ITPN (with a size above 1 cm), which is characterized by p53 overexpression and Smad4 retention in endoplasmic reticulum. In some cases, alteration on genes related to phosphatidylinositol 3-kinase pathway (*i.e.*, *PIK3CA*, *PIK3CB* and *PTEN*) and chromatin remodelling (*i.e.*, *MLL1*, *MLL2*, *MLL3*, *BAP1* and *PBRM1*) can also be detected. Recently, IOPN

(with a size above 1 cm) was categorized as additional PDAC cystic nodular lesion, which is characterized by mutation on *KRAS*. Finally, MCNs are the last PDAC precursor lesions, distinguished as uni- or multi- cystic neoplasms. About 40–70% of people with PanNETs present a mutation on *MEN1*, while alterations on *KRAS* are usually not detectable. Other genes frequented mutated are *DAXX*, *mTOR* and *ATRX* [25].

The accumulation of mutations favours the development of pre-cancer cells to invasive cancer ones.

Table 1. Differential biological, histological and genetic characteristics of pancreatic precursor lesions

Precursor Lesion	**Location in the pancreatic duct**	**Gross**	**Histology structure**	**Mucin glycoprotein expression**	**Genetic alteration**
PanIN	Any	Not resectable	Flat/Papillary	Muc5AC^{+}, Muc6^{+}	*KRAS*, *p16*
IPMN	Head	Papillary mass	Papillary	Muc5AC^{+}, Muc6^{+} or Muc2^{+}, Muc5AC^{+}, Muc1^{+}, Muc5AC^{+}, Muc5AC$^{\pm}$	*KRAS*, *GNAS*, *p53*, *SMAD4*, *RNF43*
ITPN	Head	Intraductal solid nodular mass	Cribriform	Muc1^{+}, Muc6^{+}	*MLL1*, *MLL2*, *MLL3*, *BAPI*, *PBRM1*
IOPN	Head	Cystic nodule	Cribifrom/Complex arborizing papila	Muc1^{+}, Muc6^{+}, Muc5AC^{+}, Muc2^{+}	*ARHGP26*, *ASXL1*, *EPHA8*, *ERBB4*
MCN	Tail	Uni/multilocular cyst	Ovarian-type stroma	Muc1^{+}, Muc5AC^{+}	*KRAS*, *p53*, *SMAD4*, *p16*

1.2.1. Genetic background of pancreatic ductal adenocarcinoma cell lines and its influence in cell metabolism

As reported in Table 2, the four PDAC cell lines (*i.e.*, PaCa3, PaCa44, MiaPaCa2 and PC1J) used during this project are characterized by different mutations on *p16, p53, KRAS* and *SMAD4* genes.

Table 2. PDAC cell lines and their relative genes alterations.

Cell line	***p16***	***p53***	***KRAS***	***SMAD4***	**n°**
PaCa3	Methylated / Absent	None / wt	None / wt	None / wt	1
PaCa44	Methylated / Absent	176 / Cys to Ser	12 / Gly to Val	None / wt	3
MiaPaCa2	Deletion / Absent	248 / Arg to Trp	12 / Gly to Cys	None / wt	3
PC1J	Deletion / Absent	175 / Arg to His	12 / Gly to Val	355 / Asp to Gly	4

Among the gene alteration of the four PDAC lines, p16 loss of function was a factor in common. This mutation is usually associated with early stages of pancreatic carcinogenesis, large tumour masses and patients with a short survival period. *p16* mutation describes an aggressive state of pathology, which along with *KRAS* mutations can promote PDAC tumour growth [26, 27]. On the other hand, the PDAC cell lines are characterized by different *KRAS* mutation: G12C (in MiaPaCa2), G12V (in PaCa44 and PC1J) and G12C (in MiaPaCa2). These alterations were associated with Ras-Like (Ral) signalling activation, which

modulates tumorigenesis and cancer progression. This pathway also plays a fundamental role in CSC biology, favouring resistance to apoptosis [28].

Moreover, $Kras^{G12C}$ can also mediate metabolic reprogramming, favouring glutamine metabolism which improves cell growth and proliferation [29]. PaCa44, MiaPaCa2 and PC1J also have the mutation on *p53* gene in common, which determines protein GOF. Proteins $p53^{C176S}$ (in PaCa44) and $p53^{R248W}$ (in MiaPaCa2) can promote apoptosis evasion and can favour N-glycosylation and glycoprotein folding, cell proliferation, invasion and metastasis, as well as chemoresistance [30, 31].

On the contrary, $p53^{R175H}$ protein (in PC1J) can favour cell survival improving glucose uptake [32] and cell invasion promoting epithelial mesenchymal transition (EMT) pathway [33, 34]. In addition, it can mediate histone acetylation and can promote DNA synthesis, thus enhancing cell aggressiveness and chemoresistance [35]. Interestingly, both $p53^{R248W}$ (in MiaPaCa2) and $p53^{R175H}$ (in PC1J) can promote the activation of mevalonate pathway and can promote sterol biosynthesis through the direct binding and the upregulation of the sterol regulatory element-binding protein [35].

Finally, PC1J is the only line with mutated *SMAD4* gene. In pancreatic cancer the encoded protein $Smad^{D355G}$ is usually associated with *RAS* mutations and it is usually related to more advanced stages and metastasis, as well as to low survival rates of PDAC patients [36].

1.3. Diagnosis

Pancreatic cancer diagnosis includes medical imaging and endoscopic techniques, such as computed tomography (CT scan), magnetic resonance imaging (MRI), positron emission tomography, magnetic resonance cholangiopancreatography, abdominal ultrasonography and endoscopic ultrasound (EUS) [37, 38]. These techniques are used for diagnostic purposes to help to decide whether the tumour can be surgically removed [37]. The selection of the appropriate diagnostic technique has advantages and limitations: for example, abdominal ultrasonography

is low sensitive, but it is non-invasive, inexpensive and an accessible procedure useful for a quick first examination.

The most widely used high-quality imaging examination for the detection and staging of pancreatic carcinoma is CT scan. This technique includes an arterial and a portal venous phase. PDAC is detected in the arterial phase as a hypodense, homogeneous pancreatic lesion with ill-defined margins [38]. CT scan and MRI show similar sensitivity: they are very useful to resolve specific problems, such as identifying the presence of liver lesions and cystic neoplasm and assessing biliary anatomy. However, MRI is costly and not as readily usable as CT scan, so it is rarely used.

The other technique is EUS, which is superior to CT scan and MRI for the detection of small tumours. It assesses interactions between adjacent structures, localizing suspicious lymph nodes, vascular tumour infiltration or metastases. In addition, EUS can be used to collect cytological material by fine-needle aspiration or can take tissue cores (technique under development) with a sensitivity of around 90-98% [38]. In general, CT scan helps to initially assess the stage of pancreatic cancer, providing an evaluation of local and distant sites. Successively, more information is added by using MRI and EUS. The first technique brings information about both the biliary and pancreatic ducts and the presence or absence of vascular invasion, while the second one includes vascular and nodal or bone involvement of the disease.

Another largely used technique for PDAC detection is ^{18}F-fluorodeoxyglucose (FDG) positron emission tomography (PET). It has high sensitivity, specificity and reproducibility. In 2018, Okano *et al*. suggested FDG-PET as a promising approach for selecting patients with initially unresectable locally advanced pancreatic cancer with complete surgical resection [39]. In some cases endoscopic procedures (including gastroscopy and duodenoscopy) are also used to diagnose PDAC, even though they are invasive techniques and are not able to detect tumours infiltrated into the duodenum [38].

Biomarkers have also been considered as a tool to diagnose PDAC. Carbohydrate antigen (CA) 19-9 is the most widely used biomarker for PDAC. The

CA 19-9 serum level provides information about prognosis, overall survival, response to chemotherapy and post-operative recurrence; however, it lacks sensitivity and specificity, which limits its applicability in pancreatic cancer management. In addition, CA 19-9 shows a non-specific expression in benign and malignant diseases and it can give some false negative results in a specific Lewis negative genotype (5% of people) and false positive results in the presence of obstructive jaundice. The sensitivity (80%) and specificity (73%) of CA19-9 in PDAC permits its use for following the progression of the disease rather than for diagnosis [3, 37].

Among the biomarkers used to diagnose PDAC, antigen (CEA) and the human cancer antigen 242 (CA242) can be found. CEA is a carbohydrate antigen which appears as a more robust predictor of advanced PDAC compared to CA19-9 [40]; while CA242 is a sialic acid-containing carbohydrate antigen on the cell surface or in serum which represents a systemic malfunction biomarker associated with cancers and other chronic diseases [41]. It has been reported that PDAC patients with positive expression of CEA, CA19-9 and CA242 simultaneously are characterized by a shorted survival rate [42].

1.4. Staging

Staging refers to the stage of the disease: the extent of the cancer and whether the cancer has spread to other organs in the body. The American Joint Committee on Cancer (AJCC) in collaboration with the Union for International Cancer Control (UICC) elaborated the staging system for exocrine and neuroendocrine pancreatic cancers, based on tumour size, spread to lymph node and metastasis (TNM) [43]. TNM classification distinguishes four main overall stages, from early to advanced disease respectively [44].

Figure 3 shows the two possible classifications. Based on tumour diameter size T1 (< 2 cm), T2 (2 to 4 cm), T3 (> 4 cm) and T4 (the cancer has grown outside the pancreas) can be distinguished. On the contrary, N1 or N2 (where the cancer has spread into 1-3 or more than 4 lymph nodes, respectively) refer to the spread in

lymph nodes. Finally, metastasis (M) is used to refer to the stage where the cancer has extended to different parts of the body. M0 means that there are no metastasis, while M1 means that the cancer has spread to other organs [45].

Finally, based on the possibility to surgically remove the tumour, three broader categories are recognisable: "resectable" (stage I and II), "borderline resectable" (stage III), or "unresectable" (stage IV), which is usually characterized by vascular invasion [44].

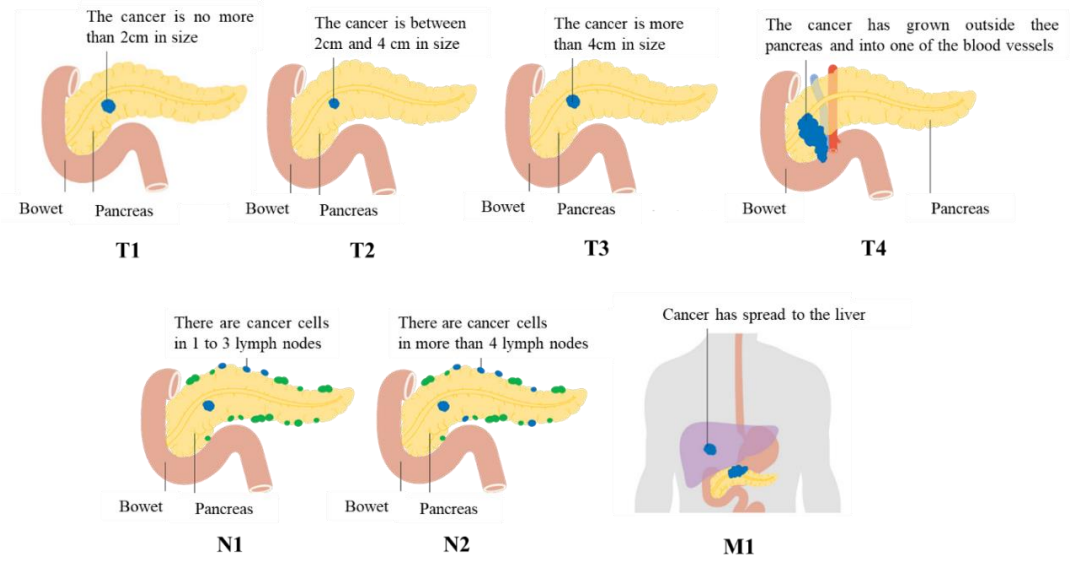

Figure 3. Different stages of PDAC (from T1 toT4) and spread to lymph nodes (N1 and N2) or organs (M1) [45].

1.5. Treatment and prevention

PDAC is therapeutically challenging because only 15%-20% of patients have resectable (at stages I and II), or borderline resectable tumours (at stage III) at the time of diagnosis. Initially, many patients are treated with chemotherapy which may or may not be associated with radiotherapy. Nowadays, the only potentially curative treatment available is surgical removal which is usually considered if patients show a down staging response after chemotherapy [37, 43]. In general, chemotherapy can be useful to reduce tumour size and to extend or to improve the quality of life of

patients. Radiotherapy can be also used to shrink a tumour to a resectable state but its use on unresectable tumours (stage IV) remains controversial as clinical trials show conflicting results [3].

Drug treatment of PDAC is mainly performed using Gemcitabine which is effective in only 23.8% of PDAC cases. The low efficacy may depend on the dense tumour stroma which prevents drug diffusion to the tumour bulk, favouring chemoresistance [46, 47]. Usually, gemcitabine is combined with other chemotherapeutic drugs (*i.e.*, Nab-paclitaxel, cisplatin, capecitabine) to improve overall survival in advanced PDAC patients [48].

It is widely known that the refractory aspect of PDAC depends on the pronounced general radio- and chemo- resistance of pancreatic cancer cells, but also on the presence of pancreatic cancer stem cells (PCSCs) [6].

2. Pancreatic cancer stem cells

Cancer stem cells (CSCs) are a small subset of undifferentiated, quiescent and immortal cells with highly aggressive features. Nowadays, the origin of this subpopulation of cells remains quite unknown. Two different hypotheses have been postulated: the first one refers to CSCs as tissue stem cell, while the second one provides for the existence of progenitor cells, so stem cells derived from bone marrow, or dedifferentiated cells that result from genetic mutation [6].

As shown in Figure 4, CSCs are characterized by their ability for self-renewal (by a symmetric differentiation) and to cell differentiation (by an asymmetric division), coupled with unique plasticity and metabolism [49]. The production of differentiated progeny is responsible for tumour growth and heterogeneity [50, 51]. Each pancreatic cancer can be characterized by genetically and/or epigenetically different CSC clones, which in turn could induce intermediate progenies or transitory/hybrid cells formations. Cancer microenvironment is highly dynamic, so CSC clones can dominate or shrink into the tumour bulk [52]. However, the symmetric differentiation never leads to the extinguishing of CSC pools.

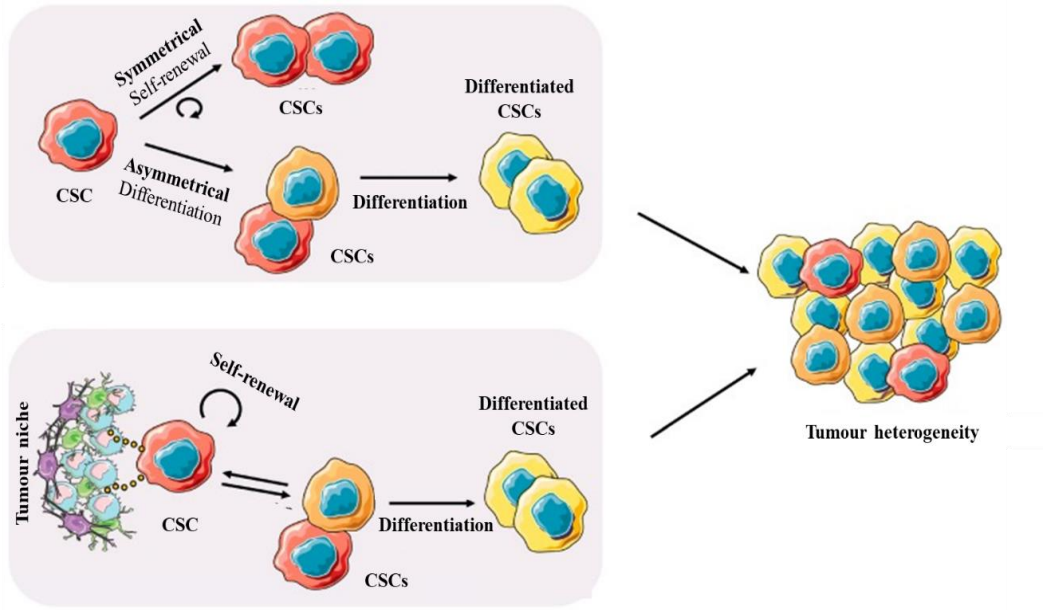

Figure 4. Models of the CSC concept to explain the tumour heterogeneity [53].

Specifically, PCSCs represent only 1% of primary pancreatic tumour cells and they are considered as the main triggering factor responsible for PDAC growth (initiation, progression and recurrence), maintenance, metastasis and chemoresistance [54, 55]. The existence of cancer stem cells was first reported in the context of acute myelogenous leukaemia and subsequently verified in breast and brain tumours [56]. PCSCs identification was demonstrated in 2007 from a xenograft model in which primary human pancreatic adenocarcinomas were grown. Li C *et al*. identified $CD44^+$, $CD24^+$, ESA^+ cells with specific properties [55].

In PDAC, CSCs were empirically defined by two major techniques: using tracing of genetic lineage markers or by assessment of tumorigenesis after transplantation into immuno-deficient mice [57, 58]. *In vitro*, these cells form non-adherent spheroids, also called tumour-spheres, which are usually used to effectively enrich subpopulations with stem-cell properties [50, 59].

2.1. Characteristics of pancreatic cancer stem cells

PCSCs possess characteristics that ensure their survival, chemo- and radio-resistance, multipotency and ability to metastasize [53]. The high chemoresistance of PCSCs depends on several mechanisms, such as the metabolic inactivation of the drug, the efflux of the drug from the cells and the mutation or deregulation of drug targets [60], which are also related to the presence of a high expression of anti-apoptotic, ATP-binding cassette (ABC) transporters and multidrug resistance proteins [61].

Other factors responsible for CSC chemoresistance are altered drug transport activity. This mechanism is modulated by the over-expression of aldehyde dehydrogenase (ALDH) and proteasome, as well as a decreased expression of the human equilibrative nucleoside transporters (ENTs) and human concentrative nucleoside transporters (CNTs) in this subpopulation of cells [62]. For this reason, the anti-PDAC drugs can usually eliminate the bulk of the tumour, but do not affect PCSCs which survive treatments. Consequently, this activated subpopulation of cells starts to proliferate to restore tumour bulk deficiency, orchestrating tumour recurrence and relapse [50, 62, 63].

Moreover, PCSC phenotype is generally supported by the EMT process. This characteristic confers on PCSCs the ability to lose their epithelial characteristics acquiring stem cell-like features [63]. The EMT process has a fundamental role in invasive and metastatic behaviour of PDAC cells, leading to changes in many aspects of cellular physiology [54, 64]. This signalling pathway can induce alterations in the cytoskeletal organization and changes in cell morphology, such as acquisition of a spindle-like and elongated form or dissolution of epithelial cell-to-cell junctions. Moreover, EMT can also determine loss of apical-basal polarity and concomitant gain of front-rear polarity, acquisition of cell motility and of the ability to degrade and reorganize the extracellular matrix (ECM).

This ECM reorganization can enable cell invasion and is related to the reconfiguration of expression patterns of at least four hundred distinct genes [65]. In pancreatic cancer cells, EMT is controlled by several transcription factors, including Zeb1, which suppresses the adhesion molecule E-cadherin by repressing

the miR-203 (an inhibitor of stemness) and the miR-200 family members which regulate the expression of stem cell factors [64]. CSCs and EMT are strictly interconnected: in PDAC mouse model it was demonstrated that the cellular dissemination , which leads to metastasis formation, occurs prior to the formation of an identifiable primary tumour [66]. This behaviour has been associated with the presence of circulating pancreatic cells with a mesenchymal phenotype, which express typical stem markers [64].

Finally, it is important to notice that PCSCs reside in *niches*, where they are stopped in a G0 phase, so in a quiescent state. This condition is responsible for the protection of cancer cells, tumour growth, phenotypic and metabolic plasticity. Specifically, CSCs can adjust their metabolism by acquiring intermediate metabolic phenotypes or by shifting from oxidative phosphorylation (OXPHOS) to glycolysis. Wnt/Rspo, c-Jun N-terminal protein kinase (Jnk), Nodal/Activin, Notch, or Hedgehog proteins are critical components for the ever-changing tumour microenvironment and for the construction of PCSC *niche* [62]. This specific microenvironment has also been suggested as contributing to drug resistance, since quiescence protects PCSCs from chemotherapeutic drugs which usually target rapidly proliferating cells [6].

2.2. Markers of pancreatic cancer stem cells

Due to CSC heterogeneity, no universal stem cell markers have been identified yet to distinguish this subpopulation unequivocally from the non-stem (parental) cancer cells. In 2007, PCSCs were identified by investigating the expression of CD44, CD24 and epithelial-specific (EpCAM) antigens involved in pancreatic cancer. Specifically, CD44 is a membrane receptor which interacts with c-Myc, improving the anti-apoptotic activity of cells [67] and prevents E-cadherin activation promoting EMT pathway [68]. Interestingly, its alternative form CD44v6 can promote tumour progression and motility, metastases formation and drug resistance [69, 70].

The other antigen is CD24, a mucin-like glycosyl phosphatidylinositol (GPI)-linked cell surface protein, involved in cell adhesion [68], metastasis formation, tumour invasion and drug resistance [71]. Its overexpression is related to poor prognosis in PDAC patients [72].

Finally, EpCAM (ESA) is a transmembrane type I glycoprotein usually expressed in epithelia able to modulate EMT pathway and *in vivo* metastasis formation. Its upregulation can reduce Pten expression and improve Akt and mTOR phosphorylation [73].

During the last decade, CD133 and CXCR4 have been identified as other PCSCs markers, able to induce tumour metastasis in pancreatic cancer [74]. CD133 is a transmembrane protein in lipid rafts able to promote tumour progression and EMT pathway [68, 75]. Instead, CXCR4 is a G-protein-coupled receptor for stromal-derived-factor-1 related to metastasis formation and poor prognosis of resected PDAC patients [76]. The double depletion of $CD133^+$ $CXCR4^+$ CSCs can eliminate the metastatic phenotype of pancreatic tumour [74].

Two additional PCSC markers are aldehyde dehydrogenase 1 (ALDH1) and hepatocyte growth factor receptor (cMet). The first one belongs to a superfamily of enzymes which detoxify endogenous and exogenous aldehydes and promote the biosynthesis of retinoic acid and other regulators of cellular functions [77]. $ALDH^+$ cells showed stem-like features, including self-renewal, clonogenic growth, tumour initiating capacity and drug resistance [77]. On the contrary, cMet is a membrane tyrosine kinase which interacts with the hepatocyte growth factor stimulating cell invasion, motility and metastasis (Tab. 3) [78].

Finally, PCSCs also express stem cell markers: octamer-binding transcription factor 4 (Oct4), homeobox protein (Nanog) and Sex-determining region Y-box 2 (Sox2). As shown in Figure 5, these three transcription factors have a fundamental role in several pathways, including the regulation of cell differentiation, reprogramming of cancer cells into stem cells and maintenance of stemness in pancreatic cancer cells and pluripotent embryonic stem cells.

Table 3. Cell membrane markers of PCSCs.

Marker	Type	Characteristics
CD44	Membrane receptor	Tumorigenicity; metastasis formation
CD24	Cell membrane	Tumorigenicity; metastasis formation
EpCAM	Transmembrane protein	Tumorigenicity; metastasis formation
CD133	Transmembrane protein	Tumorigenicity; tumour progression; drug resistance
Cxcr4	Cell membrane	Metastasis formation
ALDH1	Cell membrane	Tumorigenicity; tumour initiation;
ALDH	Cell membrane	Tumour invasion and progression; drug resistance; self-renewal;
cMet	Transmembrane protein	Tumour invasion and motility; metastasis formation

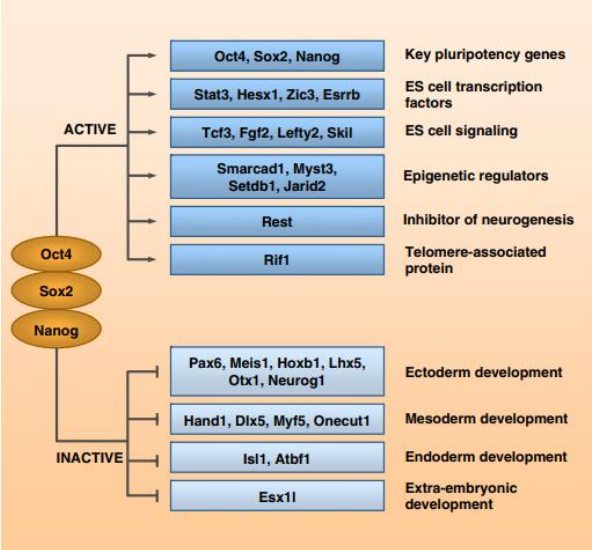

Figure 5. OCT3/4, SOX2 and NANOG genes and the related pathways in which the encoded proteins (Oct4, Sox2 and Nanog) are implicated [79].

Oct4 controls proliferation, invasion and migration of PCSCs in pancreatic cancer [68]. Its loss of function was associated with AKT pathway repression and the consequent inhibition of several biological processes, including EMT pathway [80]. As for Oct4, Sox2 not only regulates EMT but also stemness and self-renewal of CSCs [81]. Finally, Nanog regulates several CSC aspects, including self-renewal, invasive and metastatic ability and is also considered a prognostic marker [82].

The mRNA transcripts of the stem related genes (*i.e.*, *OCT3/4*, *SOX2* and *NANOG*) are usually overexpressed in CSCs compared to non-tumour cells [83].

2.3. Dysregulated signalling pathways of pancreatic cancer stem cells

The main dysregulated signalling pathways of PCSCs are Wnt/β-catenin, Sonic Hedgehog (SHH) and Notch. Additionally, autophagy, phosphatidylinositol 3kinase (PI3K), NF-κB cell cycle regulator forkhead box protein M1 (FoxM1), polycomb complex protein Bmi-1, and Nodal/Activin pathways also support PCSC activity [6].

As shown in Figure 6, Wnt/β-catenin pathway consists of two major ways: a canonical and a non-canonical pathway. The canonical pathway is essential for cell fate decisions during development and for the regulation of stem cell pluripotency [84]. Depending on the presence or not of Wnt signal, the canonical pathway can be in “off” or “on” state, respectively. During the "off" state β-catenin is phosphorylated and successively ubiquitinated for proteasome degradation [85]. During the "on" state, Wnt binds Frizzled (Frz) receptors and Lrp5/6 coreceptor, activating Dishevelled (Dv1), leading to the accumulation of β-catenin into the nucleus and the activation of the transcription of target genes [84].

On the other hand, the non-canonical pathway can be sub-divided into Wnt/calcium (Ca^{2+}) pathway which regulates the intracellular Ca^{2+} levels [86] and the Wnt/PCP pathway which regulates actin cytoskeletal reorganization and cell survival [87].

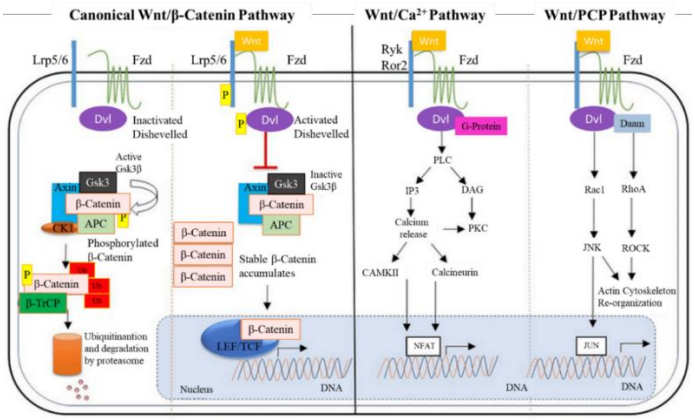

Figure 6. Wnt/β-catenin canonical and non-canonical pathways [88].

The Hedgehog signalling (HH) regulates cancer cell proliferation, malignancy, metastasis and the expansion of CSCs, promoting tumorigenesis and chemoresistance [89]. It is also associated with self-renewal and stemness maintenance of CSCs [90, 91]. HH pathway is regulated by three Hh proteins: SHH, Desert Hedgehog (DHH) and Indian Hedgehog (IHH).

As shown in Figure 7, a canonical and a non-canonical way are distinguishable. The canonical way depends on the interaction between Shh and Patched (Ptch) proteins which lead to the transcription of target genes (Fig. 7a) [92]. The non-canonical pathway involves two different mechanisms: one that modulates Ca^{2+} release and actin cytoskeleton (Fig. 7b); and the other one called Smo independent pathway (Fig. 7c) [92, 93].

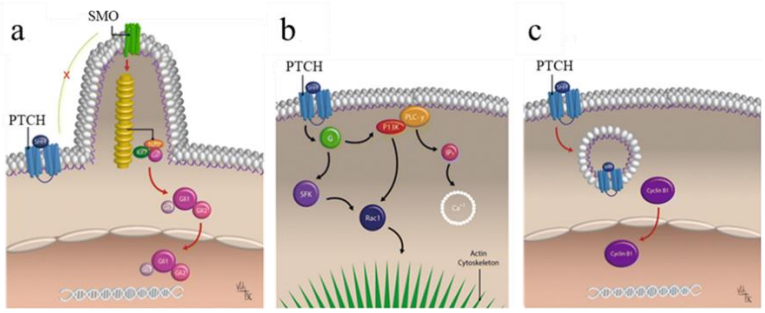

Figure 7. HH signalling pathway a. canonical way; b. and c. SMO independent non-canonical way [92].

Notch signalling regulates CSC self-renewal and survival [94, 95]. This pathway involves five ligands, namely delta-like (Dll1, Dll3 and Dll4) and Jagged (Jag1 and Jag2) proteins, and four transmembrane receptors (Notch1, Notch2, Notch3 and Notch4) and Intracellular effector molecules such as RBP-Jκ (recombination signal binding protein-jκ) [96]. The Notch signalling pathway is divided into canonical and non-canonical pathways, depending on whether RBP-Jκ is involved in pathway conduction.

Autophagy is associated with several crucial CSC characteristics: in the maintenance of pluripotency and aggressiveness of different type of CSCs (including PCSCs) [97] and in the migration and invasion regulation [97, 98], CSC growth and resistance [98-100]. For instance, in gastric CSCs, autophagy regulates chemoresistance via the already mentioned Notch signalling pathway [101].

In addition, PI3K signalling pathway, it regulates cell proliferation, survival, metabolism, apoptosis, growth and migration processes (Fig.8) [102]. PI3K is recruited and activated, stimulating an increase in phosphatidylinositol-3,4,5-trisphosphate (PIP3) levels. After several steps, Akt is activated, and it promotes cellular growth, survival and proliferation. Additionally, PI3K can also influence downstream targets, including mTORC1 [103].

PI3K/Akt/mTOR pathway is altered in most of the pancreatic cancer cases [104] and its inhibition can decrease the capability of $CD133^{+}$ pancreatic cancer cells to create spheres *in vitro* [104]. Moreover, The PI3K/Akt signal pathway is involved in gemcitabine resistance of pancreatic cancer [105].

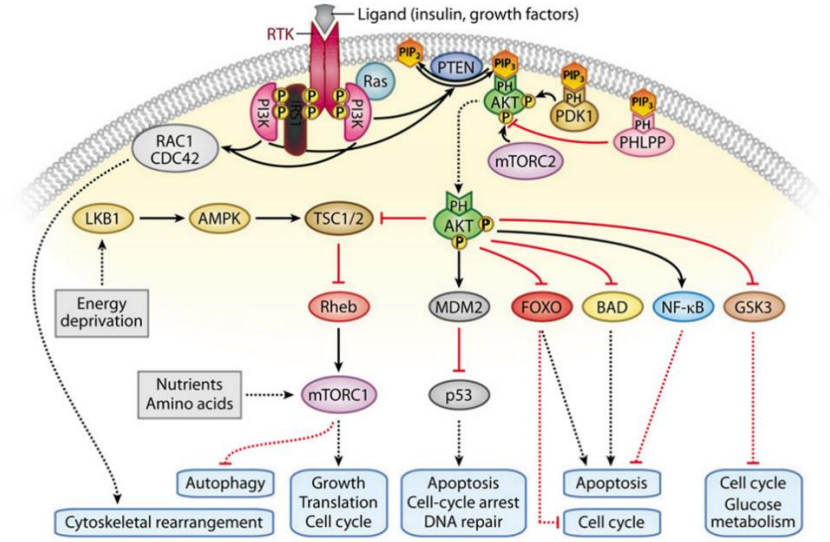

Figure 8. PI3K signalling pathway [106].

Another crucial pathway for CSCs is NF-κB signalling which is distinguished by canonical and non-canonical pathways (Fig. 9).

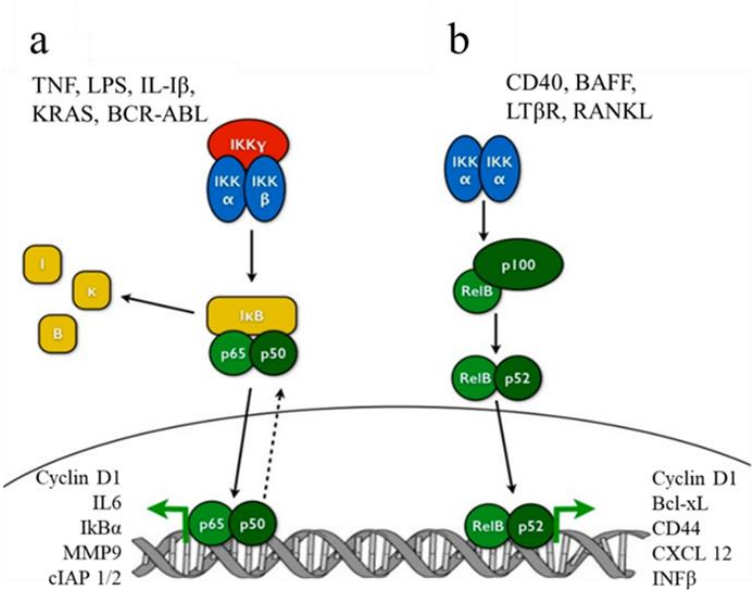

Figure 9. NF-κB signalling a. canonical pathway; b. non-canonical pathway [107].

In pancreatic cancer, NF-κB can control Hif1-α, EMT and angiogenesis factors, such as the vascular endothelial growth factor (Vegf) [108]. It has been reported that the inhibition of NF-κB activity in metastatic human PDAC mouse model blocks the formation of liver metastasis [108].

3. Pancreatic cancer stem cell targeted therapy

The development of anticancer drugs able to target fundamental pathways and proteins of PCSCs could improve therapeutic outcomes and prognosis of PDAC patients. Several potential strategies have been developed to direct eliminate CSCs (targeted therapy) and to avoid cancer progression, metastasis and relapse. Unfortunately, none of them turned out to be effective [6].

3.1. Non-cancer related drugs

Some non-cancer related drugs that show anticancer effects against different human CSCs could also represent an option against PCSCs (Tab. 4) [6]. These drugs can act through different mechanisms of action, including the inhibition of some important PCSC pathways [6].

Antibiotics are among the molecules that exhibit extraordinarily diverse biological activities. For example, Salinomycin, an antibacterial and coccidiostat ionophore drug, interferes with the activity of Kras-4B, Wnt and EMT pathways reducing the viability of breast CSCs and blocking the tumour growth and the metastatic spread of PDAC in a genetically engineered mouse model [109]. Azithromycin is another antibiotic, which acts by binding to the bacterial ribosome 50S subunit, that can prevent tumour-sphere formation in PDAC and in other cancers [110].

There are also some antimalarial agents among the non-cancer related drugs that target CSCs: for example, Chloroquine has shown significant effects on PCSCs through the inhibition of both CXCR4 and Hedgehog pathways [111]. Atovaquone

is another similar agent that selectively inhibits OXPHOS and CSC sphere-formation in breast cancer [112].

Metformin, an antidiabetic drug, is also able to counteract PCSCs. It inhibits the mTOR and PI3K/Akt pathways, reducing the expression of PCSC markers in pancreatic tissue, as well as the size and number of tumour spheres. Contrary to the very promising preclinical data, the efficacy of this compound in patients was rather inconclusive: indeed, *in vivo* experiments demonstrated that metformin prevents progression and metastasis in PDAC even though it does not improve outcome of patients at advanced metastatic stages treated with standard therapies [113].

Salicylic acid, also known as aspirin, is another non-cancer related drug that may be a candidate for eliminating PCSCs. Aspirin, commonly used as an antipyretic and anti-inflammatory drug, counteracts PCSC features such as ALDH1 activity, NF-κB signalling, self-renewal potential and gemcitabine resistance [114].

Table 4. Non-cancer related drugs and their potential effects on PCSCs [6].

Drug	**Function**	**Relative pathway/process**
Salinomycin Azithromycin Nigericin Tigecycline	Anti-bacterial antibiotic	Wnt, EMT Mitochondria EMT OXPHOS
Chloroquine Atovaquone	Anti-malaria	OXPHOS
Aprepitant	Anti-emetic	Wnt
Ketamine	Anti-depressant	Wnt
Aspirin	Anti-pyretic Anti-inflammatory	ALDH1, NF-κB
Metformin	Anti-diabetic	mTOR, PI3K/Akt
Disulfiram	Anti-alcoholism	NF-κB
Atorvastatin	Anti-cholesterol	Mevalonate

3.2. Drugs that target dysregulated pathways and proteins of cancer stem cells

Other target therapies rely on targeting stem cells related pathways, such as Wnt/β-catenin, SHH, Notch and mTOR signalling (Tab. 5).

Sanguinarine is an isoquinoline alkaloid compound obtained from *Sanguinaria canadensis* that is effective for the inhibition of PCSCs, blocking self-renewal, migration, invasion and EMT capability through SHh pathway suppression [6].

Notch signalling is another crucial pathway of CSCs: studies demonstrated that its inhibition using γ-secretase inhibitor (RO4929097) or Hes1 shRNA reduced tumour-spheres formation and PCSCs. Moreover, Quinomycin A, a quinoxaline antibiotic, was able to downregulate Notch pathway proteins, causing tumour growth inhibition *in vivo* [6].

Differential protein expression of PCSCs may allow the study and the detection of further therapeutic targets. Recently, Brandi *et al*. showed that Cerulenin, a specific fatty acid synthase (Fasn) inhibitor, reduced viability and spheroid formation in PCSCs of a specific PDAC line, called Panc-1 [54]. Another promising therapeutic target could be Galectin-3 (Gal3), a protein involved in RAS signalling activation which is overexpressed and oversecreted in Panc1 CSCs. Several studies connected this protein with stemness, by activation of Notch signalling [54, 115].

Among potential targets there is the estrogen-related receptor gamma (ERRγ), an upstream regulator of PCSC deregulated proteins that can promote metabolic reprogramming, pluripotency, OXPHOS and glycolytic pathways [116].

Table 5. Compounds that act on dysregulated pathways and proteins of pancreatic cancer stem cells. Adapted from [6].

Deregulated pathways	**Compound or strategy**
Hedgehog	Crocetinic acid; Sanguinarine; GANT61
Notch	RO492909, shRNA; Quinomycin A
mTOR	Rapamycin; AZD8055
Deregulated proteins	**Compound or strategy**
Fasn	Cerulenin
AnxA1	siRNA
Marcks	MANS peptide
Galectin-3	Polysaccharide RN1
PKM2	Lapachol; Diallyl disulphide
ERRγ	GSK5182

3.2.1. Nanoparticles against dysregulated pathways of cancer stem cells

A great obstacle to drug delivery in PDAC is represented by its dense desmoplastic stroma and the highly hypoxic tumour microenvironment, which impairs cancer cell response to chemotherapy. Therefore, a novel strategy to improve drug delivery has been developed which exploits nanoparticles (NPs) to carry the desired drug into the cell [117]. Liposomal NPs (liposomes) are small spherical vesicles delimited by a phospholipid bilayer capable of containing drugs. They are the most common drugs used against PCSCs due to their reduced size, biocompatibility and low toxicity [117]. However, their limited loading capacity can prevent an optimal drug diffusion [6]. Nanocarriers represent a promising drug delivery system for clinical applications, but further studies are needed to improve this technology.

To improve the delivery of the drug, NPs have been developed to target CSCs, reducing cytotoxicity and increasing the efficacy of treatments specifically and effectively. Some NPs have been developed to target pancreatic cancer and liposomal formulations have gained regulatory approval [6]. The first clinical trial of NPs conducted in PDAC patients was done using a PEGylated colloidal gold-rhTNF nanomedicine, termed CYT-6091, which demonstrated that NPs greatly reduce the toxicity of chemotherapeutics and may target tumours [6]. Recently, HA-modified poly (dl-lactic-co-glycolic acid)-poly (ethylene glycol) NPs have been developed for targeted delivery of thio-tetrazolyl analogue of a clinical candidate to CD44 over-expressing cancer cells.

In vitro results showed that cellular uptake led to higher cytotoxicity and enhanced intracellular accumulation of these NPs in high expressing CD44 MiaPaCa2 cells [118]. However, the most used NPs against PCSCs are liposomes. However, their limited loading capacity can prevent an optimal drug diffusion [6].

In conclusion, nanocarriers represent a promising drug delivery system for clinical applications, but further studies are needed to improve this technology.

4. Research on pancreatic cancer stem cells

4.1. *In vitro* model of pancreatic cancer stem cells

Since PCSCs represent an intriguing target for therapy, a development of reliable model of this subpopulation of cells and a complete molecular characterisation of PCSC biology becomes crucial for basic and clinical cancer research [6, 119].

Up to now, it has been demonstrated that PCSCs can be isolated from PDAC cell lines using cell surface markers by flow cytometry [120]. Alternatively, they can be obtained from parental cells *in vitro* by transferring them to a specific stem medium: DMEM/F-12 supplemented with glucose, B27, epidermal growth factor (EGF) and fibroblast growth factor (FGF), fungizone, penicillin/streptomycin, heparin, where they can produce differentiated cell progeny, forming non-adherent spheroids *in vitro*, also known as tumour-spheres [50, 59]. Yet the mechanism by which this medium induces CSCs remains unknown, even if it was demonstrated that B27

supplement (which contains, among other components, vitamins, BSA, catalase, insulin, transferrin, SOD, galactose, glutathione, progesterone) is necessary for sustained propagation and enrichment of cancer stem cells *in vitro* [121].

The EGF favours pluripotency favouring the activation of EGF signalling by EGF receptors, while FGF plays an important role in creating tumour spheres and increasing a sub-population of cells that is distinct from the main population on the basis of the markers employed [122].

In 2015, Dalla Pozza *et al*. characterized PCSCs generated *in-vitro* by adherent cells demonstrating their high resistance, plasticity and aggressiveness [123]. This study suggested the importance of PCSC *in vitro* model to investigate the biology of PDAC, to discover new biomarkers and to test new therapeutic drugs against PCSCs [123].

4.2. Proteomics and lipidomics

Proteomics represents the large-scale analysis of proteins at a given time under defined conditions in a complex and dynamic system, such as a cell, tissue or whole organism. Analysis of protein derangements on a proteome-wide scale reveals insight into dysregulated pathways and networks involved in the pathogenesis of disease. The field of proteomics has grown due to improvements in the accuracy, sensitivity, speed and throughput of mass spectrometry (MS) and the development of powerful bioinformatic software. Proteomics has expanded from protein profiling to accurate and high-throughput protein quantification between two or multiple biological samples.

Quantitative analysis at global protein levels (called ‘quantitative proteomics’) is fundamental to understand protein functions and mechanisms of biological systems. Different strategies were developed for proteomic analysis, such as two-dimensional gel electrophoresis (2-DE) and shotgun proteomics which is based on liquid chromatography tandem mass spectrometry (LC-MS/MS).

On the other hand, lipidomics is a newly developing field of study that represents a fundamental area of metabolomics, whose object of study is the lipidome (the totality of lipids) in a complex system [124]. Figure 10 shows that this emerging field refers to eight different groups: fatty acyls, glycerophospholipids (also known as phosphoglycerides), glycerolipids, sphingolipids, sterol lipids, prenol lipids, saccharolipids and polyketides [125]. These groups are characterized by different head groups and chain lengths that define properties and function of lipids. The lipid species can be identified and quantified.

In this study, a label free strategy based on high resolution mass spectrometry (SWATH-MS) analysis was adopted to perform quantitative proteomics by using a TripleTOF 5600 plus MS instrument. Samples were subjected first to an untargeted data-dependent acquisition (DDA) analysis to generate the SWATH-MS spectral library, and then to cyclic data independent analysis (DIA), based on a 25-Da window, using three technical replicates of each sample.

Untargeted lipidomics analyses were performed by using an Orbitrap Elite mass spectrometer (Thermo Fisher Scientific, Waltham, MA, USA), while targeted analysis of lysolipids, ceramides and dihydroceramides lipid sub-classes, was performed using triple quadrupole analyser worked in multiple reaction monitoring (MRM) mode for the quantification of the analytes.

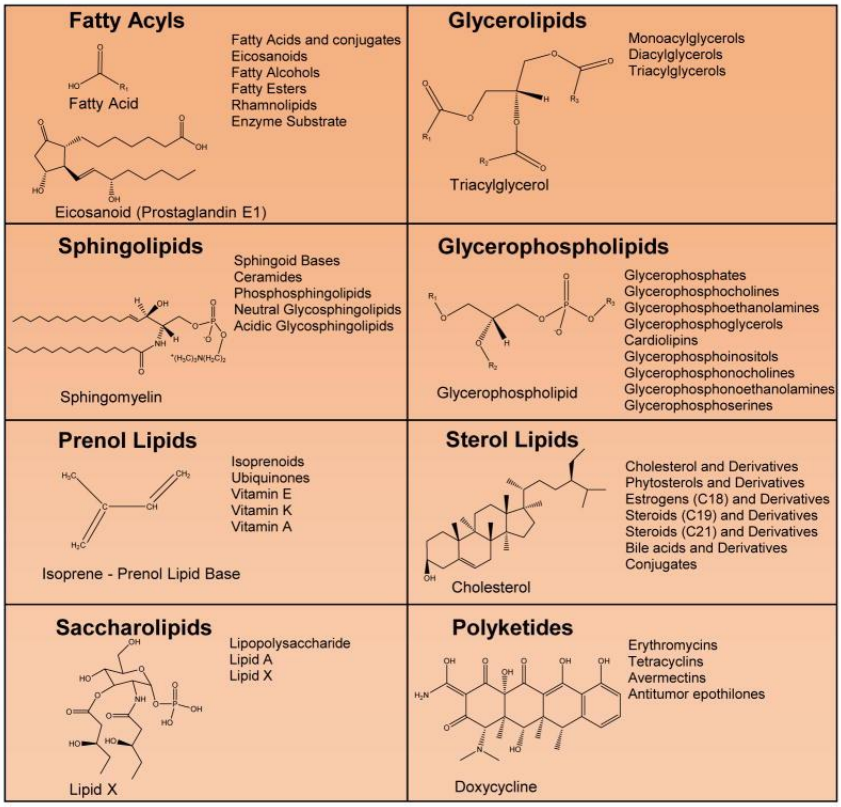

Figure 10. Lipid group composing the lipidome: fatty acyls, glycerolipids, sphingolipids, glycerophospholipids, prenol lipids, sterol lipids, saccharolipids and polyketides. Different classes are also reported for each group [125].

4.2.1. Proteomics and lipidomics in pancreatic cancer research

Proteomics and lipidomics analyses can be useful to identify prognostic biomarkers for PDAC. In 2018, Hu D. *et al.* analysed tumour tissue samples isolated from PDAC patients with different survival rates to identify prognostic biomarkers which can be related to their outcome [126]. A total of 171 proteins resulted differentially modulated in patients with "short" compared to those with "long" survival rate. The dysregulated proteins were mainly involved in the metabolic switch from OXPHOS to glycolytic state [126].

Another interesting study on tumour and metastatic samples obtained from PDAC patients suggested that those with "short" survival rate were characterized

by an upregulation of proteins located to the stroma, indicating the importance of tumour microenvironment in this pathology [127], while the analysis of the proteomic profile of three different PDAC cell lines (*i.e.*, Panc-1, BxPC-3 and HPDE) revealed that the overexpression of proteins related to the EMT pathway and glutathione metabolism can be associated with gemcitabine resistance [128]. Interestingly, in gemcitabine resistant pancreatic cancer cells, the environmental stress caused by the treatment with this drug may be modulated by the overexpression of different proteins (*i.e.*, transitional endoplasmic reticulum ATPase, LIM/homeobox protein, prelamin A/C, 60 kDa heat shock protein and alpha enolase) [128].

Over recent years, few studies have been published on the lipidomic profile of PDAC. In 2017, Saison-Ridinger M. *et al*. showed that primary cancer-associated pancreatic stellate cells obtained from PDAC patients were characterized by an increase of triacylglycerols and cholesterol ester sub-classes, which caused the accumulation of lipid droplets [129]. Afterwards, it was demonstrated that PDAC cells favour the production of lysophosphatidic acid, which is an oncogenic signalling lipid able to promote cell proliferation and migration [130]. More recently, Urman J.M. *et al*. (in 2020) performed multi-omics analyses of bile from PDAC patients to select potential biomarkers. A total of 10 lipid species of phosphatidylethanolamine, ceramides, phosphocholines and monoacylglyceride sub-classes were selected as able to discriminate PDAC compared to normal patients [131].

4.2.2. Proteomics and lipidomics in pancreatic cancer stem cell research

Currently, few data have been collected concerning the proteome dysregulation of PCSCs. In 2010, the global proteome profiling of PCSCs from xenograft tumours in mice was first explored using a capillary scale shotgun technique by coupling offline capillary isoelectric focusing (cIEF) with nano reversed phase liquid chromatography (RP-LC) followed by spectral counting peptide quantification

[132]. A total of 169 dysregulated proteins were identified in these PCSCs compared to non-tumorigenic cell sample, which were mainly involved in inflammation, apoptosis, cell proliferation and metastasis [132].

Successively, Zhu J. *et al.* performed two proteomics studies of PCSCs. In 2012, sixteen differentially expressed glycoproteins were identified in $CD24^{+}CD44^{+}$ PCSCs by nano-LC-MS/MS and tissue microarray. Among them, the increased expression of CD24 protein was related to advanced PDAC, while the decreased expression of CD13 protein was associated with tumour progression. Therefore, CD24 and CD13 were suggested as promising prognostic markers for pancreatic cancer [133]. In 2013, proteomic profile of $CD24^{+}$ PDAC cells obtained from biopsies was analysed in comparison with $CD24^{-}$ cells. A total of 375 differentially regulated proteins were identified in $CD24^{+}$ PDAC cells. Some of them were related to tumour promotion (*i.e.*, TGFBI) and immune escape (*i.e.*, CD59, CD70 and CD74) [134].

Successively, Matsukuma S. *et al*. analysed PCSCs, obtained from pancreatic cancer cell lines, by 2-D electrophoresis and MS. This study revealed the upregulation of calreticulin in PCSCs and the association of this protein with poor survival in PDAC patients. For these reasons, calreticulin was suggested as novel biomarker for PDAC [135]. The most recent papers concerning the proteomic analysis of Panc-1 CSCs, a specific PDAC cell line, were published by our research group [54, 115]. PCSCs were obtained from Panc-1 parental (P) cells by transferring them in a specific stem medium and then proteome and secretome profiles of these cells were analysed. The data revealed a pivotal role of FA synthesis and mevalonate pathway in PCSCs [54]. Moreover, ceruloplasmin was also suggested as promising biomarker for PDAC patients negative for CA19-9 [115].

Up to now, there are no studies about the lipidome of PCSCs which is totally unexplored. However, there are few papers about lipid metabolism of CSCs. In colon CSCs an increase of monounsaturated FAs and a reduction of FA levels compared to bulk cancer cells was detected [136], while in ovarian CSCs was demonstrated a higher ratio of unsaturated to saturated FAs in comparison with non-

CSCs was demonstrated. This feature was directly correlated to the enhanced activity of NF-κB and of lipid desaturases. The induction of lipid unsaturation was defined as a stable, universal and functional metabolic marker and potential target for ovarian CSCs [137].

Another study on chronic myelogenous leukaemia stem cells (LSCs) revealed the pivotal role of lysophospholipid metabolism in stem cell maintenance. Instead, the reduction of some lysophosphatidic acid species determined a reduction in LSCs in promoting *in vivo* tumour initiation [138]. In addition, some lipid signalling species (*i.e.*, some phosphatidic acid and diacylglycerols species) can mediate homing of bone marrow-derived mesenchymal stem cells to glioma stem cell xenografts. By electrospray ionization-tandem mass spectrometry (ESI-MS/MS) analysis, which firstly provided the implication of lipid signalling in this inflammation process [139].

More recently, Serna I.M.R. *et al.* investigated the lipidomic changes of hepatic CSCs by LC-MS/MS analysis. The increased levels of sphingomyelin sub-class together with decreased levels of both phosphatidylcholine and lysophosphatidylcholine sub-classes were suggested as specific lipidomic signatures able to modulate malignant phenotype and stemness [140].

On the other hand, it was demonstrated that some lipids could affect CSC vitality. A treatment with eicosapentaenoic acid, an omega-3 polyunsaturated FA, was able to reduce the population of CSCs which were enriched to chemoresistant colorectal cancer cells [141].

Chapter 2

Characterization of pancreatic cancer stem cells

1. Introduction

Pancreatic cancer stem cells (PCSCs) are a heterogeneous population that represents a small percentage of PDAC tumour bulk, whose isolation and identification is challenging. As previously described, PCSCs express heterogeneous markers, which makes it difficult to isolate these cells by using flow cytometry. On the contrary, the *in-vitro* generation of this subpopulation from pancreatic cancer cells, here called parental (P) cells, is a well-established strategy to obtain PCSCs which represent the different subpopulations of a tumour very well. This chapter addresses the generation of PCSCs from P cells using a specific culture media and the analysis of some PCSC characteristics. Therefore, the in-depth study of PCSC features will allow us to delineate the most critical aspects of these cells.

PCSCs were subjected to a morphological analysis by microscopy. Successively, stemness and quiescence-related markers were analysed by qPCR and/or immunoblotting analyses. Specifically, Sox2, Nanog, Oct3/4 were investigated due to their importance in pluripotency and self-renewal [142], while Cyclin B1 and Frizzled 2 were studied due to their role in quiescence [143] and drug resistance [144, 145].

2. Materials and methods

2.1. Cell lines and culture conditions

Four different PCSC lines, *i.e*., PaCa3, PaCa44, MiaPaCa2 and PC1J, together with their relative P cells, were analysed. As described in the Introduction (Chapter 1, Section 1.2.1.), these cell lines are characterized by a different genetic background that may influence phenotype and cell metabolism [146, 147].

The PDAC PaCa3, PaCa44, MiaPaCa2 and PC1J P cell lines obtained from American Type Culture Collection (ATCC) were grown in RPMI-1640 media, supplemented with 10% FBS, 2 mM glutamine and 50 µg/ml gentamicin sulphate (all from Gibco/Life Technologies), at 37°C in a humidified 5% CO_2 incubator for the entire duration of cell culture. PCSCs were generated from PDAC cells as previously described [119]. P adherent cells were washed twice in 1X PBS (Gibco/Life Technologies) and then cultured in stem-selective medium (SsM) to obtain PCSCs. SsM contains DMEM/F-12 without glucose (US Biological Life Sciences) supplemented with 1 g/l glucose, B27, 1 µg/ml fungizone, 1% penicillin/streptomycin (all from Gibco/Life Technologies), 5 µg/ml heparin (Sigma/Merck), 20 ng/ml epidermal growth factor (EGF) and 20 ng/ml fibroblast growth factor (FGF) (both from PeproTech).

PCSCs obtained from P cells were cultivated in SsM for two weeks, refreshing the cell culture media twice a week.

2.2. Examination of cells by light microscope

Bright field images of PCSC and P cells in the cultured dish were acquired with an inverted microscope (Axio Vert. A1, Zeiss) using 20x objective lens coupled with an Axio Cam MRC Zeiss camera and Zen 2012 software for image acquisition. The captured images were qualitatively assessed for cell morphology to differentiate P and PCSCs. The initial visual observation was conducted three times.

2.3. Viability assay

P cells were collected using trypsin and centrifuged at 800 X g for three minutes to remove the supernatant. PCSCs, derived from P cells (PaCa3, PaCa44, MiaPaCa2, and PC1J), were passed through a cell strainer (40 μm) to separate and maintain only the cell aggregates/spheres. Cells were centrifuged at 800 X g for three minutes to remove the media, and then pelleted cells were resuspended in RPMI-1640 or SsM media for P and PCSCs, respectively.

The viability percentage for P and PCSCs was evaluated through trypan blue assay (Thermo Fisher Scientific). PCSCs and P cells with viability higher than 85% were counted (using Countess™ II Automated Cell Counter, Thermo Fisher Scientific) and $1*10^6$ cells of live cells were washed twice with 1X PBS, pelleted and stored at -80°C for further experiments.

2.4. RNA extraction and qPCR

Total RNA was extracted from $1x10^6$ cells (PaCa3, PaCa44, MiaPaCa2 and PC1J P and CSCs) using TRIzol Reagent (Life Technologies). The extracted RNA was quantified by NanoDrop™ One (Thermo Fisher Scientific) and checked for integrity loading on 1.5% agarose gel. 1 μg of RNA was reverse transcribed using first-strand cDNA synthesis. The real-time PCR reaction was performed according to the protocol of the SYBR-Green detection chemistry with GoTaq qPCR Master Mix (Promega) on a QuantStudio 3 Real-Time PCR System (Thermo Fisher Scientific).

The primers used are described by Lemma and Avnet *et al.*, 2016 and are shown in Table 1. The cycling conditions, used for the reverse transcription, were 95˚C for ten minutes, 40 cycles at 95˚C for fifteen seconds, 60˚C for one minute, 95˚C for fifteen seconds, and 60˚C for fifteen seconds. Reactions were run in triplicate in three independent experiments. The average of cycle threshold, of each triplicate, was analysed according to the $2^{-\Delta\Delta Ct}$ method. *p*-values <0,05 are considered as significantly different. The range of individual double delta Ct values for the mRNA as compared to the house keeping gene was from 0.01 to 0.04.

Table 1. Primers used for qPCR analysis.

Primer name	Forward primer	Reverse primer
Cyclin B1	5'-CATGGTGCACTTTCCTCCTT-3'	5'-AGGTAATGTTGTAGAGTTGGTGTCC-3'
Frizzled 2	5'-TCCTCAAGGTGCCATCCTATCTC -3'	5′-TGGTGACAGTGAAGAAGGTGGAAG-3'
NANOG	5'-AGTCCCAAAGGCAAACAACCCACTTC-3'	5'-TGCTGGAGGCTGAGGTATTTCTGTCTC-3'
OCT3/4	5'-GACAGGGGGAGGGGAGGAGCTAGG-3'	5'-CTTCCCTCCAACCAGTTGCCCCAAAC-3'
SOX2	5'-GGGAAATGGGAGGGGTGCAAAAGAGG-3'	5'-TTGCGTGAGTGTGGATGGGATTGGTG-3'
Succinate dehydrogenase (housekeeping gene)	5'-GGACCTGGTTGTCTTTGGTC-3'	5'-CCAGCGTTTGGTTTAATTGG-3'

2.5. Protein extraction

Protein extraction from PaCa3, PaCa44, MiaPaCa2 and PC1J P and PCSCs lines was performed as previously reported [148]. Cells were collected (three biological replicates for each P and PCSC lines), washed and lysed in 1× protease inhibitor cocktail (Roche) and 1% SDS. Protein extraction was performed by three cycles of sonication with an amplitude of 35% for 10 seconds, incubation at −80 °C for 30 minutes, and then sonication again three times for 10 seconds. Samples were then centrifuged at 14000 X g for ten minutes at 4°C to remove debris. The supernatant was collected, and the proteins were precipitated with ice cold acetone to further

clean up the protein solution. Proteins were quantified by bicinchoninic acid (BCA) protein assay (Sigma-Aldrich), using bovine serum albumin (BSA) as a protein standard.

2.6. Immunoblotting analysis

Protein extracts were diluted 1:1 with Laemmli sample buffer (62.5 mM Tris-HCl at pH 68, 25% glycerol, 2% SDS, 0.01% Bromophenol Blue). The protein solution was heated for five minutes at 90 °C using a thermoblock followed by separation on the SDS/polyacrylamide gel electrophoresis (PAGE) using 4-20% T acrylamide gels in Tris-HCl, glycine, and SDS buffer. Proteins were then electroblotted onto polyvinylidene fluoride (PVDF) membranes (Roche) at 80 V for 1.3h at 4°C.

Amido black staining was used to confirm equal protein loading in different lanes. Non-specific binding sites were blocked by incubating the PVDF membranes with 5% w/v BSA in 0.1% Tween-20 in Tris-buffered saline at 37°C for one hour. PVDF membranes were incubated overnight at 4^{o}C with dilutions of primary antibodies specified in Table 2, using 5% w/v BSA, 0.1% Tween-20 and Tris-buffered saline, and then 1h at room temperature with the corresponding horseradish peroxidase (HRP)-conjugated secondary antibody (Tab. 3). The protein-immunocomplexes were visualized by chemiluminescence using the ChemiDoc MP Imaging System (Bio-Rad). The assay was conducted as three independent experiments with triplicate samples.

Table 2. Primary antibodies used for Western Blot analysis

Gene name	Antibody	Source	Supplier	Dilution
Sox2	SRY-Box Transcription Factor 2	Rabbit	Cell signalling technology (#3579)	1:600
Nanog	Nanog Homeobox	Mouse	Cell signalling technology (#4903)	1:200
Oct4	Octamer-Binding Transcription Factor 3	Mouse	Cell signalling technology (#2750); Santa Cruz Biotechnology (sc-5279); GeneTex (GT486);	1:100

Table 3. Secondary antibodies used for Western Blot analysis

Antibody	Supplier	Dilution
Mouse anti-rabbit IgG-HRP	Santa Cruz Biotechnology (sc-2004)	1:1500
Goat anti-mouse IgG-HRP	Santa Cruz Biotechnology (sc-2005)	1:1000

3. Results

3.1. Morphological characteristics of pancreatic cancer stem cells

Different growth patterns between P and PCSC lines were clearly distinguishable through shape and size observation (see Fig. 1). PaCa3, PaCa44, MiaPaCa2 and PC1J P lines grew as adherent cells in monolayers, showing an epithelial morphology with clear intact cell-to-cell contacts (Fig. 1a to 1d). PCSCs were observed as spheroids (Fig. 1e to 1h).

Figures 1e and 1f showed similar PCSC morphology in PaCa3 and PaCa44, displaying compacted spheroids, where cell boundaries were indistinguishable. MiaPaCa2 CSCs was observed as spheroids (Fig. 1g) with a defined cell wall. However, MiaPaCa2 tumour spheres appeared less compact and smaller than PC1J (Fig. 1h). PC1J CSCs also have a sphere morphology, with a distinguishable cellular membrane, which showed a greater aggregated structure than MiaPaCa2 CSCs.

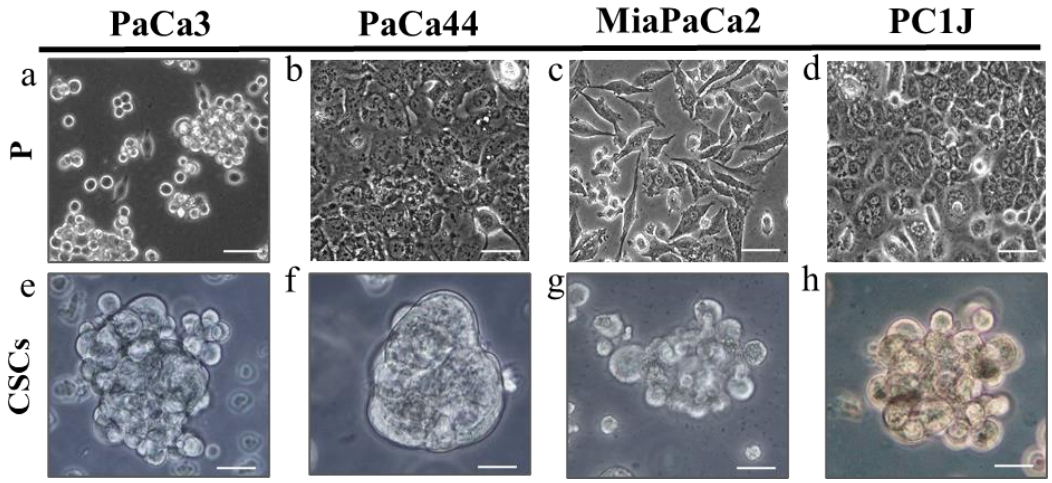

Figure 1. Bright-field microscopy of parental and PCSC lines (20x magnification) obtained after two weeks of culture. a. PaCa3 P cells; b. PaCa44 P cells; c. MiaPaCa2 P cells; d. PC1J P cells; e. PaCa3 CSCs; f. PaCa44 CSCs; g. MiaPaCa2 CSCs; h. PC1J CSCs. Scale bar = 50 and 25 μm for P cells and PCSCs, respectively. Scale bar 50 μm.

3.2. Analysis of stemness and quiescence-related markers

qPCR analyses were performed to detect the genes related to stemness (*i.e.*, *OCT3/4*, *SOX2* and *NANOG*), cell cycle (*CYCLIN B1*), and Wnt signalling pathway (*FRIZZLED 2*, here reported as *FZD2*). qPCR analyses of the four PDAC lines were plotted as a bar graph for easier interpretation. Figure 2 shows mRNA expression level of stemness-related genes in the four PDAC lines.

A general increase of *OCT3/4*, *SOX2*, and *NANOG* mRNA expression levels in PaCa3, PaCa44, and MiaPaCa2 CSCs compared to each respective P line were detected. *OCT3/4* was statistically significantly increased in PaCa3, PaCa44 and MiaPaCa2 CSCs compared to P cells, whilst *SOX2* was statistically significantly induced in PaCa44 and MiaPaCa2 CSCs and *NANOG* resulted statistically significantly enhanced in PaCa3 and MiaPaCa2 CSCs. However, no statistically significant changes were observed in PC1J line, whose stemness has been further investigated by immunoblotting analyses.

In addition to *OCT3/4*, *SOX2* and *NANOG* mRNA expression, *CYCLIN B1* and *FDZ2* mRNA levels were also measured. The qPCR results for PaCa3, PaCa44, MiaPaCa2, and PC1J cell lines are shown in Figure 3. qPCR analysis shows a statistically significant decrease of *CYCLIN B1* mRNA levels in all four PCSCs compared to P cells. On the contrary, a statistically significant increase of *FDZ2* mRNA expression levels was observed in PaCa3, PaCa44 and MiaPaCa2CSCs, while a trend of increment was detected in PC1J CSCs (Fig. 3).

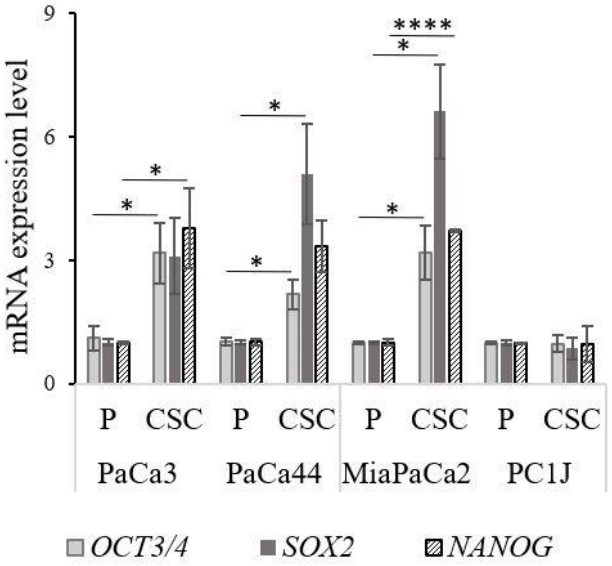

Figure 2. q-PCR analysis of OCT3/4, SOX2 and NANOG genes. Results are reported as means (± SE) of three independent biological replicates; p <0,05 (*) and p <0,0001 (****).

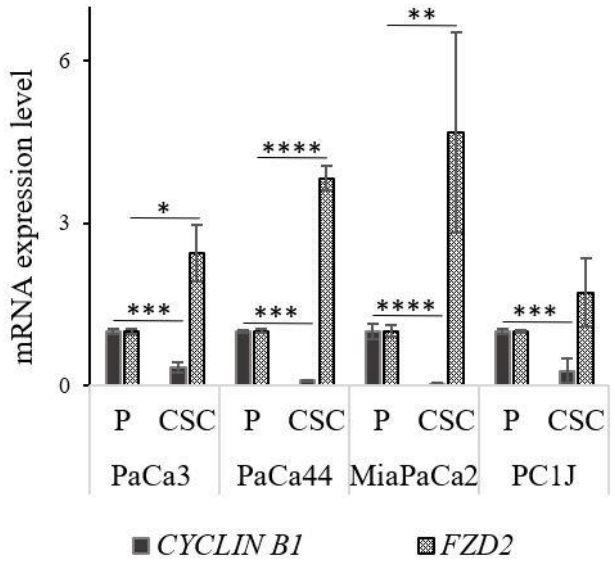

Figure 3. mRNA expression of CYCLIN B1 and FDZ2. Results are reported as means (± SE) of three independent biological replicates; p <0,05 (*), p <0,001 (***) and p <0,0001 (****).

Western Blot analysis was carried out to observe any changes at protein levels encoded by the genes related to stemness: see Figure 4. Hence, analyses of the proteins Sox2, Nanog and Oct3/4 were performed in all the four PCSCs and P cell lines.

The data obtained indicated that Oct3/4 was not detectable in either PCSCs or P lines (data not shown); Nanog and Sox2 were upregulated in PaCa3, PaCa44 and PC1J CSCs, while non-observable levels were detected in MiaPaCa2 line (Fig. 4). The results on protein immunoblotting in MiaPaCa2 line suggested that these cells have low levels of protein expression under the experimental conditions (*i.e.*, different type of membranes, PVDF or nitrocellulose, different primary antibody concentration and exposition time).

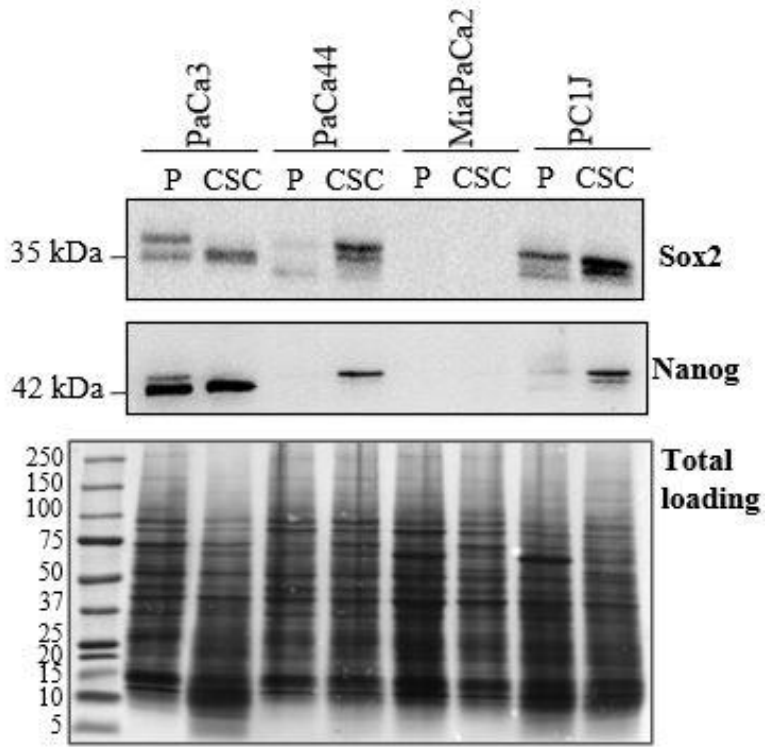

Figure 4. Western blot analysis of Sox2 and Nanog protein expression in PaCa3, PaCa44, MiaPaCa2 and PC1J P and CSCs, respectively. Proteins were resolved on 4-20% SDS-PAGE gels, transferred onto PVDF membranes, and probed with specific antibodies against the indicated targets.

4. Discussion

Pancreatic cancer stem cells (PCSCs) are characterized by sphere-forming capacity [6] and stemness properties. Accordingly, the data obtained during this phase of the PhD project indicate that PaCa3, PaCa44, MiaPaCa2 and PC1J CSCs in SsM medium grow as floating cell aggregates, called tumour sphere or spheroids, which may correlate with an acquired mesenchymal morphology of cells [143]. Mesenchymal morphology may be associated with an improved capability of PCSCs to promote *in vitro* expansion compared to their parental cells [119]. It was interesting to observe different compacted spheroids for the four PDAC lines. The different sphere-forming activity of PCSC lines may be related to a distinct resistance of PDAC lines [149, 150].

The increased observed levels of *OCT3/4*, *SOX2* and *NANOG* in PaCa3, PaCa44 and MiaPaCa2 CSCs (Fig. 2) agreed with previous published results [151, 152]. Increased *SOX2* mRNA level correlates with cell proliferation, dedifferentiation and impartment of stem cell-like features of pancreatic cancer cells [81]. Interestingly, *SOX2* upregulation in PCSCs may be related to the promotion of tumour sphere formation *in vitro* as well as to the induction of other stem-markers [81]. Moreover, the observed enhanced protein expression of Oct3/4 and Nanog in PCSCs compared to P cells, confirms that PC1J also has stemness characteristics. These transcription factors have a role in the maintenance of self-renewal and in the pluripotency state of these cells [82, 153]. Indeed, PCSC proliferation, migration, invasion, chemoresistance and tumorigenesis could be increased by the upregulation of Oct3/4 and Nanog proteins [153-155]. It was reported that Nanog, in combination with Oct3/4 and Sox2, can efficiently induce the reprogramming of pluripotent stem cells (iPSCs) and CSCs generation [82]. It is believed that Nanog controls cell proliferation and motility, malignancy conversion, immune evasion and drug resistance and could mediate the communication between cancer cells and the surrounding stroma [82].

The mRNA expression levels of *CYCLIN B1* were also analysed (Fig. 3). This gene encodes for a protein that plays a role in the transition from the G2 to M phase of the mitotic process. Consequently, the observed reduced expression of *CYCLIN*

B1 in the four PCSCs might suggest a G2/M phase arrest [156]. Accordingly, PCSCs proliferate more slowly than differentiated cells, showing a less cycling/quiescence state of the stem cells [157]. Quiescence of PCSCs may represent one of the mechanism able to explain chemotherapy resistance and recurrence in post-therapy cancer patients [143]. Moreover, recent studies on Cyclin B1 showed its involvement in the coordination of mitochondrial energy metabolism with cell cycle and tumour aggressive phenotype [158]. During G2/M phase, mitochondria relocation of Cyclin B1 and its interactor, CDK1, is related to activation of several substrates, including p53. This activation can enhance mitochondrial function and homeostasis and energy production of PCSCs [145, 158], which is supposed to be upregulated in mut-p53 cell lines (*i.e.*, PaCa44, MiaPaCa2, and PC1J).

The quantitative PCR analysis also showed an induction of *FDZ2* in PCSCs (Fig. 3) suggesting a possible activation of Wnt signalling pathway [159]. *FDZ2* upregulation has been suggested as a new potential target for pancreatic cancer therapy [160]. Recently, it was demonstrated that Fdz2 can modulate the epithelial-mesenchymal transition, playing a role in metastasis and tumour recurrence [161]. Moreover, its overexpression might promote PCSC stemness and drug resistance [144].

5. Conclusions

PaCa3, PaCa44, MiaPaCa2 and PC1J CSCs were examined from a morphological point of view using a bright-field inverted microscope. Bright-field microscopy is very easy to use, and it can produce high quality images can be obtained by using this microscopy, which permits the analysis of the cell components of PCSCs and P cells. However, confocal microscopy could be well suited to observe PCSC tumour spheres since it permits the acquisition of optical sections to reconstruct the three-dimensional model.

To better investigate the characteristics of the four PCSC lines, the mRNA expression levels of stem and quiescence related genes were analysed and compared to relative P cells. qPCR and immunoblotting analyses resulted suitable to reveal the PCSC markers. The high efficiency and sensitivity of qPCR analysis allows the detection and the investigation of stem and quiescence related genes, even if the cells express low mRNA levels. Moreover, immunoblotting analysis permitted the detection of the modulation of encoded proteins by stem related genes.

The obtained results confirmed the qPCR data and also clarified the stemness characteristics also for PC1J CSCs. qPCR and immunoblotting analyses of stem and quiescence related markers well accomplished the aims of investigating PCSC characteristics. Therefore, these techniques can also be applied to the analysis of other CSCs. However, further analyses of genes related to epithelia to mesenchymal transition (EMT), such as Cadherin 1 (*CDH1*), Mitotic Arrest Deficient 2 Like 1 (*MAD2L1*) and/or Zinc Finger E-Box Binding Homeobox 1 (*ZEB1*) could be useful for a more complete characterization of PCSCs.

In conclusion, PCSCs generated by P cells were first evaluated confirming their stemness properties. Consequently, the investigation of proteome alterations of PCSCs was performed as described in the next chapter.

SECTION 2

Chapter 3

Proteomic analysis of pancreatic cancer stem cells and parental pancreatic ductal adenocarcinoma cell lines

1. Introduction

Despite the importance of a global molecular characterization of PCSCs to identify molecules or drugs that can affect them, the in-depth characterization of PCSCs from a multi-omics point of view is still missing. Therefore, in this PhD thesis project proteomic and lipidomic analyses were integrated to investigate the metabolic and signalling dysfunctions implicated in the pathophysiology of PCSCs.

This chapter addresses the proteomic characterization of pancreatic cancer stem cells (PCSCs) and their comparison with parent PDAC cell lines. PCSCs were obtained from PDAC cell lines having different genotypic status from commonly altered genes for this pathology (*i.e.*, *KRAS*, *p53*, *p16* and *SMAD4*).

A label-free strategy based on sequential window acquisition of all theoretical mass spectra (SWATH)-MS analysis was applied to study the proteome of PCSCs. Successively, dysregulated proteins and pathways of PCSCs were investigated through bioinformatics tools.

The results obtained are characterized by novelty, since in the past decade few data were collected concerning the proteome dysregulation of PCSCs (as discussed in Chapter 1, Section 4.2.2). Up to now, no proteomic study has been performed on different PCSC lines with a different genetic background.

2. Materials and methods

2.1. Sample preparation for proteomics

PCSCs and P cells were grown and collected as described in Chapter 2, Section 2.1, while intracellular proteins were extracted as described in Chapter 2, Section 2.5.

30 µg aliquot of protein extract was resuspended in 25 µl of 100 mM NH_4HCO_3 and subjected to protein reduction and alkylation. Reduction step was performed using 2.5 µl of 200 mM dithiothreitol (DTT) at 90°C for twenty minutes. Proteins were alkylated with 10 µl of 200 mM iodoacetamide (IAA), a cysteine blocking reagent, for one hour at room temperature in the dark. 2.5 µl of DTT were added to remove IAA excess, by incubating for one hour in the dark. Before protein digestion pH was adjusted between 7.5 and 8 by adding 300 µl of water and 100 µl of NH_4HCO_3.

Protein digestion was performed adding 1 µg/µL of sequencing grade modified trypsin (Promega) and incubating overnight at 37°C. 2 µl of formic acid were added to stop trypsin activity. Peptides were dried through MaxiDry Plus Speed-vacuum centrifuge (Heto) and stored at -80°C until LC-MS/MS analysis.

2.2. Mass spectrometry analysis and data processing

Tryptic peptides were analysed in collaboration with researchers of ISALIT (spin-off at University of Eastern Piedmont) by label-free LC-MS/MS, performed by using a micro-LC system (Eksigent Technologies, Dublin, USA) interfaced with a 5600+ TripleTOF mass spectrometer (AB SCIEX, Concord, Canada). Samples were subjected first to DDA analysis to generate the SWATH-MS spectral library, and then to cyclic DIA analysis, based on a 25-Da window, using three technical replicates of each sample. The MS data were acquired by Analyst TF v.1.7 (AB SCIEX), while PeakView v.1.2.0.3, Protein Pilot v.4.2 (AB SCIEX) and Mascot v. 2.4 (Matrix Science) programs were used to generate the peak-list. The database search was performed using the UniProt/Swissprot (v.2018.01.02, 42271 sequences entries). Samples were input to the Protein Pilot software v. 4.2 (AB SCIEX, Concord, Canada), with the following parameters: cysteine alkylation, digestion by

trypsin, no special factors and false discovery rate (FDR) at 1% were used for database search with Protein Pilot, while for Mascot search the following parameters were used: trypsin as digestion enzyme, 2 missed cleavages, search tolerance of 50 ppm for the peptide mass tolerance and 0.1 Da for the MS/MS tolerance. The charges of the peptides to search for were set to 2 +, 3 + and 4 +, and the search was set on monoisotopic mass.

The instrument was set to electrospray ionization-quadrupole-time of flight (ESI-Q-TOF) and the following modifications were specified for the search: carbamidomethyl cysteines as fixed modification and oxidized methionine as variable modification. FDR was fixed at 1%. The obtained files from the DDA acquisitions were used for the library generation using a FDR threshold of 1%. Protein quantification was performed by PeakView v.2.0 and MarkerView v.1.2. (AB SCIEX) programs by extracting from SWATH files six peptides per protein with the highest MS1 intensity, and up to six transitions per peptide (MS2). Peptides with FDR lower than 1.0% were exported, and up- and downregulated proteins were selected using *p*-value <0,05 and fold change ±1.5. The average between the three technical replicates was carried out, while statistical comparison between the tree biological replicas using the paired t-test ($p < 0.05$) was performed. No multi-testing correction was applied.

2.3. Bioinformatic analysis of proteomics data

2.3.1. STRING analysis

Search Tool for the Retrieval of Interacting Genes/Proteins (STRING) is a database and web resource of known and predicted protein–protein interactions [162]. STRING v.11.0 platform (http://string-db.org) was used to characterize the function of proteins, gene ontology (GO) annotation, Kyoto encyclopaedia of genes and genomes (KEGG) and Reactome pathways enrichment analyses. Two STRING criteria were selected: “database” which involves observation that functionally associated proteins have known interactions from curated databases and

"experiments" which indicates experimentally proven interactions from published studies.

Functional annotation was used to identify GO biological processes, molecular function, and cellular component enriched terms (p <0,01), with a threshold of minimum gene counts belonging to an annotation set to 2.

KEGG and Reactome pathway enrichment analyses were performed to analyse up- and down- regulated proteins of PCSCs separately by using as background the human genome.

2.3.2. Ingenuity pathway analysis

Ingenuity Pathway Analysis (IPA © 2000-2019 QIAGEN, Ingenuity Systems, Redwood City, CA) was used to predict activated upstream regulators that can further explain the observed expression changes in PCSCs.

The IPA program uses a knowledge database derived from the literature to relate the proteins to each other based on their interaction and function. The knowledge database consists of a high-quality expert-curated database containing 1.5 million biological findings, consisting of more than 42,000 mammalian genes and pathway interactions extracted from the literature. The IPA analysis settings were as follows: i) Reference set: Ingenuity Knowledge Base; ii) Relationship to include: Direct and Indirect; iii) Filter Summary: Consider only molecules and/or relationships where (species = Human) AND (confidence = Experimentally Observed).

The activated upstream regulators were assumed as valid effectors of gene/protein expression if the corresponding p-value obtained by Fisher's exact test was ≤0,01. Z-score algorithm was used to allow for prediction whether an upstream regulator is activated (Z ≥2) or inactivated (Z ≤−2) based on the direction of expressional change of the associated genes.

2.4. Immunoblotting analysis

Western blot analyses were performed as described in Chapter 2, Section 2.6 in two independent experiments. Membranes were incubated with the different primary antibodies at the appropriate dilutions (as reported in Tab. 1) in 1% non-fat dried milk, 0.05% Tween-20 in Tris-buffered saline.

The incubation with primary antibody lasted for 3 h at room temperature or overnight if required. Then, blots were incubated 1h at room temperature with the appropriate horseradish peroxidase (HRP)-conjugated secondary antibody (Tab. 2).

The immunocomplexes were visualized by enhanced chemiluminescence using the Chemidoc MP imaging system (Bio-Rad).

Table 1. Primary antibodies used for Western Blot analysis.

Gene Name	Antibody	Source	Supplier	Dilution
phospho-LDHA	Phospho-L-lactate dehydrogenase A chain	rabbit	Cell signaling technology (#8176)	1:1000
LDHA	L-lactate dehydrogenase A chain	mouse	Santa Cruz Biotechnology (sc-515615)	1:250
HADHA	Trifunctional enzyme subunit alpha, mitochondrial	mouse	Santa Cruz Biotechnology (sc-374497)	1:200

Table 2. Secondary antibodies used for Western Blot analysis.

Antibody	Source	Supplier	Dilution
Goat anti-mouse IgG-HRP	mouse	Santa Cruz Biotechnology (sc-2005)	1:1000
Mouse anti-rabbit IgG-HRP	rabbit	Santa Cruz Biotechnology (sc-2004)	1:2000

3. Results

3.1. Dysregulated proteins of pancreatic cancer stem cell lines

A total of 765, 885, 830 and 894 intracellular proteins were identified in PaCa3, PaCa44, MiaPaCa2 and PC1J CSCs, respectively. More specifically, 121, 212, 186 and 235 differentially expressed proteins (*p*-value ≤0,05; fold change ±1,5) were identified in PaCa3, PaCa44, MiaPaCa2 and PC1J CSC compared to relative P cells, respectively. Table 3 summarizes the trend of modulation of the up- and down-regulated proteins in the four PCSC lines.

Table 3. Up- and down-regulated proteins of PaCa3, PaCa44, MiaPaCa2 and PC1J CSCs compared to relative P cells (p-value ≤0,05; fold change ±1,5).

Cell lines	Total n° of modulated proteins	Upregulated proteins (PCSCs *vs* P cells)	Downregulated proteins (PCSCs *vs* P cells)
PaCa3 CSCs	121	68	53
PaCa44 CSCs	212	119	93
MiaPaCa2 CSCs	186	110	76
PC1J CSCs	235	80	155

Overlapping and non-overlapping differentially expressed proteins of the four PCSC lines were indicated using Draw Venn Diagram tool (http://bioinformatics.psb.ugent.be/webtools/Venn/), as shown in Figure 1.

Among the modulated proteins, six were in common between PaCa3, PaCa44, MiaPaCa2 and PC1J CSCs (Fig. 1): trifunctional enzyme subunit alpha (HADHA), voltage-dependent anion-selective channel protein 2 (VDAC2), L-lactate dehydrogenase A chain (LDHA), heterogeneous nuclear ribonucleoprotein A/B Isoform 2 (HNRNPAB), dolichyl-diphosphooligosaccharide-protein glycosyltransferase subunit 2 Isoform 2 (RPN2) and 40S ribosomal protein S7 (RPS7). The trend of modulation of the six-common proteins in the four PCSC lines

was also analysed as shown in Table 4. Both HADHA and VDAC2 were upregulated, while HNRNPAB and LDHA were downregulated in PaCa3, PaCa44, MiaPaCa2 and PC1J CSCs. On the contrary, RPN2 and RPS7 proteins showed a different trend of modulation in four PCSC lines.

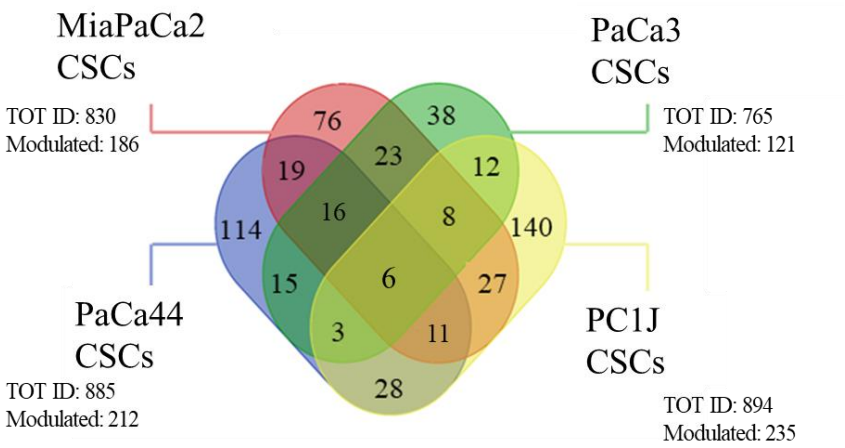

Figure 1. Venn diagram of identified intracellular proteins differentially modulated in PaCa3, PaCa44, MiaPaCa2 and PC1J CSCs compared to their relative P cells
(p-value ≤0,05; fold change ±1,5).

Table 4. Modulation of the six proteins dysregulated in all four PCSC lines. The related fold changes of the up- and/or down- regulated proteins were also reported.

	fold change (CSCs/P cells)			
Protein	**PaCa3**	**PaCa44**	**MiaPaCa2**	**PC1J**
HADHA	1,97	1,76	3,38	1,58
VDAC2	2,54	2,59	2,35	1,88
HNRNPAB	-1,76	-1,86	-1,51	-1,94
LDHA	-1,71	-1,77	-3,21	-1,76
RPN2	6,62	2,55	-4,17	2,09
RS7	1,76	-1,73	-1,61	-1,82

Proteomics data were further investigated by immunoblotting analysis. Western Blot of HADHA, phosphorylated and non-phosphorylated LDHA proteins were performed in PaCa3, PaCa44, MiaPaCa2 and PC1J CSC and P cells (Fig. 2). Sample loading was confirmed by β-actin immunodetection.

Western blot data indicated that LDHA and p-LDHA were downregulated in PaCa3, PaCa44, MiaPaCa2 and PC1J CSCs. On the other hand, HADHA was overexpressed in the four PCSC lines compared to P cells, especially in both MiaPaCa2 and PC1J CSCs.

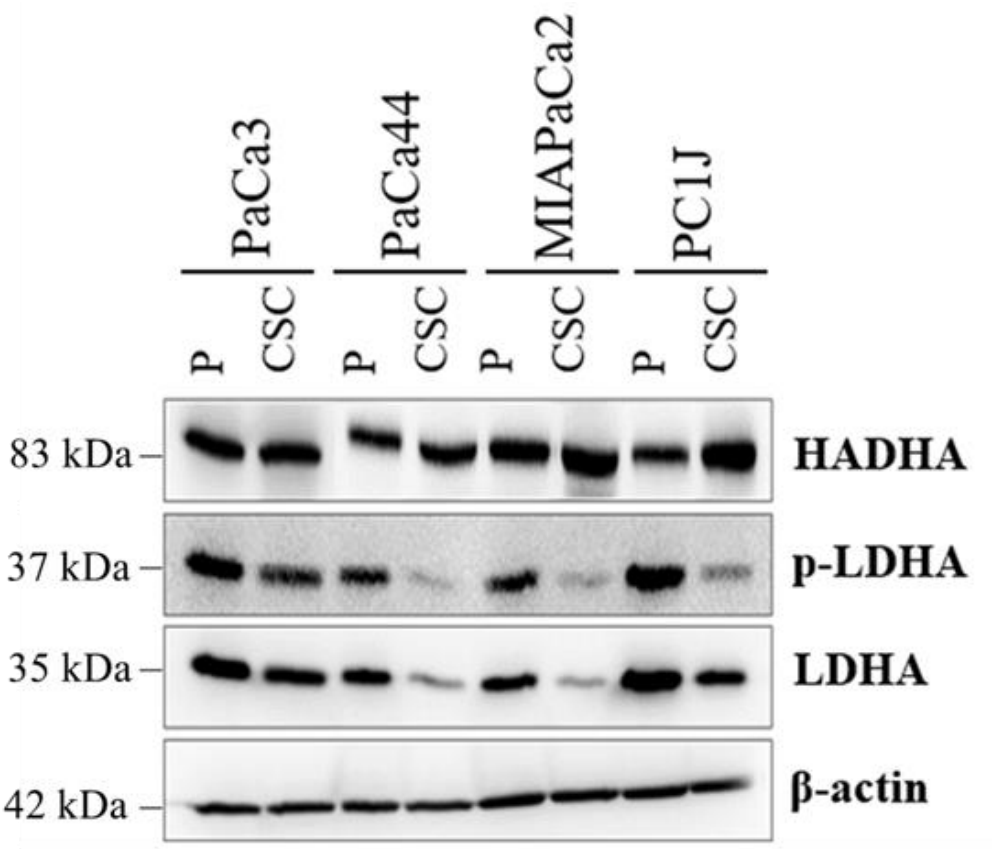

Figure 2. Western blotting analysis of HADHA, p-LDHA, and LDHA in PaCa3, PaCa44, MiaPaCa2 and PC1J P and CSCs. Proteins were resolved on 4-20% SDS-PAGE gels, transferred onto PVDF membranes, and probed with specific anti-bodies against the indicated targets. β-actin was used as a loading control.

3.2. Alteration of proteome of pancreatic cancer stem cells

3.2.1. Upregulated proteins of pancreatic cancer stem cell are mainly cytosolic and mitochondrial

Bioinformatics analysis of proteomic data permitted the annotation of dysregulated proteins and to reveal possible alterations in the signalling and metabolic pathways of the four PCSC lines. The analysis of modulated proteins was performed according to GO, using STRING database v11.0 [163] to search for enriched GO cellular component, molecular function, and biological process terms.

Figures 3 and 4 show the cellular component enrichment analysis of up- and down- regulated proteins in PaCa3, PaCa44, MiaPaCa2 and PC1J CSCs. This analysis revealed that overexpressed proteins were mainly of intracellular and cytoplasmic parts. The upregulated proteins were also of mitochondrial organelle (*i.e.*, mitochondrial part, mitochondrion, matrix, membrane and nucleoid) (Fig. 3). Additionally, in both PaCa3 and PaCa44 CSCs it was possible to identify upregulated proteins of vesicles and endocytic vesicle lumen.

On the other hand, downregulated proteins in PaCa3, PaCa44, MiaPaCa2, and PC1J CSCs also belonged to the cytosolic and intracellular part (Fig. 4). Moreover, some down modulated proteins were of complexes (*i.e.*, protein-containing and ribonucleoprotein complexes), in both MiaPaCa2 and PC1J CSCs, of melanosome and secretory granule lumen in PaCa3 CSCs, mitochondrial part in PaCa44 CSCs and nuclear part in PC1J CSCs.

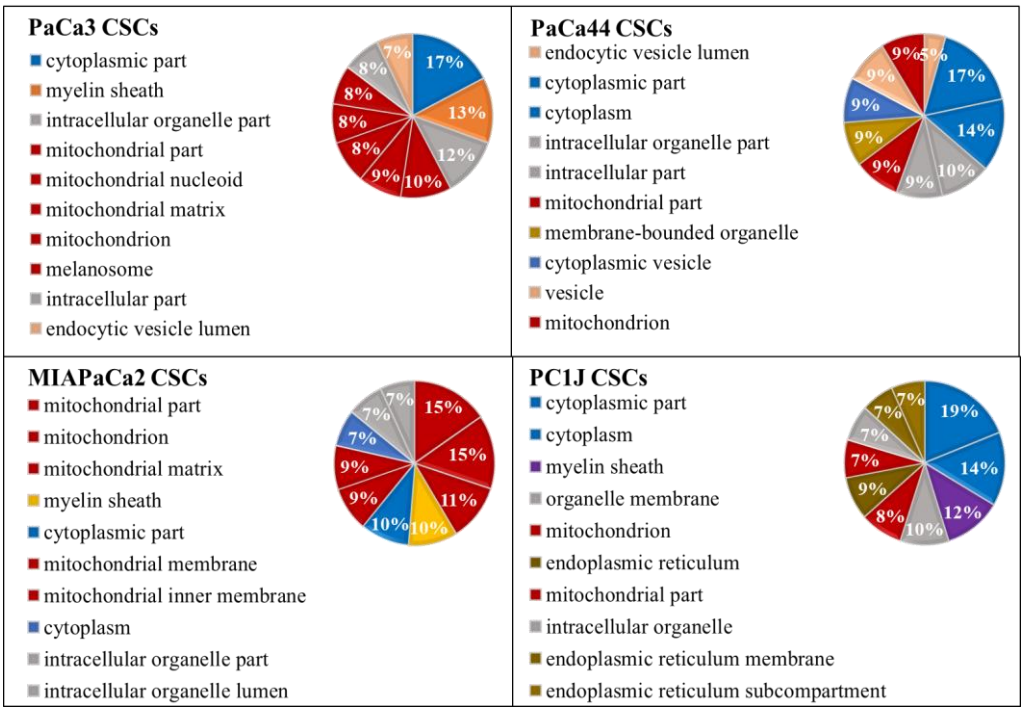

Figure 3. Top 10 GO terms in the cellular component category related to upregulated proteins of PaCa3, PaCa44, MiaPaCa2 and PC1J CSCs (p-value ≤0,05; fold change ≥1,5).

The area of each sector is proportional to the number of observed gene count.

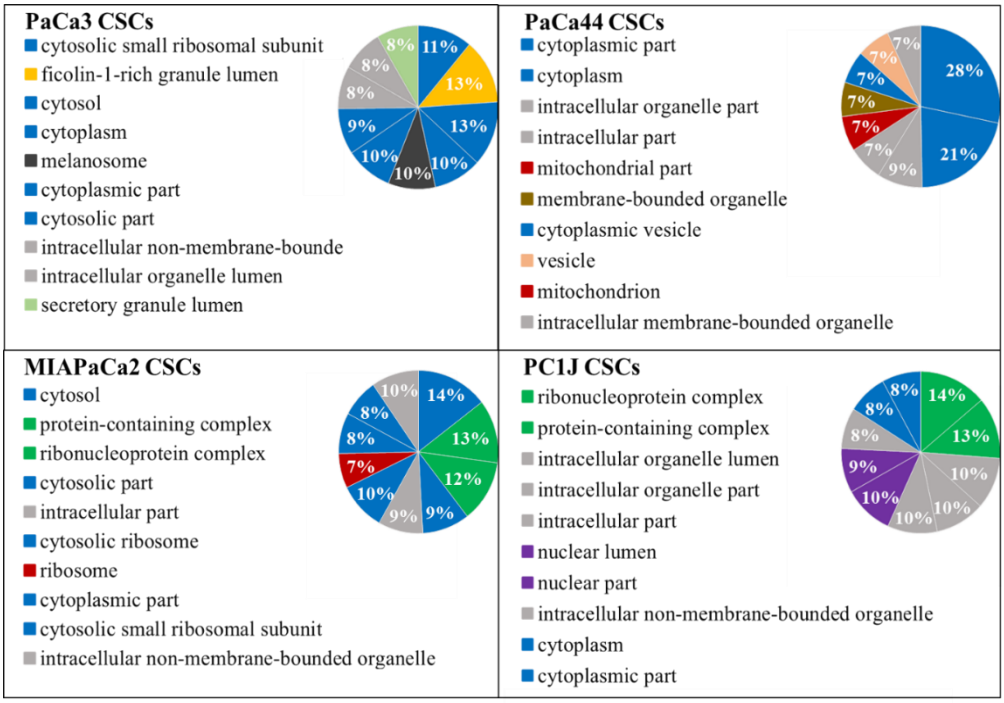

Figure 4. Top 10 GO terms in the cellular component category related to downregulated proteins of PaCa3, PaCa44, MiaPaCa2 and PC1J CSCs (p-value ≤0,05; fold change ≤-1,5).

The area of each sector is proportional to the number of observed gene count.

According to the molecular function category, Table 5 reports the top 10 most significant enriched GO terms of up- or down- modulated proteins in PaCa3, PaCa44, MiaPaCa2 and PC1J CSCs compared to relative P cells. This analysis suggested that the dysregulated proteins in PCSCs were implicated in binding activity. Moreover, in PaCa3, PaCa44, MiaPaCa2 and PC1J CSCs a dysregulation of proteins involved in different activities, such as the oxidoreductase, catalytic and antioxidant proton transporting processes, was identified.

Table 5. Top 10 GO terms in the molecular function category related to up- and down-regulated regulated proteins of PCSC lines (p-value ≤0,05; fold change ±1,5).

	Enriched molecular function for upregulated proteins	*p*-value	Enriched molecular function for downregulated proteins	*p*-value
PaCa3 CSCs	RNA binding	3,60E-04	structural constituent of ribosome	9,15E-08
	oxidoreductase activity	3,60E-04	mRNA binding	1,14E-05
	3-hydroxyacyl-CoA dehydrogenase activity	1,10E-03	RNA binding	3,18E-05
	structural constituent of epidermis	2,50E-03	structural molecule activity	1,30E-04
	translation elongation factor activity	2,80E-03	identical protein binding	5,60E-04
	unfolded protein binding	2,80E-03	unfolded protein binding	6,50E-04
	oxidoreductase activity	3,60E-03	fructose-bisphosphate aldolase activity	3,00E-03
	ATP:ADP antiporter activity	5,60E-03	kinase binding	3,00E-03
	adenine transmembrane transporter activity	5,60E-03	protein homodimerization activity	3,00E-03
	antioxidant activity	5,60E-03	protein binding	4,30E-03
PaCa44 CSCs	oxidoreductase activity	1,85E-16	structural constituent of ribosome	4,06E-48
	catalytic activity	1,23E-12	structural molecule activity	4,27E-37
	antioxidant activity	7,84E-06	RNA binding	1,09E-30
	proton transmembrane transporter activity	1,20E-04	nucleic acid binding	8,95E-15
	coenzyme binding	1,20E-04	rRNA binding	1,29E-12
	oxidoreductase activity	1,60E-04	translation regulator activity	6,71E-11
	NAD binding	1,60E-04	mRNA binding	6,18E-10
	proton-transporting ATP synthase activity, rotational mechanism	1,70E-04	translation factor activity, RNA binding	6,48E-10
	aldehyde dehydrogenase (NAD) activity	2,30E-04	organic cyclic compound binding	6,83E-10
	electron transfer activity	2,30E-04	heterocyclic compound binding	1,42E-09
MiaPaCa2 CSCs	oxidoreductase activity	1,92E-11	structural constituent of ribosome	3,16E-13
	catalytic activity	5,38E-10	structural molecule activity	1,24E-11
	cofactor binding	8,09E-10	RNA binding	6,06E-11
	small molecule binding	8,69E-08	rRNA binding	1,47E-05
	proton-transporting ATP synthase activity, rotational mechanism	8,69E-08	binding	1,50E-05
	coenzyme binding	8,69E-08	unfolded protein binding	1,50E-05
	anion binding	2,15E-07	heterocyclic compound binding	1,50E-05
	unfolded protein binding	1,05E-06	organic cyclic compound binding	1,80E-05
	proton transmembrane transporter activity	2,55E-06	S100 protein binding	2,01E-05
	acetyl-CoA C-acyltransferase activity	8,79E-06	protein-containing complex binding	2,01E-05
PC1J CSCs	small molecule binding	4,42E-06	RNA binding	1,01E-13
	cofactor binding	1,68E-05	structural constituent of ribosome	4,75E-11
	lyase activity	1,00E-04	mRNA binding	2,33E-09
	catalytic activity	1,20E-04	nucleic acid binding	1,47E-07
	oxidoreductase activity	1,20E-04	heterocyclic compound binding	1,90E-07
	anion binding	1,20E-04	organic cyclic compound binding	3,17E-07
	nucleotide binding	3,70E-04	structural molecule activity	4,91E-07
	ADP binding	6,80E-04	protein binding	1,33E-06
	coenzyme binding	7,40E-04	binding	2,05E-05
	oxidoreductase activity	8,50E-04	chromatin DNA binding	4,59E-05

3.2.2. Dysregulated proteins of pancreatic cancer stem cells are particularly involved in metabolic pathways and lipid metabolism

Finally, Figures 5 and 6 show the GO enrichment analysis concerning the biological process category, in which up- and down-regulated proteins of PCSCs are involved, respectively. The results revealed that most of the enriched terms which comprised upregulated proteins were transport and metabolic processes (*i.e.*, RNA catabolic, nucleobase-containing compound catabolic, mRNA metabolic and nuclear-transcribed mRNA catabolic processes) (Fig. 5). In particular, the overexpressed proteins of PaCa3, PaCa44 and MiaPaCa2 CSCs were involved in the generation of both precursor metabolites and energy. The upregulated proteins of PaCa3 and PaCa44 CSCs were also involved in endocytosis, while those of MiaPaCa2 and PC1J CSCs in mitochondrion organization and localization.

On the other hand, the enrichment analysis of downregulated proteins of PCSCs suggested that they were implicated in translational processes, SRP-dependent co-translational protein targeting the membrane, localization, catabolic and metabolic process (Fig. 6).

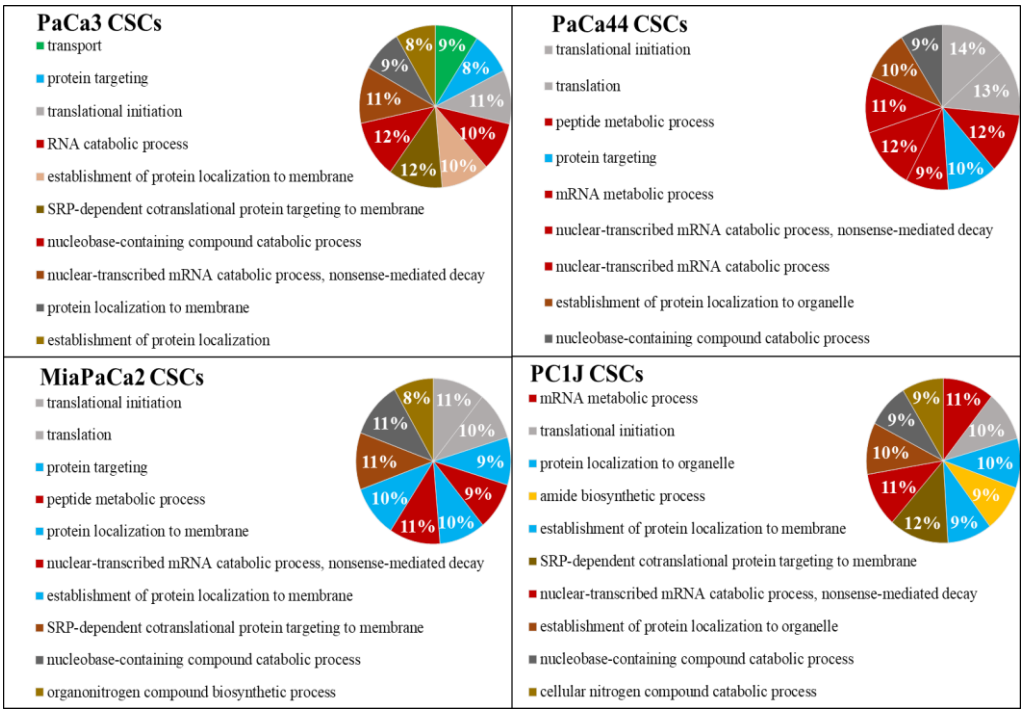

Figure 5. Top 10 GO terms in the biological process category related to upregulated proteins of PaCa3, PaCa44, MiaPaCa2 and PC1J CSCs (p-value ≤0,05; fold change ≥1,5).

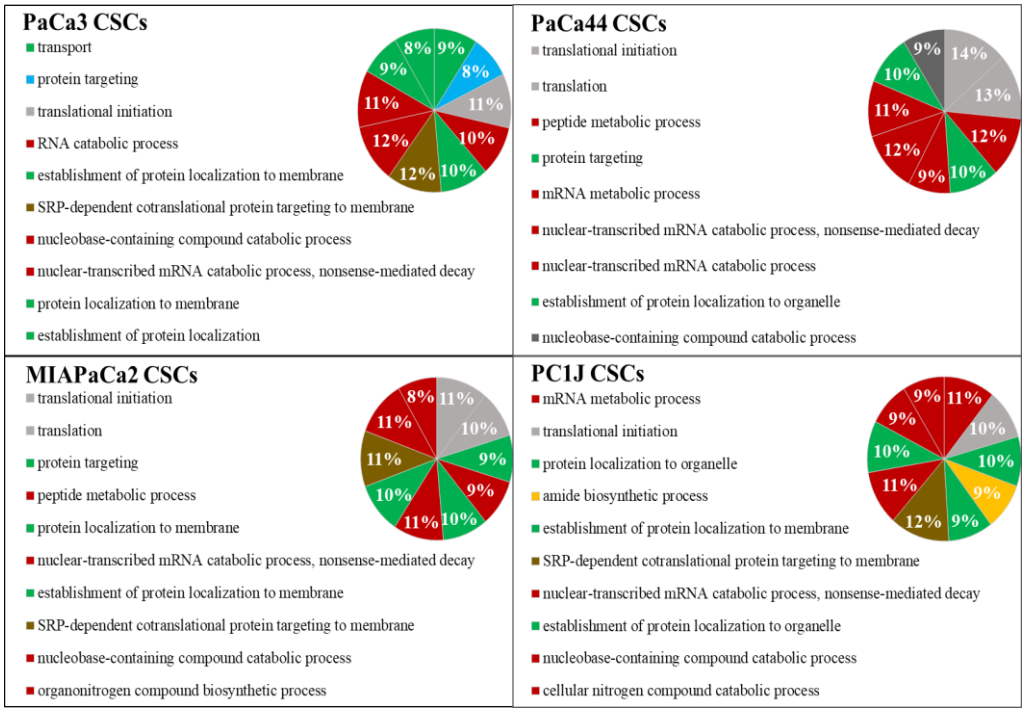

Figure 6. Top 10 GO terms in the biological process category related to downregulated proteins of PaCa3, PaCa44, MiaPaCa2 and PC1J CSCs (p-value ≤0,05; fold change ≤-1,5).

The dysregulated proteins of PCSCs were further analysed for assignment to both KEGG (Fig. 7) and Reactome (Fig. 8) databases. Looking at the top 10 KEGG and Reactome enriched pathways, it was possible to observe that the upregulated proteins of PaCa3, PaCa44, MiaPaCa2 and PC1J CSCs were involved in metabolic, amino acids (aa) and lipid pathways. Among the identified metabolic pathways, the upregulation of "oxidative phosphorylation" (OXPHOS) was detected in PaCa3, PaCa44 and MiaPaCa2 CSCs. In addition, "carbon metabolism" was detected in PaCa44, MiaPaCa2 and PC1J CSCs, while "TCA cycle" was in both PaCa44 and MiaPaCa2 CSCs (Fig. 6). Among aa pathways "phenylalanine metabolism" was upregulated in PaCa44, "alanine, aspartate glutamate metabolism" in PC1J, "valine (Val), leucine (Leu), and isoleucine (Ile) degradation" in MiaPaCa2, and in PaCa3 (with a *p*-value of 4,70E-03) and PaCa44 (with a *p*-value of 1,87E-02) over the top 10 KEGG pathway (data not shown).

Upregulated proteins were also implicated in “mitochondrial calcium ion transport” in PaCa3 and PaCa44 CSCs, and in “cellular responses to stress” in PaCa44 and MiaPaCa2 CSCs (Fig. 6). Specific enriched pathways were detected for each PCSC line: “necroptosis” for PaCa3 CSCs; “detoxification of reactive oxygen species” for PaCa44 CSCs; “transport pathways and proximal tubule bicarbonate reclamation pathway” for PC1J CSCs.

Focusing on the significantly enriched KEGG pathways (p <0,05) of the upregulated proteins in PCSCs that were related to lipid metabolism (Fig. 9), it was possible to detect: “FA elongation” in PaCa3, PaCa44, MiaPaCa2 and PC1J CSCs; “biosynthesis of unsaturated FAs”, “FA degradation and metabolism” in PaCa3, PaCa44 and MiaPaCa2 CSCs; and “cholesterol metabolism” as an enriched pathway in PaCa3, PaCa44 and PC1J CSCs. “Butanoate and propanoate metabolism” were enriched in PaCa3 and MiaPaCa2 CSCs, “non-alcoholic FAs” in PaCa3 and PaCa44 CSCs and “thyroid hormone synthesis” in MiaPaCa2 and PC1J CSCs. The KEGG pathways analysis also revealed “steroid hormone biosynthesis” in PaCa3 CSCs and “terpenoid backbone biosynthesis” in MiaPaCa2 CSCs. Additionally, the Reactome pathway analysis of upregulated PCSC proteins indicates “acyl chain remodelling of cardiolipin” (CL) as an enriched pathway in both MiaPaCa2 and PC1J CSCs (with a p-value of 0,0051 and 0,0062, respectively). Notably, “remodelling of cardiolipin (CL)” is not reported in Fig. 8 which for simplicity showed only the TOP 10 enriched pathways for each PCSC line.

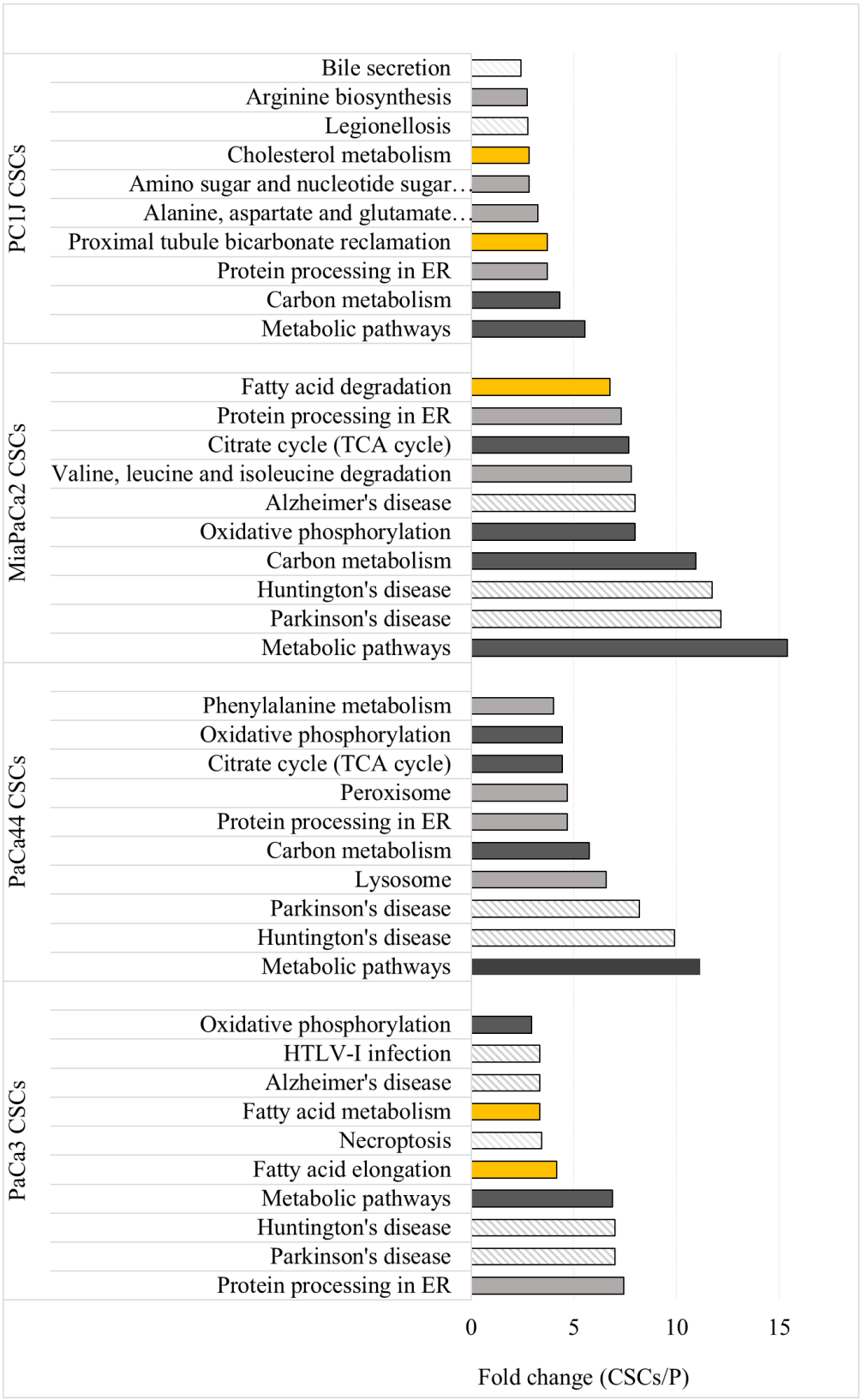

Figure 7. Top 10 enriched KEGG pathways related to upregulated proteins of PCSCs compared to P cells (p-value ≤0,05; fold change ≥1,5).

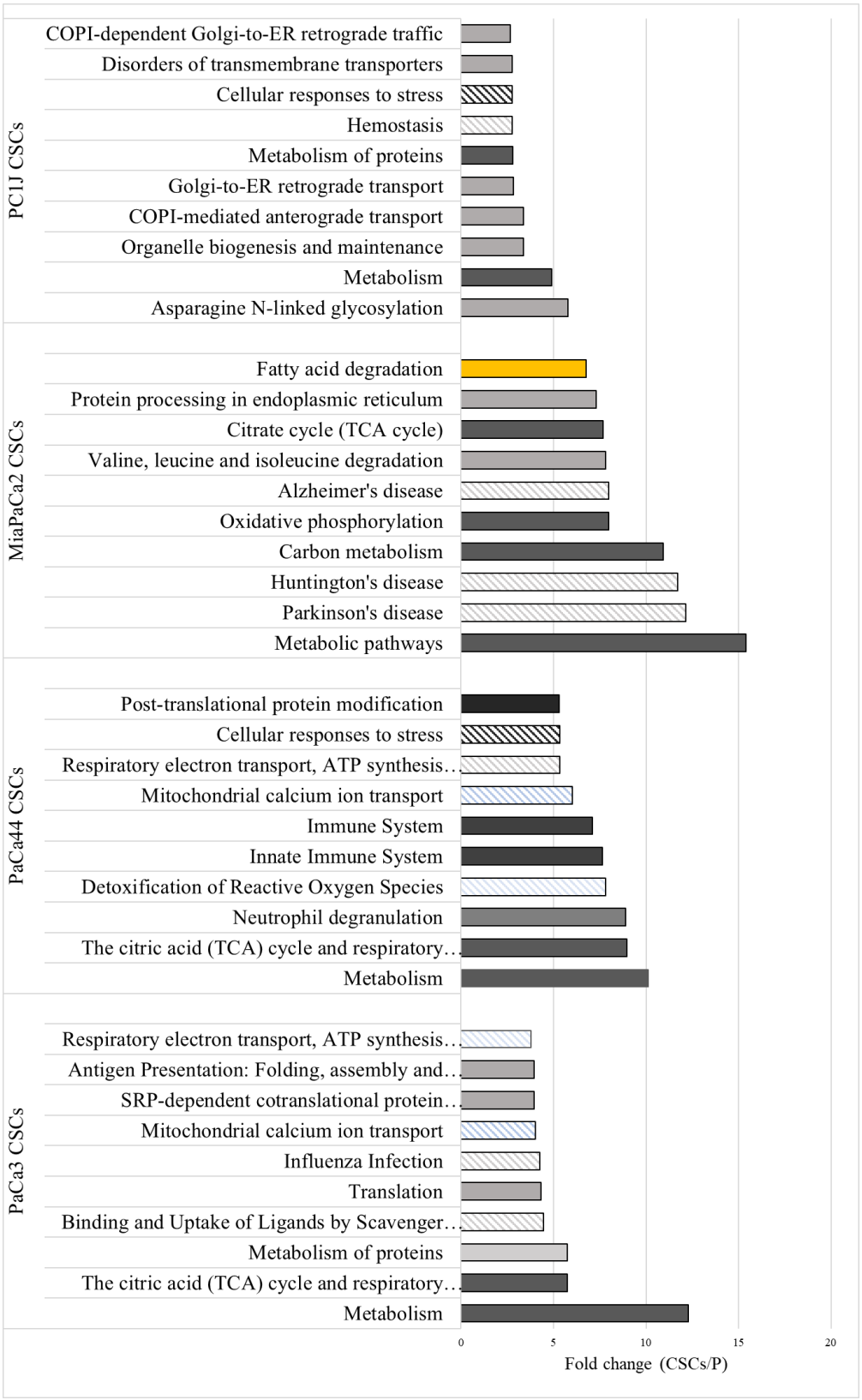

Figure 8. Top 10 enriched Reactome pathways related to upregulated proteins of PCSCs compared to P cells (p-value ≤0,05; fold change ≥1,5).

Figure 9 also shows the involvement of HADHA in the significantly enriched lipid pathways (*i.e.*, "biosynthesis of unsaturated FA", "butanoate metabolism" and "FA degradation, elongation, and metabolism") of PaCa3, PaCa44, MiaPaCa2 and PC1J CSCs.

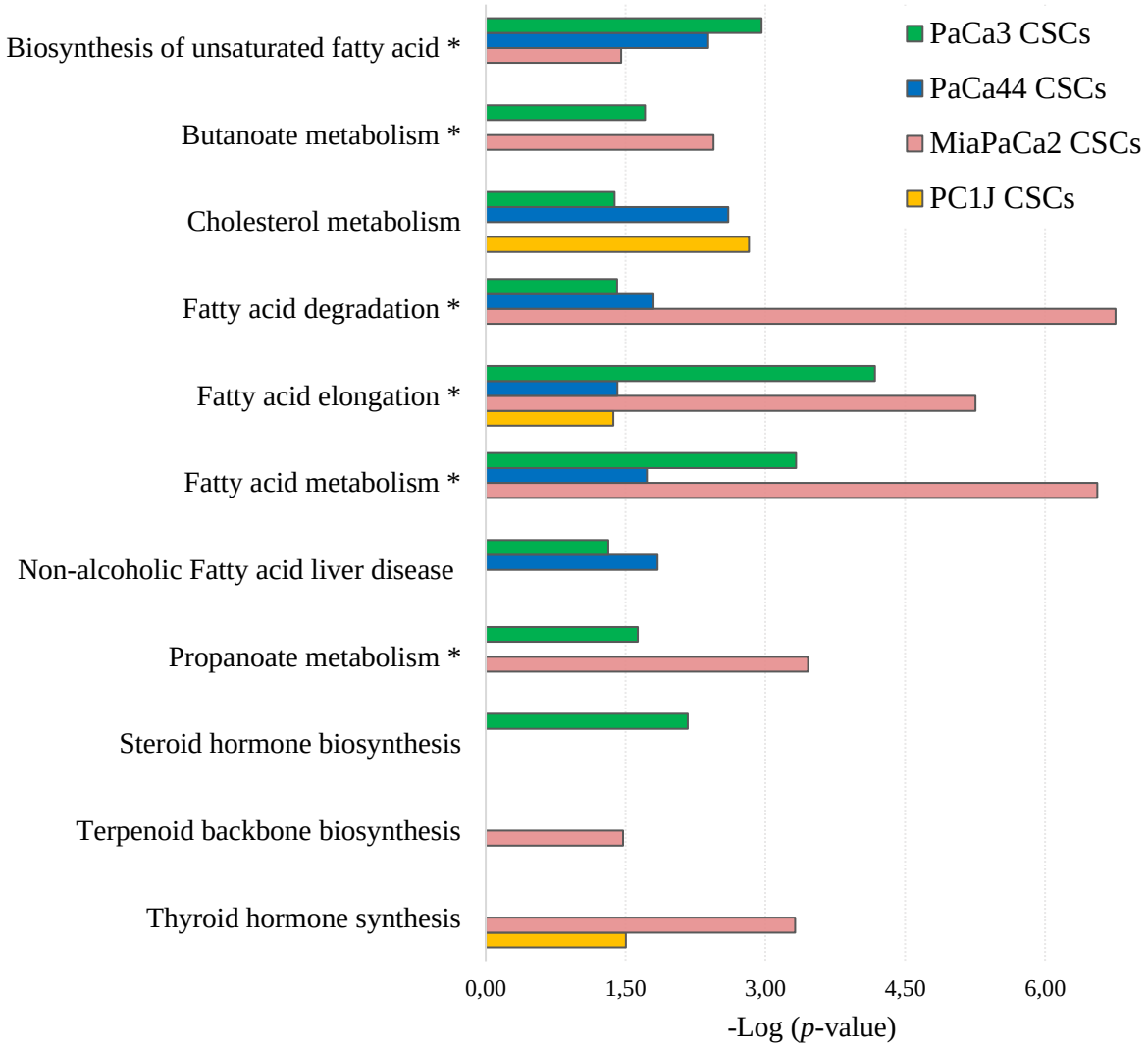

Figure 9. The significantly enriched KEGG pathways (p <0,05) of the upregulated proteins in PaCa3, PaCa44, MiaPaCa2 and PC1J CSCs that are related to lipid metabolism. The asterisk indicates the pathways in which HADHA is involved.

3.2.3. Predicted activation of upstream regulators of pancreatic cancer stem cells

Table 6 shows the IPA Upstream Regulator analysis which predicted a putative cascade of upstream regulators of PCSCs. The upstream regulators were assumed as valid effectors of gene/protein expression if the corresponding *p*-value obtained by Fisher's exact test was ≤0,01. Activation Z-score algorithm was used to allow for the prediction of whether an upstream regulator is activated (Z-score ≥2) based on the direction of the expressional change of the associated genes. The upstream regulators can be represented by molecule from transcription factors to microRNAs, kinases, compounds or drugs.

Among the activated upstream regulator, insulin receptor (INSR) was in common between PaCa3, PaCa44, MiaPaCa2 and PC1J CSCs. The results also predicted the activation of X-box binding protein 1 (XBP1) in PaCa3, PaCa44 and MiaPaCa2 CSC, while the activation of insulin-like growth factor 1 (IGF1R) was detected in PaCa44 and MiaPaCa2 CSCs. The most interesting line-specific activated upstream regulators were: vascular endothelial growth factor receptor 1 (FLT1) for PaCa3 CSCs; PGC-1α (PPARGC1A) and -1β (PPARGC1B), TP53 and phosphatidylinositol 3-kinases (PI3K) for MiaPaCa2 CSCs; Rapamycin-insensitive companion of mTOR (RICTOR) for PC1J CSCs.

Table 6. Activated upstream regulators related to dysregulated proteins of the four PCSC lines. Molecule type, Z-score and p-value are reported for each pathway.

	Activated upstream regulator	Molecule type	Z-score	*p*-value
PaCa3	FLT1 (Vascular endothelial growth factor receptor 1)	kinase	2,24	1,00E-04
	INSR (Insulin receptor)	kinase	2,80	0,00E+00
	lactacystin	chemical	2,00	4,10E-03
	mir-122	microRNA	2,00	1,40E-03
	NFKBIA (NFKB inhibitor alpha)	transcription regulator	2,12	2,60E-03
	thapsigargin	chemical toxicant	2,14	2,70E-03
	XBP1 (X-box binding protein 1)	transcription regulator	2,26	1,00E-04
PaCa44	sirolimus	chemical drug	3,96	4,50E-62
	5-fluorouracil	chemical drug	2,78	1,62E-57
	metribolone	chemical reagent	2,65	1,42E-21
	tretinoin	chemical	2,91	3,38E-19
	INSR (Insulin receptor)	kinase	4,90	6,81E-19
	IGF1R (insulin-like growth factor 1)	transmembrane receptor	2,89	1,30E-14
	mono-(2-ethylhexyl) phthalate	chemical toxicant	2,79	1,84E-14
	arsenic trioxide	chemical drug	2,71	3,99E-13
	XBP1 (X-box binding protein 1)	transcription regulator	4,41	4,2E-13
MiaPaCa2	APP (Amyloid precursor protein)	other	2,00	1,48E-17
	ATF4 (Activating Transcription Factor 4)	transcription regulator	2,59	7,12E-06
	butyric acid	chemical	3,53	2,29E-07
	COMMD1 (Copper Metabolism Domain 1)	transporter	2,24	1,90E-06
	Esrra (Estrogen-related receptor alpha)	transcription regulator	2,72	6,74E-12
	HBA1/HBA2 (Haemoglobin subunit alpha)	transporter	2,45	1,83E-06
	IGF1R (insulin-like growth factor 1)	transmembrane receptor	2,53	7,25E-08
	INSR (Insulin receptor)	kinase	4,84	2,95E-22
	KLF15 (Krüppel-like factor 15)	transcription regulator	2,21	3,42E-05
	NFKBIA (NFKB inhibitor alpha)	transcription regulator	2,35	1,31E-02
	NRF1 (nuclear respiratory factor 1)	transcription regulator	2,21	9,29E-05
	PI3K (family) (phosphatidylinositol 3-kinases,)	group	2,18	2,66E-03
	PPARA (PPAR-alpha)	ligand-dependent nuclear receptor	2,28	6,74E-08
	PPARD (PPAR-delta)	ligand-dependent nuclear receptor	2,21	1,03E-02
	PPARGC1A (PGC-1α)	transcription regulator	3,27	2,62E-08
	PPARGC1B (PGC-1beta)	transcription regulator	2,38	4,53E-07
	TP53 (p53)	transcription regulator	2,83	9,40E-14
	tretinoin	chemical	2,20	7,82E-06
	VEGFA (Vascular endothelial growth factor A)	growth factor	2,53	4,38E-05
	XBP1 (X-box binding protein 1)	transcription regulator	2,50	2,45E-07
PC1J	INSR (Insulin receptor)	kinase	2,80	0,00E+00
	NUPR1 (Nuclear Protein 1)	transcription regulator	2,12	1,76E-01
	RICTOR (Rapamycin-insensitive companion of mTOR)	other	3,13	0,00E+00

4. Discussion

One of the goals of this thesis was to investigate the proteome alterations of PaCa3, PaCa44, MiaPaCa2 and PC1J CSCs and to identify dysregulated pathways. Quantitative proteomic analysis permitted the identification of many differentially expressed proteins of the four PCSC lines compared to relative P cells.

Among the activated upstream regulators, XBP1 may be implicated in chemoresistance [164]; PGC-1α and PI3K in stemness [165, 166]; IGF1R in both stemness and chemoresistance [167]; and RICTOR connected to quiescence of CSCs [168].

Two common modulated proteins of PaCa3, PaCa44, MiaPaCa2 and PC1J CSCs, *i.e.*, HADHA and LDHA enzymes, were better investigated due to their pivotal role in cancer metabolism. LDHA catalyses the conversion of L-lactate and NAD to pyruvate and NADH in the final step of anaerobic "glycolysis". The phosphorylation of this enzyme on tyrosine 10 (Y10) (p-LDHA) determines its activation [169], which orchestrates the Warburg effect [170]. Consequently, the downregulation of both LDHA and p-LDHA proteins may suggest a higher reliance of PCSCs on "OXPHOS" as energy source rather than on "glycolysis" [143, 171]. This finding could be also supported by the upregulation of mitochondrial proteins as well as by the dysregulation of several metabolic pathways in PCSCs. Specifically, the predicted activation of "OXPHOS" in PaCa3 and MiaPaCa2 CSCs, and its enrichment in PaCa44 CSCs, together with the predicted inactivation of "glycolysis" and "gluconeogenesis" in PaCa44, MiaPaCa2 and PC1J CSCs, can suggest a metabolic shift of these cells from a more glycolytic to a more oxidative metabolism. In addition, the predicted activation of the upstream regulators estrogen-related receptor alpha (ERRα) and PGC-1α (PPARGC1A) in MiaPaCa2 CSCs are in line with a more active OXPHOS metabolism [172].

However, it should be reported that studies on CSC metabolism revealed inconsistent phenotypes among them. Some studies suggested a higher dependency of PCSCs on "glycolysis" [143], while others on "OXPHOS" [173]. Due to the still open debate on PCSC metabolism, it would be interesting to better investigate this

metabolic aspect using other approaches (*i.e.*, metabolomics analysis and/or oxygen consumption rate assay).

The other common modulated protein was HADHA (overexpressed in all fours PCSCs) which catalyses the last three steps of mitochondrial "β-oxidation of FAs" [174] and also plays a role in the acylation of monolysocardiolipin to form cardiolipin (CL). HADHA resulted mainly involved in dysregulated lipid pathways (*i.e.*, "the biosynthesis of unsaturated FA", "butanoate and propanoate metabolism", and "FA degradation, elongation and metabolism" and "CL remodelling") of PCSCs, indicating the crucial role of this enzyme in the metabolic alteration of these cells. The enrichment of "FA synthesis" and "mevalonate pathway" have been already observed in PCSCs [54], in which they may support cell survival in some conditions, including glucose deficiency [175].

Notably, the data also suggested the enrichment of pathways able to promote lipid metabolism, such as the predicted activation of "TCA cycle" in MiaPaCa2 CSCs and its enrichment in PaCa44 CSCs. The citrate produced by "TCA cycle" can move into the cytoplasm to fuel "FA synthesis" in PCSCs [176], while the enrichment of "Val, Leu and Ile degradation" in PaCa3, PaCa44, and MiaPaCa2 CSCs can promote the formation of carbon sources to support "lipid biosynthesis" [177].

Interestingly, HADHA also displays a role in both "FA elongation and metabolism", which may promote key CSC pathways (such as "Wnt signaling") [178] and may help to maintain stemness of PCSCs [54]. Notably, HADHA plays a key role in cardiolipin (CL) remodelling and shows high activity for some FA species (*i.e.*, FA 16:0, FA 18:1 and FA 18:2), which have been recently related to cardiolipin (CL) remodelling [179]. This process can modify the CL species in the inner mitochondrial membrane, affecting its stability and organization [180]. "CL remodelling" can also promote the enzymatic activities of the mitochondrial respiratory complexes [181, 182]. It has been reported that these respiratory supercomplexes favour "OXPHOS" by the modulation of oxidative stress. They can decrease superoxide levels and act on proton pump homeostasis and energy metabolism [183]. In addition, CL species function as a proton trap within the

membranes of the mitochondrial organelle to modulate the pH change caused by the activity of respiratory complexes [184]. In particular, the negative charge of $PO4^{-}$ groups of CL acyl chains are neutralized by their interaction with H^{+} ions, determining the reduction of the size of the hydrate coat around the polar head [185]. This process changes the CL structure from a bilayer packing to a reverse molecular shape, containing inverted micelles near highly protonated regions of membranes. These non-bilayer structures favour the oligomerization of the F0 sector of the ATP synthase complex and act as a proton trap to shuttle protons to the ATP synthase complex leading to enhanced ATP synthesis [185, 186]. Recently, it has been demonstrated that the inhibition of "CL remodelling" can promote the differentiation of acute myeloid leukaemia cells, decreasing their stemness [187, 188].

Altogether these data suggested the importance of HADHA and of lipid metabolism in PCSC biology [189].

5. Conclusions

In conclusion, a differential proteomics approach was applied to investigate the proteome profile of PaCa3, PaCa44, MiaPaCa2 and PC1J CSCs compared to relative P cells. Many differentially expressed proteins of PCSCs were identified. Among them, six were in common between the four PCSC lines, and in particular the downregulated LDHA and the upregulated HADHA were also analysed by immunoblotting analysis. The modulations of these two enzymes suggest that PCSCs are subjected to a metabolic shift.

Bioinformatic analyses were performed to better understand the role of dysregulated proteins and pathways able to distinguish PCSCs from their counterpart. Several proteins and pathways related to stemness, chemoresistance and quiescence were identified. More interestingly, GO enriched analyses of upregulated proteins of PCSCs showed that they were mainly cytosolic and mitochondrial.

The enriched pathway analyses indicated a statistically significant enrichment of lipid-related pathways (such as “unsaturated FA biosynthesis”, “FA elongation”, “CH biosynthesis”, *etc*.), in which HADHA was mainly involved, underlining the pivotal importance of this protein in PCSCs. In addition, Reactome pathway analysis revealed the “acyl chain remodelling of CL” as an enriched pathway of both MiaPaCa2 and PC1J CSCs. Notably, the HADHA play a role in “CL remodelling”, which is a pathway that could be involved in the promotion of “OXPHOS”.

Taken together, the proteomics data obtained suggested the importance of lipid metabolism in PCSCs, which has therefore been investigated in depth, as described in the next chapter.

Chapter 4

Lipidomic analysis of pancreatic cancer stem cells and parental pancreatic ductal adenocarcinoma cell lines

1. Introduction

Proteomics analysis showed alteration of lipid metabolism in PCSCs and upregulation of the mitochondrial HADHA enzyme.

Therefore, as described in this chapter, the lipid profiles of PaCa3, PaCa44, MiaPaCa2 and PC1J CSCs were analysed by LC-MS and LC-MS/MS to evidence their differences compared to related P cells. In addition, since HADHA plays a role in cardiolipin (CL) remodelling, the levels of CL species were investigated in depth. The levels of each lipid molecular species were quantified relative to a non-endogenous IS. Statistical and bioinformatic evaluation of lipidomic data was carried out and the dysregulated pathways, with related genes, were predicted.

Additionally, colorimetric enzymatic assay and confocal microscopy analysis were employed to investigate fatty acid (FA) concentration and to determine lipid droplets (LDs) content in all four PCSCs.

As described in Chapter 1 (Section 4.2.), few studies concerning the lipidome of CSCs have been published and up to now no studies have been performed to characterize the lipid profile of PCSCs. Therefore, the data reported here represent the first attempt to study the lipid metabolism of PCSCs.

2. Materials and methods

2.1. Sample preparation for lipidomic analyses

PCSCs and P cells were grown and collected as described in Chapter 2, Section 2.1. The cell pellets of four biological replicas (each of around $1*10^6$ cells) were washed twice with 1X cold PBS, fluxed with liquid nitrogen to prevent lipid oxidation and stored at -80°C until further analyses.

Free FAs, phospholipids, sphingolipids and neutral lipids were extracted from frozen cell pellets using the Folch method with chloroform/methanol/water (2:1:1 ratio) [190].

Lysolipids and phosphatidylinositol phosphates were obtained from frozen cell pellets by butanol and acidified extraction with butanol/water (1:1 ratio) and chloroform/methanol/acidified aqueous solution (1,25:2,5:1 ratio) [191] respectively.

The DNA concentration was determined for each sample, for normalization purpose, by using NanoDrop (Thermo Fisher Scientific, Waltham, MA).

Extracted lipids were dried by SpeedVac (Savant SP131DDA, Thermo Scientific, Runcorn, UK), and resuspended in chloroform/methanol (1:1) prior to lipidomics analyses. An IS was also added at the beginning of the extraction process accounting for the percentage of recovery in the final re-suspension. Collision energy was optimized previously.

2.2. Mass spectrometric based lipidomics analysis and data processing

Lipids were analysed by mass spectrometry in collaboration with the Lipidomics facility at the Babraham Institute in Cambridge (UK), during my three-months placement abroad.

Chromatographic separation was achieved upon a Waters Acquity UPLC C4 (100 x 1 mm, 1.7 μm particle size) column (Milford, MA, USA). The column was

kept at 45 °C and 7 µl of samples were eluted using a mobile phase composed of solvent A (water) and B (acetonitrile), each containing 0.025 % formic acid. The gradient started at 45 % B for 5 min, then increased to 90 % B for five minutes and 100 % B was reached after an additional 10 minutes and held for seven minutes before re-equilibration at 45% B for five minutes. The flow rate was maintained constant at 100 µL/min. Accurate mass (with an error below 5 ppm) was acquired on an Orbitrap Elite mass spectrometer (Thermo Fisher Scientific, Waltham, MA, USA). Source parameters for positive polarity were: capillary temperature 275 °C; source heater temperature 200 °C; sheath gas 10 AU; aux gas 5 AU; sweep gas 5 AU; Source voltage was 3.8 kV. Full scan spectra in the range of *m/z* 340 to 1,500 were acquired at a target resolution of 240,000 (FWHM at *m/z* 400).

The transitions were selected based on the abundance of the fragment and the specific to the acyl chain composition, while water losses of carbo dioxide were not considered because of its no-specificity. Therefore, manual inspection of the results was carried out using Xcalibur and further processed using Lipid Data Analyzer (LDA) 2.7.0_2019 software [192]. Targeted analysis of lysolipids, Cer and dhCer, was performed by using Q-TRAP 6500 LC-MS/MS System (AB SCIEX) operating in MRM mode. Quantification of multiple species of ceramides was carried out by the integration of the peak area as normalized against the peak area of the unnatural odd-chain ceramide C17:0. C17 was present at a known concentration and served as the IS. The level of confidence in hight resolution-MS-based identifications was with an error at 5 ppm.

Thirty-seven lipid sub-classes were identified, including CE, triacylglycerol (TG), CH, dihydrosphingosine (dhSG), sphingosine (SG), sphingomyelin (SM), ceramides (Cer), dihydroceramides (dhCer), dihydrosphingomyelin (dhSM), alkyl−acylglycerol (O-DG), alkyl−triacylglycerol (O-TG), cardiolipin (CL), phosphatidic acid (PA), phosphatidylcholine (PC), phosphatidylethanolamine (PE), phosphatidylglycerol (PG), phosphatidylserine (PS), diacylglycerol (DG), phosphatidylinositol (PI), phosphatidylinositolmonophosphate (PIP), phosphatidylinositoldiphosphate (PIP2), FA, lysophosphatidic acid (LPA), lysophosphatidylcholine (LPC), lysophosphatidylethanolamine (LPE), lysophosphatidylglycerol (LPG), lysophosphatidylinositol (LPI),

lysophosphatidylserine (LPS), alkyl−lysophosphatidic acid (O-LPA), alkyl−lysolysophosphatidylcholine (O-LPC), alkyl−lysophosphatidylethanolamine (O-LPE), alkenyl−lysophosphatidic acid (P-LPA), alkenyl−lysophosphatidylcholine (P-LPC), alkyl−acylphosphatidylcholine (O-PC), alkyl−acylphosphatidylethanolamine (O-PE), alkenyl−acylphosphatidylcholine (P-PC) and alkenyl−acylphosphatidylethanolamine (P-PE).

The results from the LC-MS and LC-MS/MS experiments were reported as amount of lipid on sample (expressed as ng) and normalized to DNA concentration (ng of DNA) for each sample (PCSCs and P cells). Lipid relative quantitation levels were calculated using the R-studio (v3.2.4). Statistical comparison between the P cells and PCSCs was performed using the paired *t*-test (p <0.005), principal component analysis (PCA) and $\log_2$ ratio transformation of PCSCs *versus* P lipid levels.

2.3. Bioinformatic analysis of lipidomics data

Bioinformatics analysis of lipidomics data of PCSCs compared to P cells was performed using an open access tool BioPAN, on LIPID MAPS® Lipidomics Gateway (https://lipidmaps.org/biopan/) [193]. LIPID MAPS® is a relational database which includes annotations and structures of different biologically significant lipids. Structures of lipids in the database come from: (i) LIPID MAPS® Consortium's core laboratories and partners; (ii) lipids identified by LIPID MAPS® experiments; (iii) biologically relevant lipids manually curated from LIPID BANK, LIPIDAT, Lipid Library, Cyberlipids, ChEBI and other public sources; (iv) novel lipids submitted to peer-reviewed journals; (v) computationally generated structures for appropriate classes.

All the lipid structures in LIPID MAPS® Structure Database (LMSD) conform to the structure drawing rules proposed by its consortium. LIPID MAPS® Lipid Classification System classifies all lipids in the LMSD, correlating each lipid with a LIPID MAPS® ID (LM_ID), which reflects its position in the classification hierarchy. Moreover, this database allows users to search the LMSD using either text-based or structure-based search options, as well as the classification-based

retrieval of lipids [194, 195]. BioPAN provides *Z*-scores ($Z > 1{,}645$ at $p < 0{,}05$) using substrate and product lipid levels and includes a list of genes, which could be involved in the activation or suppression of enzymes catalysing lipid metabolic pathways [196].

BioPAN is used here to compare the lipid profile results of the CSC against the parental. Each pair CSC and P lipid results area is individually analysed as control condition (P) and condition of interest (CSC). BioPAN requires a minimum of two replicates per condition to find statistically significant changes between the conditions.

2.4. Assessment of free fatty acid concentration

The levels of free FAs were determined using a colorimetric FA Quantification Kit (MAK044, Sigma-Aldrich/Merk) according to the manufacturer's instructions. $1*10^6$ cells for each sample were lysed in 1% Triton X-100 in chloroform (w/v) and centrifuged at 13000 × g for ten minutes to remove insoluble debris. The organic phase was collected and then dried at 50 °C in a dry bath for twenty minutes. Addition of FA assay buffer to the dried extract was performed, followed by extensive vortex mixing to solubilize the dried extract. Successively, absorbances were read at 570 nm using a microplate reader (Tecan infinite PRO 200) and values reported as μM FFA/million cells.

2.5. Confocal fluorescence microscopy

PCSCs and P cell lines were grown on an L-lysine coverslip inside a 24-well plate and incubated at 37° C (5% CO_2). The supernatant was removed and, after washing with PBS, cells were fixed using 8% formaldehyde for ten minutes at room temperature. The fixed cells were incubated with Oil Red O (Bio-Optica) for twenty minutes at room temperature. Then, cells were washed again and treated with 0.1% Triton X-100 and 1% bovine serum albumin for fifteen minutes at room temperature. Cells were stained with DAPI (4',6-diamidino-2-phenylindole nuclei stain, dilution 1:1000; Sigma Aldrich) for thirty minutes and used for nuclei

visualization. Stained samples were scanned by a confocal microscope (Leica TCS SP5 AOBS) using 416 nm and 545 nm lasers under a 40x oil objective.

IMARIS X64 9.1.0 software was used to generate z- and three-dimensional (3D) projections. The 3D projections were used to analyse lipid droplets (LDs) shape and volume. Twenty images per sample were recorded and LDs were counted manually using the ImageJ multipoint tool after background correction. LDs were classified as small (with a volume between 1 and 5μm^3) and large (with a volume >5μm^3). The number of counted LDs was normalized per cell nucleus number. Thus, statistical analysis (*t*-test) was performed to identify significant changes.

3. Results

3.1. Lipidome modulations of pancreatic cancer stem cells

The LC-MS/MS results of the 37 lipid sub-classes identified in each pair of P cells and PCSCs. A total of 459, 498, 495 and 469 lipid species were detected in PaCa3, PaCa44, MiaPaCa2 and PC1J, respectively. These results were then represented as the $\log_2$ of the fold changes of PaCa3, PaCa44, MiaPaCa2 and PC1J CSCs compared to related P cells (see Fig. 1). The results showed a trend of increase in all four PCSCs in the levels of neutral lipids (*i.e.*, DG, TG, CH), sphingolipids (*i.e.*, dhSG, SG, Cer, dhCer, SM, dhSM), glycerophospholipids (*i.e.*, CL, PA, PC, PS, PG, PE, PI), FAs and some ether lipids (*i.e.*, O-PE, O-PC). A general increase in the lipid sub-classes was particularly noticeable for PC1J CSCs.

Moreover, some lysolipids and ether lipid (*i.e.*, LPA, LPC, LPE, LPI, LPS, O-LPE and P-LPC), phospholipids (*i.e.*, O-PC and P-PC), dhSM and CH sub-classes were increased in PaCa44, MiaPaCa2 and PC1J CSCs; while two sphingolipid sub-classes (*i.e.*, dhSG and dhCer) were up in PaCa3, MiaPaCa2 and PC1J CSCs.

Interestingly, 17 lipid subclasses (*i.e.*, CH, TG, dhSG, Cer, dhCer, dhSM, PC, PE, PG, PI, LPA, LPC, O-LPA, O-LPC, O-LPE, O-PC and O-PE) were significantly increased at 95 % confidence interval (CI) in PC1J CSCs.

However, it was clearly observed that some lipid sub-classes for MiaPaCa2 CSCs were not significantly dysregulated (95% CI) (such as CE, PA, O-LPA and P-LPA).

It was quickly reckoned that the $\log_2$ of the fold changes graph was more complex to interpret and posed a difficulty to find a general relationship between the PaCa3, MiaPaCa2 and PC1J CSCs compared to P cells. Consequently, all the $\log_2$ of the fold changes observed in each PDAC cell line (P and CSCs) were plotted using Draw Venn Diagram tool (http://bioinformatics.psb.ugent.be/webtools/Venn/). Figure 2a shows overlapping in the dysregulated lipid molecular species of the four PCSCs. A total of 385 lipid molecular species were common among P cells and PCSCs of the four PDAC lines (see Annex Tab. 1). Additionally, principal component analysis (PCA) of the $\log_2$

of the fold change of PCSCs compared to P cells was performed (Fig. 2b). PCA results revealed that PaCa3, PaCa44, MiaPaCa2 and PC1J lines clustered away from each other, being clearly distinguished from each other.

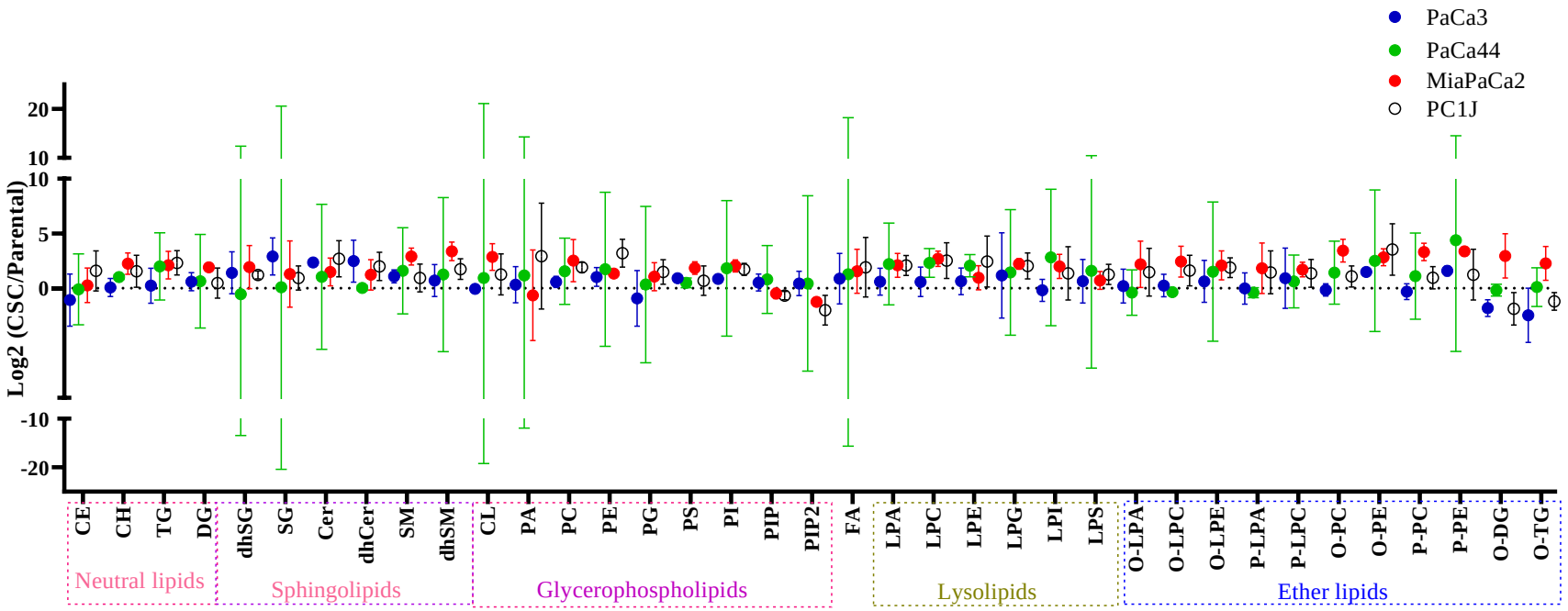

Figure 1. Log$_2$ of the fold changes of the lipidome profile of PaCa3 (blue), MiaPaCa2 (red), PaCa44 (green) and PC1J (white) CSCs compared to related P cells. The x-axis represents the analysed 37 lipid subclasses; the y-axis reports the log$_2$ ratio (CSC/P) at 95% CI.

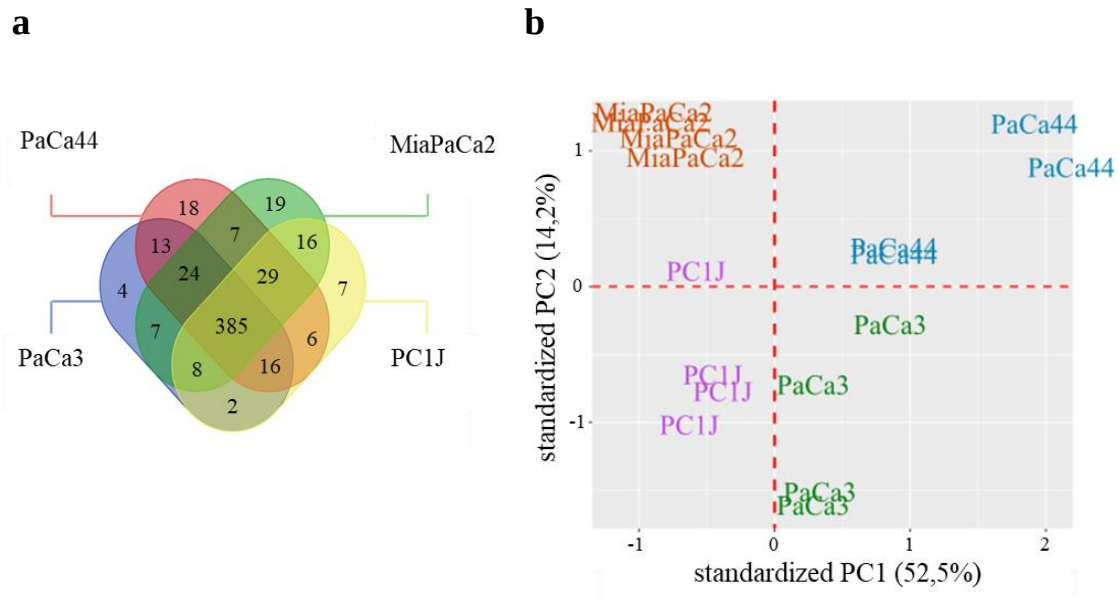

Figure 2. a. Venn diagram of identified intracellular lipid species in each pair of P cells and PCSCs of PaCa3, PaCa44, MiaPaCa2 and PC1J lines; b. PCA of the log_2 ratio of CSC/P of PaCa3 (in green), PaCa44 (in blue), MiaPaCa2 (in red) and PC1J (in purple).

3.2. Accumulation of long chain fatty acids in pancreatic cancer stem cells

By LC-MS/MS a general increase in FAs in PCSCs compared to P cells was detected. To better investigate this trend of modulation, the FA intracellular levels were evaluated in PaCa3, PaCa44, MiaPaCa2 and PC1J P and CSCs using a colorimetric enzymatic assay. Figure 3a shows the concentration levels of FAs (expressed as μM/1*10^6 cells) in all the four cell lines. A statistically significant increase of FA concentration was observed in PaCa44, MiaPaCa2 and PC1J CSCs. Although a trend of increase was also detected in PaCa3 CSCs.

Interestingly, the lipidomics results pointed out increased levels of long (16–20 carbons) and very long (≥22 carbons) chain FAs in PCSCs (Fig. 3b).

a

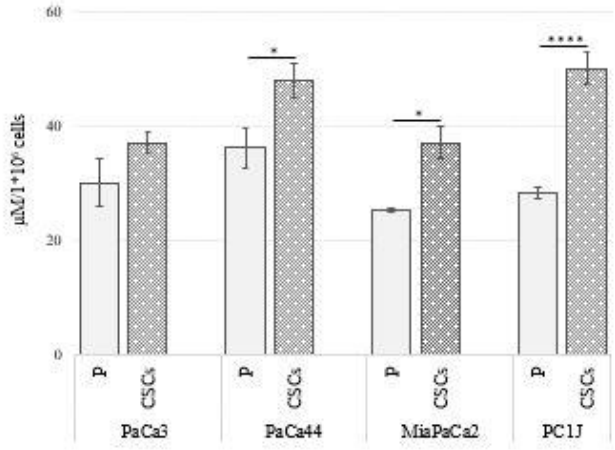

b

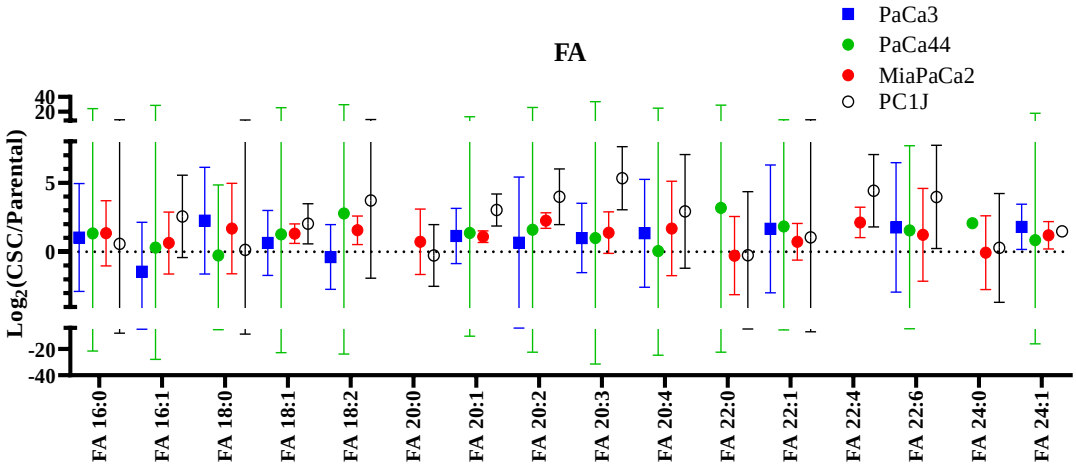

Figure 3. a. FA concentration (µM) in PaCa3, PaCa44, MiaPaCa2 and PC1J P and CSCs. Data presented as mean ± standard error (SE) of three independent experiments. p <0,05 (*) and p <0,0001 (****); b. Log₂ of the fold changes of FA species in PaCa3 (in blue), PaCa44 (in green), MiaPaCa2 (in red) and PC1J (in white) CSCs compared to relative P cells. The x-axis represents the analysed 16 FA lipid species; the y-axis represents the log₂ (CSC/P) at 95 % CI.

3.3. Accumulation of lipid droplets in pancreatic cancer stem cells

Lipidomics analysis also pointed out an increase of some neutral lipids in PCSCs (Fig. 1). For instance, CE and TG levels, that mainly constitute the core of lipid droplets (LDs), were investigated for the accumulation of these lipid bodies. Total CE and TG levels were normalized against the PC content, as the LDs core is surrounded by a PC layer (Fig. 4). The results showed an increased content of CE and TG species in both PaCa44 and MiaPaCa2 CSCs compared to relative P cells, which it was also statistically significant (at 95% CI) in PC1J CSCs. Thus, confocal microscopy was used to evaluate number and size (shape) of LDs in the four PCSCs and P cell lines.

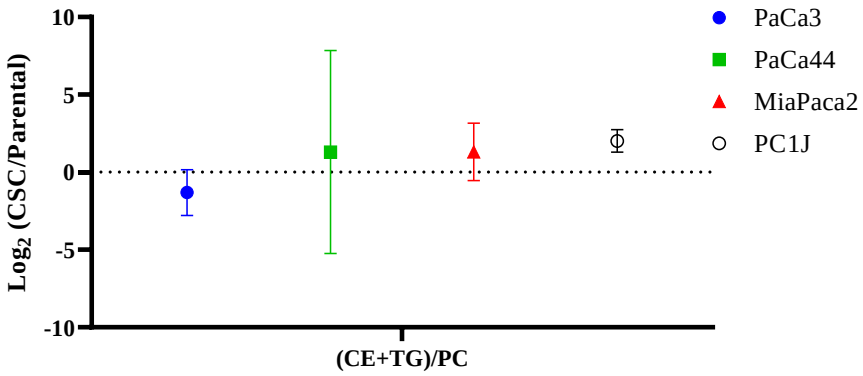

Figure 4. Results of CE+TG content (normalized to PC content) detected by LC-MS analysis reported as log_2 of the fold change at 95% CI in PaCa3 (in blue), PaCa44 (in green), MiaPaCa2 (in red) and PC1J (in white) CSCs compared to P cells.

PaCa3, PaCa44, MiaPaCa2 and PC1J P and CSCs were labelled with Oil Red O (red) to detect LDs and with DAPI (blue) to highlight the nuclei, as shown in Figure 5. LDs number (Fig. 6a) and size (Fig. 6b) were also measured in all four PCSCs and related P cells. An enhancement in the number of LDs in all four PCSCs compared to their related P was detected (Fig. 6a), which was also statistically significant for both MiaPaCa2 and PC1J CSCs. In addition, a statistically significant increment of large and small LDs was observed in PaCa3 and PC1J CSCs, respectively (Fig. 6b).

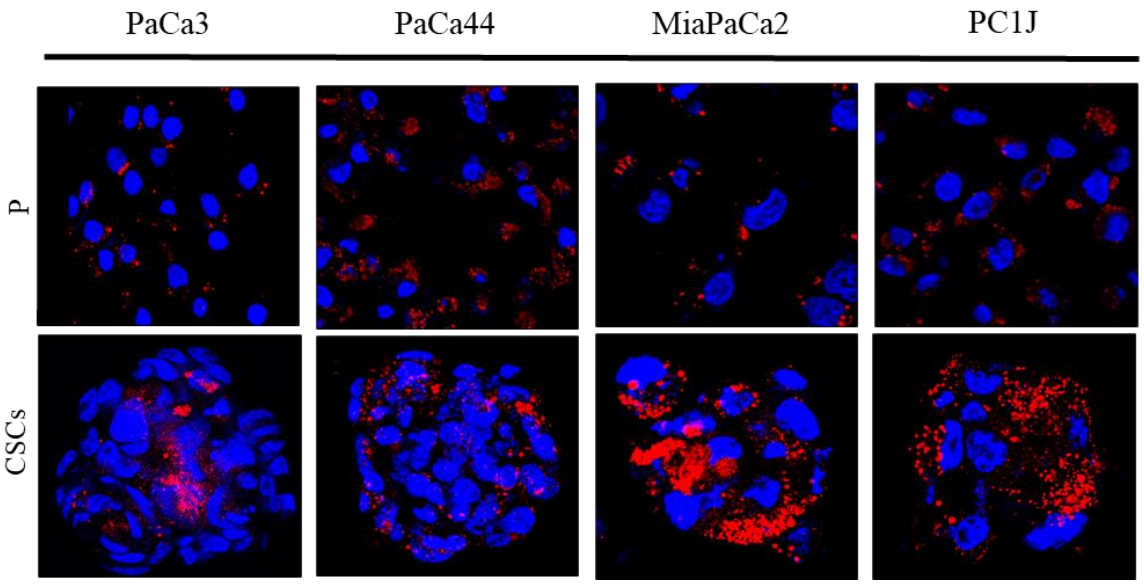

Figure 5. Confocal microscopy images of PaCa3, PaCa44, MiaPaCa2 and PC1J P and CSCs labelled with Oil Red O (red) to detect LDs and with DAPI (blue) to highlight nuclei.

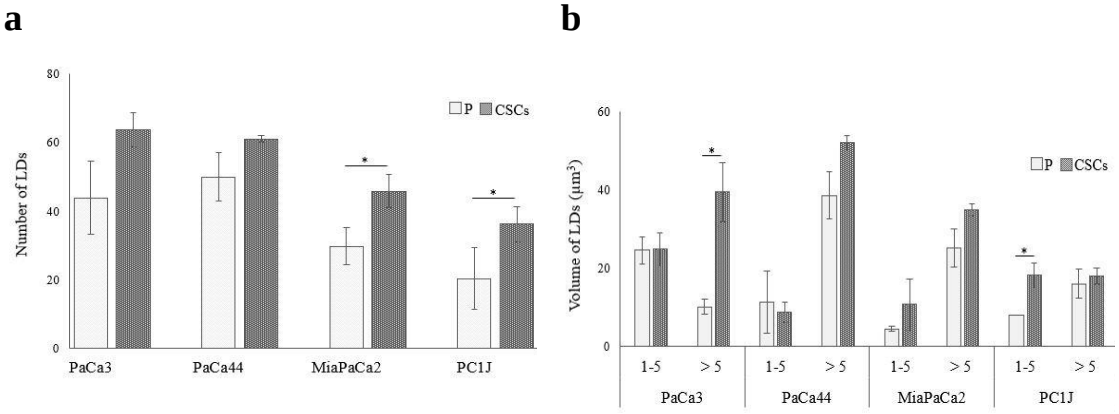

Figure 6.a. Number of LDs in PaCa3, PaCa44, MiaPaCa2 and PC1J P and CSCs. The data were normalized on cell number; b. Measure of LDs size (as volume, µm3) in PaCa3, PaCa44, MiaPaCa2 and PC1J P and CSCs. Data represented as means ± standard error (SE) of three independent experiments. p <0,05 (*).

3.4. Dysregulated lipid metabolism of pancreatic cancer stem cells

Next, lipidomic data were evaluated to predict dysregulated pathways of PCSCs and to detect genes which could be involved in the activation or suppression of enzymes catalyzing lipid metabolic pathways.

Table 1 shows the reaction chains of lipid sub-classes and FA molecular species predicted as active (with a Z-score >1,645, p <0,05) in PaCa3, PaCa44, MiaPaCa2 and PC1J CSCs by BioPAN analyses. The numbers of active reactions were: 8, 11, 13 and 15 for PaCa3, PaCa44, MiaPaCa2 and PC1J CSCs, respectively.

All four PCSC lines showed changes in the pathways comprising phospholipids, sphingolipids, ether lipids and FA elongation and desaturation. In Table 1 the genes related to the lipid reactions predicted as active can be also observed. Each gene activates enzymes catalysing lipid metabolic pathways, as shown in Figure 7. Interestingly, pathways involving PS and PE were common in all four PCSCs compared to their related P. Moreover, DG (a neutral lipid) was involved in active pathways in PaCa3, PaCa44, MiaPaCa2 and PC1J CSCs.

Notably, overall reactions involving FA species were predicted as active in all the four PCSCs, as shown in Table 1. Therefore, the FA elongation and desaturation were also investigated as they emerged as key pathways of PCSCs from the proteomics analyses (see Chapter 3). Figure 8 shows activated and supressed FA chain reactions in PaCa3, PaCa44, MiaPaCa2 and PC1J CSCs, highlighting with thick edges the most active reactions (with a Z-score >1,645).

Among the most FA active reactions (Fig. 8), the formation of monounsaturated FA 16:1 (from FA 16:0) and FA 18:1 (from FA 18:0) species was predicted in PC1J CSCs, while the elongation of FA 18:1 (from FA 16:1) and of FA 20:2 (from FA 18:2) were detected as the most active reactions in PaCa3 and MiaPaCa2 CSCs, respectively. In addition, the formation of polyunsaturated FA 18:2 (from FA 18:1) and FA 20:3 (from 20:2) species were identified in PaCa44 and PC1J CSCs, respectively.

.

The large number of genes involved in activating enzymes of lipid metabolism can also be observed in Table 1; therefore, a Venn Diagram was produced to show overlapping genes (Fig. 9). The results pointed out fourteen overlapping genes in all four PCSCs. Among these, thirteen (*i.e.*, *SYNJ1, SYNJ2, SACM1L, MTMR1, MTMR2, MTMR3, MTMR4, MTMR6, MTMR7, MTMR8, MTMR9, MTMR14* and *PTEN*) encode for phosphoinositide lipid phosphatase proteins (see Annex Tab. 3). Specifically, the well-studied *PTEN* (phosphatase and tensin homolog) encodes for a tumour suppressor, which is mutated with high frequency in different type of cancers, including PDAC. Interestingly, among the common gene *ELOVL5* (fatty acid elongase 5) was also detected. It encodes for a protein, Elovl5, which activates the enzyme involved in FA elongation. *PTEN* and *ELOVL5* are further discussed in Section 3.4.1.

Figure 9 also shows genes with different overlapping between the PaCa3, PaCa44 and MiaPaCa2 CSCs (see Annex Tab. 2). For example, the transmembrane protein 189 (*TMEM189*) and phosphatidylcholine: ceramide choline phospho-transferase 1 and 2 (*SGMS1* and *SGMS2*) were common in PaCa3, PaCa44 and MiaPaCa2 CSCs, while choline phosphotransferase 1 (*CHPT1*), choline/ethanolamine phosphotransferase 1 (*CEPT1*) and fatty acid elongase 6 (*ELOVL6*) were detected in PaCa3, PaCa44 and PC1J CSCs. Moreover, phospholipase D1 (*PLD1*) were common to PaCa44, MiaPaCa2 and PC1J CSCs.

Table 1. BioPAN predicted significantly active reaction chains (Z >1,645) of lipid class and FA species and related genes for PCSC lines compared to their P.

	Reaction chain	*Z*-score	Predicted genes
PaCa3	SM→Cer	3,013	*SMPD2, SMPD3*
	O-DG→O-PE→P-PE	2,612	*CEPT1, TMEM189*
	PIP2→PIP→PI	2,211	*FIG4, OCRL, INPP5E, PTEN, SYNJ1, SYNJ2, SACM1L, MTMR1, MTMR2, MTMR3, MTMR4, MTMR6, MTMR7, MTMR8, MTMR9, MTMR14, PTEN*
	O-DG→O-PC	2,074	*CHPT1*
	FA 16:1→FA 18:1→FA 20:1→FA22:1→FA 24:1	1,833	*ELOVL5, ELOVL6, ELOVL3, ELOVL3, ELOVL3*
	dhSM→dhCer	1,828	*SGMS1, SGMS2*
	DG→PE	1,673	*CEPT1*
	PC→PS	1,654	*PTDSS1*
PaCa44	FA 16:1→FA 18:1→FA 18:2	2,72	*ELOVL5, ELOVL6, FADS2*
	O-PE→P-PE	2,620	*TMEM189*
	dhCer→Cer→SM	2,221	*DEGS1, DEGS2, SGMS1, SGMS2, CERT1*
	O-DG→O-PC	2,022	*CHPT1*
	FA 18:1→FA 18:2	1,930	*FADS2*
	dhCer→dhSM	1,919	*SGMS1, SGMS2*
	O-DG→O-PE→P-PE→P-PC	1,895	*CEPT1, TMEM189, PLD1*
	DG→PE	1,859	*CEPT1*
	PS→PE	1,805	*PISD*
	DG→PC	1,685	*CHPT1*
	PIP→PI	1,667	*MTMR6, MTMR7, MTMR8, MTMR9, MTMR14, PTEN SYNJ1, SYNJ2, SACM1L, MTMR1, MTMR2, MTMR3, MTMR4,*
MiaPaCa2	PIP2→PIP→PI	3,731	*FIG4, OCRL, INPP5E, PTEN, SYNJ1, SYNJ2, SACM1L, MTMR1, MTMR2, MTMR3, MTMR4, MTMR6, MTMR7, MTMR8, MTMR9, MTMR14, PTEN*
	PIP→PI	2,392	*SYNJ1, SYNJ2, SACM1L, MTMR1, MTMR2, MTMR3, MTMR4, MTMR6, MTMR7, MTMR8, MTMR9, MTMR14, PTEN*
	dhCer→dhSM	2,103	*SGMS1, SGMS2*
	Cer→SM	2,049	*SGMS1, SGMS2, CERT1*
	PIP2→DG	2,007	*PLCB1, PLCB2, PLCB3, PLCB4, PLCD1, PLCD3, PLCD4, PLCE1, PLCG1, PLCG2*
	PA→DG	1,983	*PLPP1, PLPP2, PLPP3*
	O-LPE→O-LPA	1,944	*PLD1*
	PE→PC	1,941	*PEMT*
	PG→CL	1,821	*CRLS1*
	O-PE→P-PE→P-PC	1,811	*TMEM189, PLD1*
	PA→PS	1,782	*CDS1, PTDSS1*
	PE→PS	1,779	*PTDSS2*
	FA18:2→FA 20:2	1,717	*ELOVL5*
PC1J	O-DG→O-PC	3,644	*CHPT1*
	PIP2→PIP→PI	3,129	*FIG4, OCRL, INPP5E, PTEN, SYNJ1, SYNJ2, SACM1L, MTMR1, MTMR2, MTMR3, MTMR4, MTMR6, MTMR7, MTMR8, MTMR9, MTMR14, PTEN*
	PIP2→DG→PE	2,879	*PLCB1, PLCB2, PLCB3, PLCB4, PLCD1, PLCD3, PLCD4, PLCE1, PLCG1, PLCG2, CEPT1*
	FA 16:0→FA 16:1→ FA 18:1→ FA 20:1	2,527	*SCD3, ELOVL5, ELOVL6, ELOVL3*
	PIP2→DG→PC→PA	2,378	*PLCB1, PLCB2, PLCB3, PLCB4, PLCD1, PLCD3, PLCD4, PLCE1, PLCG1, PLCG2, CHPT1, PLD1, PLD2*
	FA 18:0→FA 18:1→FA 18:2→FA 20:2→FA 20:3 ↓ FA 20:4	2,349	*SCD1, FADS2, ELOVL5, FADS1, FADS1*
	DG→PC	2,343	*CHPT1*
	PIP2→DG→PA	2,265	*PLCB1, PLCB2, PLCB3, PLCB4, PLCD1, PLCD3, PLCD4, PLCE1, PLCG1, PLCG2, DGKA, DGKB, DGKD, DGKE, DGKG, DGKH, DGKI, DGKK, DGKQ, DGKZ*
	PIP→PI	2,148	*SYNJ1, SYNJ2, SACM1L, MTMR1, MTMR2, MTMR3, MTMR4, MTMR6, MTMR7, MTMR8, MTMR9, MTMR14, PTEN*
	FA 18:0→FA 18:1→FA 20:1→FA 22:1	2,098	*SCD1, ELOVL3, ELOVL3*
	DG→PE	2,022	*CEPT1*
	FA 16:0 FA 16:1→FA 18:1→FA 18:2 ↓ FA 20:2→FA 20:3→FA20:4	1,982	*SCD3, ELOVL5, ELOVL6, FADS2, ELOVL5, FADS1, FADS1*
	O-DG→O-PE	1,949	*CEPT1*
	PIP2→DG→PC→CL	1,931	*PLCB1, PLCB2, PLCB3, PLCB4, PLCD1, PLCD3, PLCD4, PLCE1, PLCG1, PLCG2, CHPT1, TAZ*
	FA 20:2→FA 20:3	1,926	*FADS1*

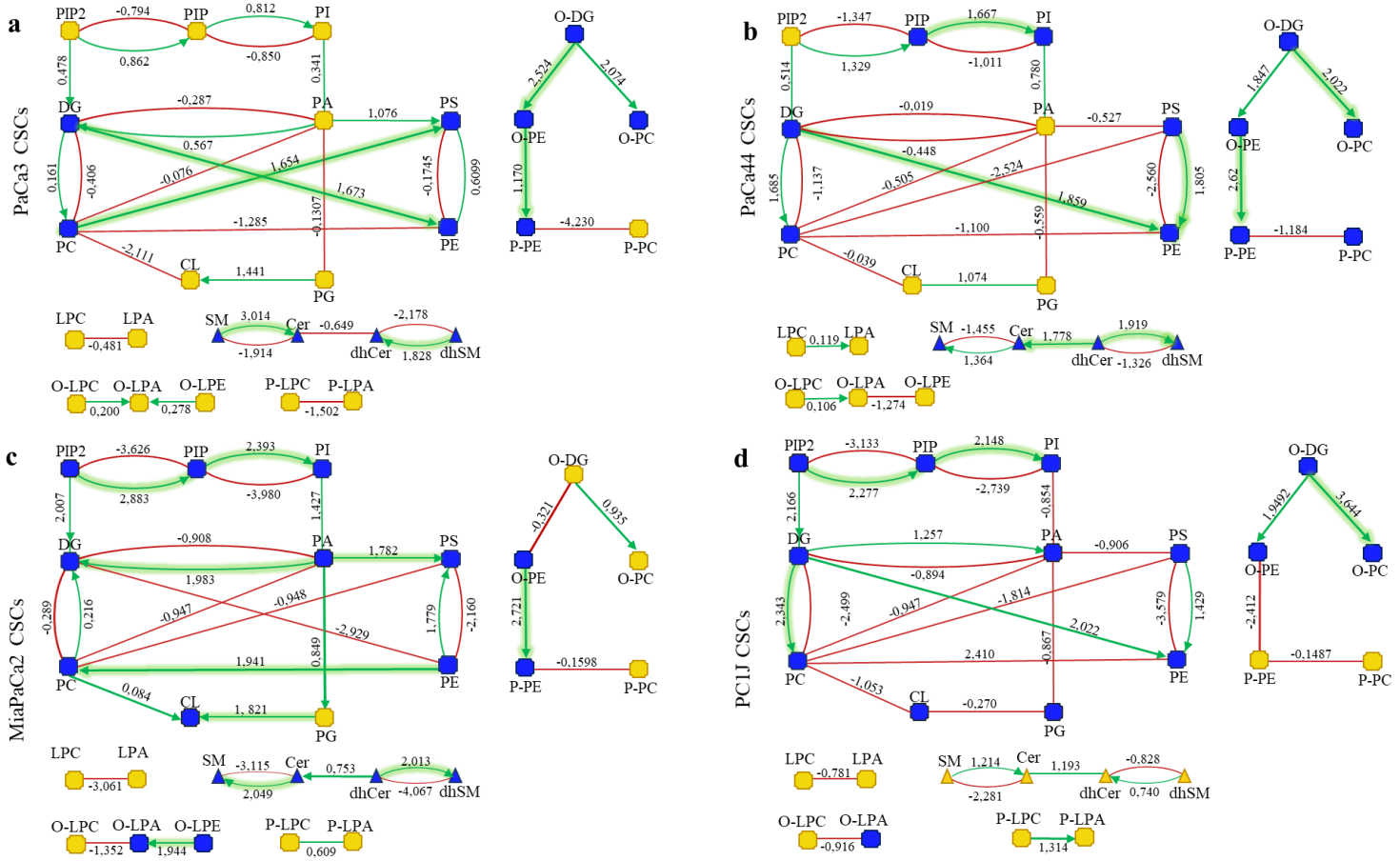

Figure 7. Pathway analysis of a. PaCa3, b. PaCa44, c. MiaPaCa2 and d. PC1J CSCs compared to relative P cells. Coloured nodes indicated active/suppressed status. Green and red edges indicated positive and negative Z-score, respectively. The edges of the most active reactions are highlighted with thick edges.

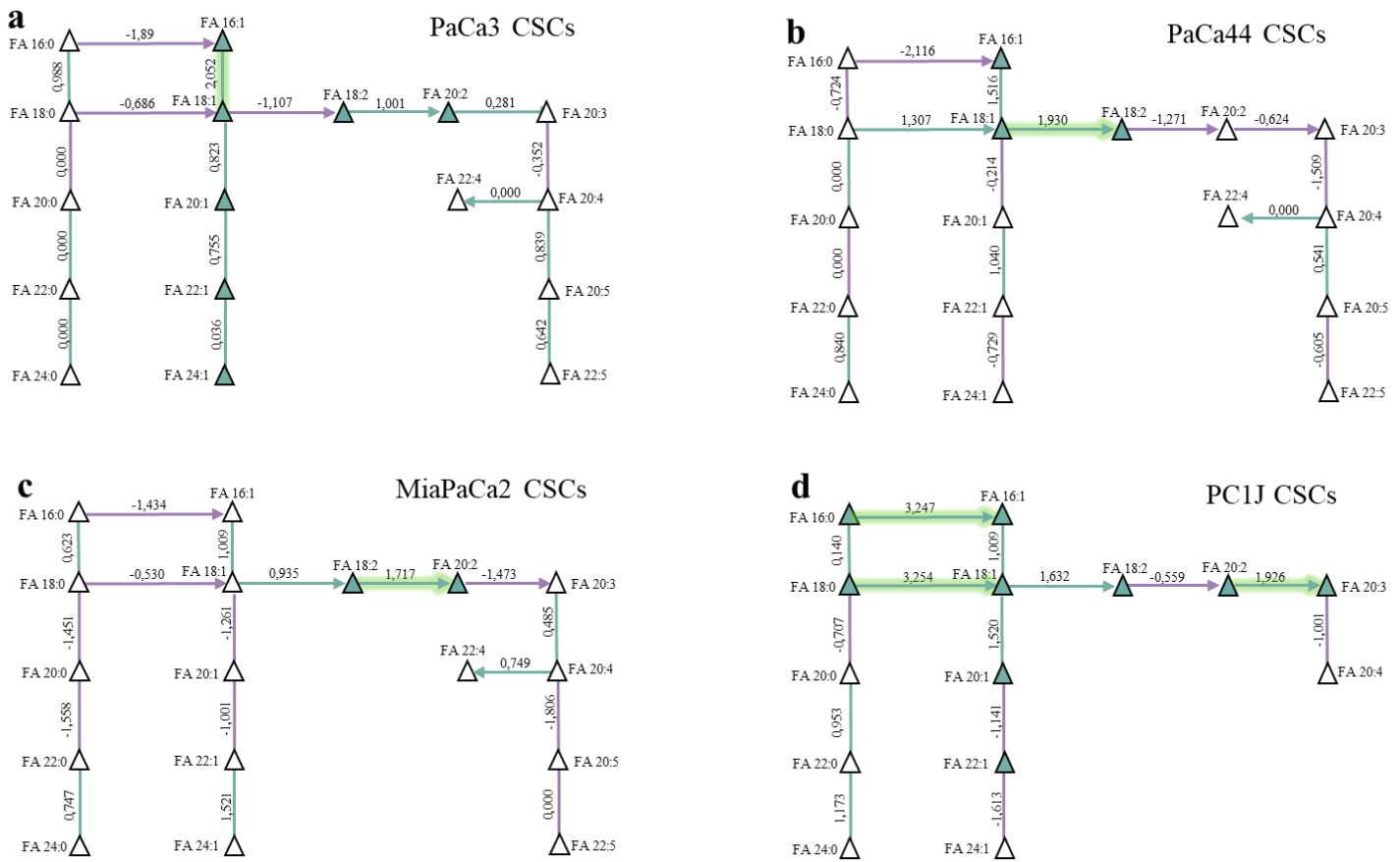

Figure 8. FA pathway analysis at molecular specie level of a. PaCa3, b. PaCa44, c. MiaPaCa2 and d. PC1J CSCs compared to relative P cells. Coloured nodes indicated the most active/suppressed status. Green and purple edges indicated positive and negative Z-score, respectively. The reactions with an active status have edges highlighted with thick edges.

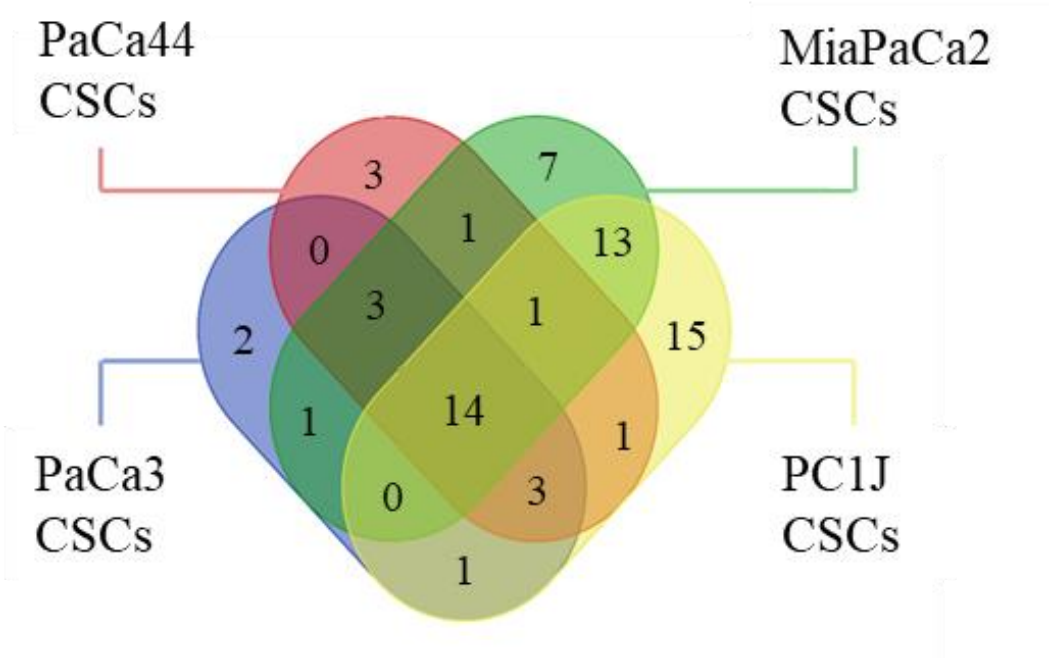

Figure 9. Venn diagram representation of genes related to predicted active pathways detected by BioPAN analysis tool.

3.4.1. Pancreatic cancer stem cells revealed induced phosphoinositides and fatty acid elongation pathways

Next the study was focalized on the analysis of pathways in which the common predicted genes of PaCa3, PaCa44, MiaPaCa2 and PC1J CSCs are involved.

A statistically significantly increase (at 95% CI) in the levels of phosphatidylinositol (PI) in PaCa3, MiaPaCa2 and PC1J CSCs was observed (Fig. 1). PI is one of the products of phosphoinositide lipid phosphatases using phosphatidylinositolmonophosphate (PIP) as a substrate. Additionally, PIP is produced from the catalytic activity of phosphoinositide lipid phosphatases on phosphatidylinositoldiphosphate (PIP2). Hence, the levels of PIP appeared not to be statistically significantly (at 95% CI) changed (Fig. 1 and Fig. 10). However, the levels of PIP2 showed a 1.2 and 2-fold decrease in MiaPaCa2 and PC1J CSCs (Fig. 10).

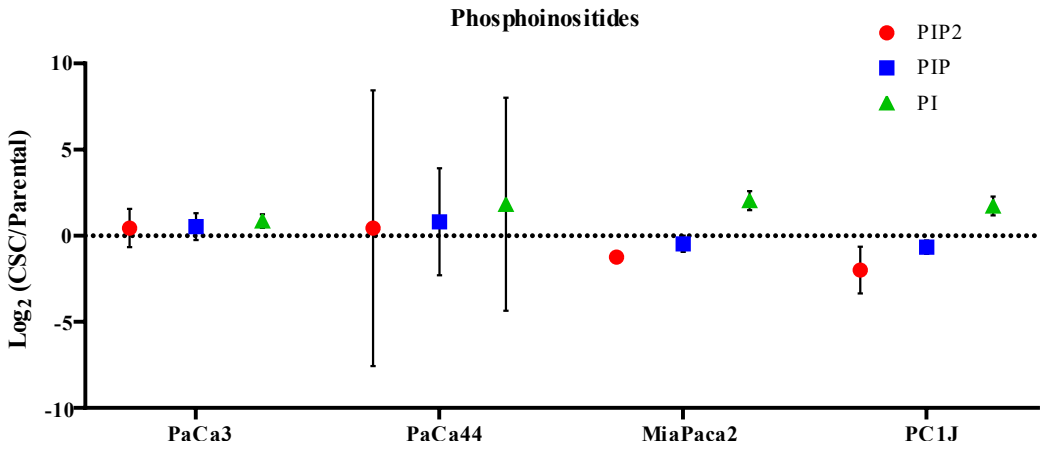

Figure 10. Log_2 of the fold change of PaCa3, PaCa44, MiaPaCa2 and PC1J CSCs compared to P cell lines of PIP2, PIP and PI sub-classes. Log_2 of the fold change at 95% CI.

Along with phosphoinositide lipid phosphatases, *ELOVL5* was also common to the four PCSCs. As presented in Section 3.4, the elongation of FA 16:1 and FA 18:1 molecular species was predicted as an active pathway, involving the catalytic activity of the encoded enzyme Elovl5 (Fig. 8 and Fig. 11). BioPAN calculated a different Z-score for each FA reaction predicted as active in PaC3, PaCa44, MiaPaCa2 and PC1J CSCs.

In addition, a statistically significantly (at 95% CI) increased levels of FA 18:1, FA 20:2, FA 20:3 and FA 22:4 species were detected in both MiaPaca2 and PC1J CSCs and of FA 20:4 species in both Paca3 and MiaPaca2 CSCs.

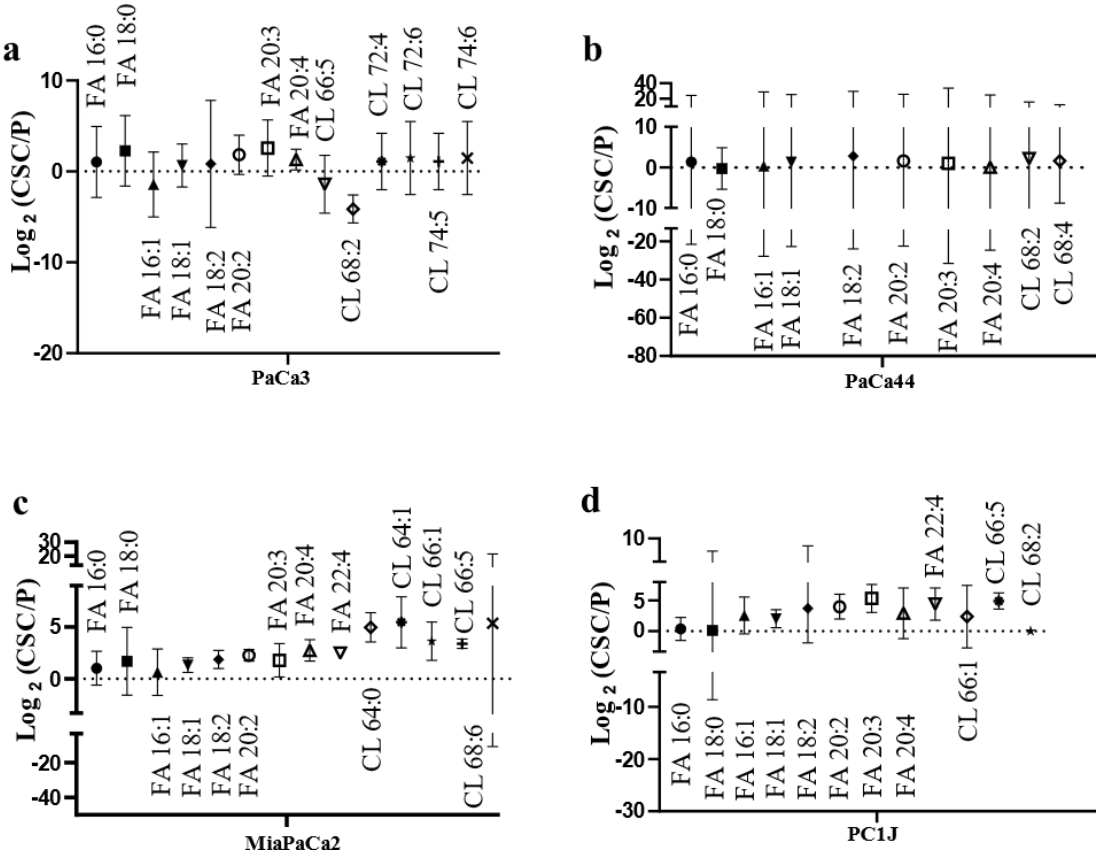

Figure 11. Log_2 of the fold change in a. PaCa3, b. PaCa44, c. MiaPaCa2 and d. PC1J (CSCs/P ratio) of the FA substrates and products catalysed by Elovl5, including FA species (i.e., 16:0, 18:1 and 18:2) related to CL remodelling by HADHA enzyme. Log_2 of the fold change at 95% CI.

3.5. Pancreatic cancer stem cells are characterized by cardiolipin remodelling

Since HADHA was detected by proteomics as upregulated in all the four PCSCs, the levels of FA and CL molecular species which could contain fatty acyl chain incorporation in the reaction of monolysocardiolipin with C18:1, C18:2 and C16:0 by HADHA were analysed.

The trifunctional enzyme subunit alpha (HADHA) has a monolysocardiolipin acyltransferase activity as discussed in Chapter 3. HADHA uses as substrates for the acylation of monolysocardiolipin: the oleoyl-CoA, for which species it displays

the highest activity, as well as linoleoyl-CoA and palmitoleoyl-CoA. Hence, levels of FA 16:0, FA 18:1, FA 18:2 and CL molecular species, which could contain fatty acyl chain incorporation of C18:1, C18:2 and C16:0 by HADHA, were analysed (Fig.11 and Fig. 12). A trend of increase was observed in some CL molecular species of PaCa3, PaCa44, MiaPaCa2 and PC1J CSCs. On the contrary, a statistically significant decrease (95% CI) of 4,2-fold was only observed in CL 68:2 of PaCa3 CSCs. Interestingly, a statistically significant (95% CI) increase was observed in CL 64:0 (of 5-fold), CL 64:1 (of 5.5-fold), CL 66:1 (of 3.5-fold) and CL 66:5 (of 3.2-fold) in MiaPaCa2 CSCs. In addition, a 5-fold increment in CL 66:5 molecular species was detected in PC1J CSCs.

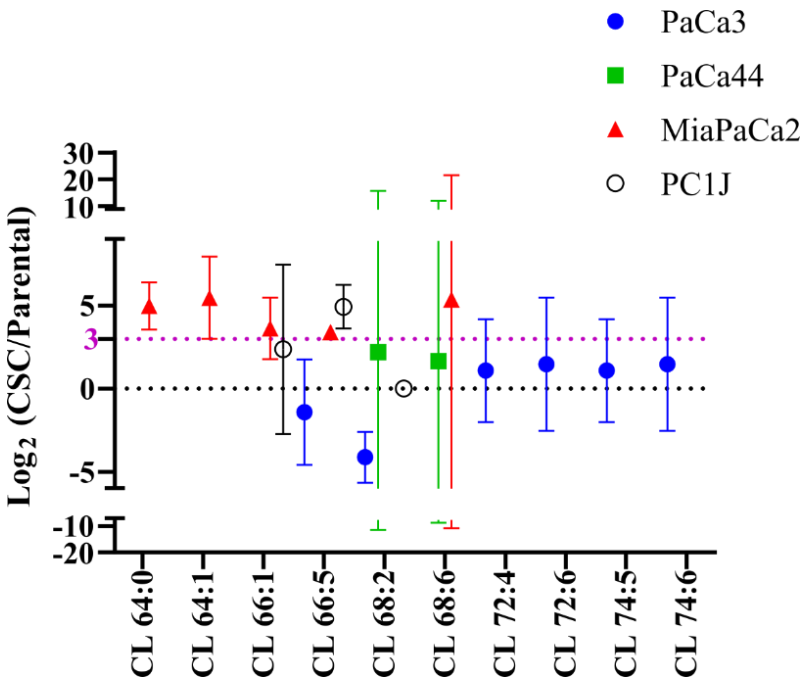

Figure 12. Log_2 ratio (CSC/P) in PaCa3 (in blue), PaCa44 (in green), MiaPaCa2 (in red) and PC1J (in white) cells CL species related to remodelling by HADHA enzyme. Log_2 of the fold change at 95% CI.

4. Discussion

4.1. Induction of long chain fatty acids and lipid droplets

High levels of long and very long FAs and accumulation of lipid droplets were observed in all four PCSCs compared to P cell lines. In accordance with previously proteomics analysis (see Chapter 3), the increase of FA levels can be related to metabolic reprogramming of PCSCs. The changes in the synthesis of FAs might represent a strategy, adopted by the PCSCs, to promote cancer development, invasion and metastasis [197]. It was well established that FA species can be used as substrates to generate more complex lipid species, such as neutral lipids (*i.e.*, DG and TG). It was demonstrated that FA incorporation is necessary to prevent the toxic effect caused by their accumulation in cells.

In regard to complex lipids, DG and TG, together with CE, are usually transferred into the intermembrane space of the endoplasmic reticulum. TG and CE are then packaged into LDs [198], where they are accumulated to eventually be used in catabolic processes. Even though the function of these lipid bodies is still not completely understood, it is well-known that they represent a principal source of energy for cells [199]. LDs are highly dynamic structures which undergo cycles of synthesis and breakdown, providing FAs to cells for mitochondrial energy production [200]. The accumulation of LDs may also protect cells against oxidative stress [201, 202], probably conferring higher aggressiveness [202] and chemoresistance to PCSCs [203, 204].

LDs presented different shapes, but the reason behind their different sizes is still unknown. Nonetheless, it was understood that the movement and fusion of small LDs can promote the formation and accumulation of larger lipid bodies [205]. Recently, it has been hypothesized that large LDs may be related to the primary function of the droplet in long-term lipid storage [201]. Large LDs were also suggested as prognostic marker for cancer progression [206]. Interestingly, it has been reported that small LDs could be highly dynamic and metabolically more active than the larger ones [206, 207].

4.2. Phosphoinositide pathway

Genes encoding for phosphoinositide lipid phosphatases were predicted as common among all four PCSC lines. The enzymes they encode can act as both protein and lipid phosphatases. As protein phosphatases they can dephosphorylate phosphatidylinositoltriphosphate (PIP3), phosphatidylinositoldiphosphate (PIP2) and phosphatidylinositolmonophosphate (PIP) substrates (see Annex Tab. 3 for more details). Among them, Pten can remove the phosphate in the D3 position of the inositol ring from PIP3, PIP2, PIP and also inositol 1,3,4,5-tetrakisphosphate (I4P) [208, 209]. If PIP is used as a substrate, the formation of phosphoinositol (PI) is favoured. Accordingly, the results presented here showed a general increase in PI levels in PaCa3, PaCa44, MiaPaCa2 and PC1J CSCs.

PI species might also serve as substrate for post-translational modification of proteins and can also modulate cell signalling [210]. This lipid sub-class plays a role in the promotion of cancer signalling, cell growth and cell survival [211, 212]. Moreover, PI levels were usually detected improved in chronic pancreatitis [213]. In addition, in glioblastoma CSCs PI levels were reported as induced [214]. Therefore, the phosphoinositide lipid phosphatases might represent a highlighted pathway, which can support key mechanisms specific for PCSCs [215].

PI species can be also regulated by phosphatidylinositol 3kinase (PI3K) [213]. This enzyme is implicated in PCSC activity [6], regulating the activation of many intracellular signalling pathways, including cell proliferation, survival, metabolism, apoptosis, growth and migration processes [216]. In addition, the activation of PI3K/AKT/mTOR signalling pathway might provide a higher resistance and aggressiveness to PCSCs [217].

4.3. Cardiolipin remodelling

Lipidomics analysis also predicted the activation of FA elongation pathways involving the *EVLOL5* gene. Its encoded protein, Elovl5, catalyses the addition of two carbon units sequentially to the carboxyl ends of both saturated and unsaturated fatty acyl CoA substrates. This elongase acts on monounsaturated FA 16:1 [218],

polyunsaturated FA 18:2 and contributes to the production of FA 20:2, FA 20:3 and FA 22:4 [219, 220]. Furthermore, some of these FA species were linked to cardiolipin (CL) remodelling by HADHA, which was detected overexpressed in all four PCSC lines (see Chapter 3) [179]. In particular, HADHA displays high activity for FA 18:1, but also for FA 18:2 and FA 16:0 species [179, 221]. Proteomics data indicated a significant enrichment of "acyl chain remodelling of CL" pathway in both MiaPaCa2 and PC1J CSCs (see Chapter 3), thus increased levels of CL species obtained by remodelling of this lipid sub-class in these two PCSC lines were identified. Recent studies demonstrated that CL remodelling might be associated with the functioning of mitochondrial membrane proteins, such as the complexes involved in the respiratory chain [181, 182]. CL mainly supports mitochondrial functions and plays a critical role in oxidative phosphorylation (OXPHOS). During this process, many protons are transferred from one side of the mitochondrial membrane to another, causing a large pH change. In this context, CL species function as a proton trap within the membranes of this organelle: this sub-class strictly localizes the proton pool, minimizing pH changes in the mitochondrial intermembrane space [184].

Moreover, recent studies have demonstrated that the inhibition of CL remodelling can reduce stemness properties and increase cell differentiation of acute myeloid leukaemia cells [222, 223]. Therefore, CL remodelling may play a pivotal role in PCSCs. This is the first time that CL remodelling has been demonstrated for a solid tumour such as PDAC and for PCSCs.

4.4. Other lipid sub-classes related to cancer stem cell maintenance

The lipid profile results detected many lipid sub-classes, some of which can be related to stemness of PCSCs. Among them some sphingolipid sub-classes, including ceramide (Cer), sphingomyelin (SM) and dihydrosphingomyelin (dhSM) were increased in all four PCSCs. Interestingly, sphingolipids play a role in tumorigenesis, metastasis and response to cancer treatments. Metabolism of these lipid sub-classes can influence the expression of genes able to regulate PCSC properties, including stemness [224]. Other authors have suggested that increased

levels of sphingolipids may promote cell survival, proliferation, adhesion and migration [225]. Specifically, Ghosh S. *et al*. (in 2020) reported that the enzymes, which mediate the degradation of Cer sub-class, can promote the activation of alternative signalling pathways of this sub-class favouring CSC chemoresistance [226].

Moreover, increased levels of some phospholipids in all four PCSCs, such as PC, PE and PS, could be related to PCSC properties [227]: particularly, the enrichment of PE species can provide a higher number of accessible binding targets on cell membranes, which could favour cell signalling [228]. Recently, several small molecules and membrane-active peptides able to bind PE and to induce membrane disruption have been identified [229, 230]. It could therefore be interesting to treat PCSCs with molecules able to target these lipid sub-classes to investigate cell response. David H.V. *et al*. (in 2019) correlated high levels of the PS sub-class with an enhanced cancer cell survival after irradiation treatment. Moreover, increased PS levels caused enhanced resistance to chemotherapy in different tumour cell lines (including the pancreatic AsPC-1, MiaPaCa2 and cfPac-1 cancer lines) in subcutaneous xenografts in nude mice [231]. However, the biological consequences of the increment of PS levels in PDAC is still unexplored.

5. Conclusions

Lipid profiles of PaCa3, PaCa44, MiaPaCa2 and PC1J CSCs and related P cells were analysed by LC-MS and LC-MS/MS analyses, which were confirmed to be powerful technologies for lipidomic analyses.

Increased levels of FAs and of neutral lipids were detected by lipidomics. The data were also confirmed by the quantification of FAs by enzymatic colorimetric assay and by the detection of LD accumulation by confocal microscopy. Confocal microscopy was especially suitable to observe LDs in PCSC spheres, allowing the acquisition of optical sections to reconstruct the three-dimensional tumour spheroids. Hence, it might be interesting to further investigate the biological consequences on the inhibition of the accumulation of FAs and LDs in PCSCs. Other analyses are necessary to better investigate these two aspects (*i.e.*, *in vitro* and/or *in vivo* tumorigenic assays, treatment with chemotherapeutic drugs, *etc.*).

The results also showed that PCSCs and P cells had major differences in the levels of lipid molecular species, accounting for significant changes in lipid metabolic pathways. Translation of the obtained lipidome into biological meaning was also performed. The data pointed out an increased synthesis of PI sub-class. In addition, the analysis revealed the crucial role of FA elongation in four PCSCs and of CL remodelling in both MiaPaCa2 and PC1J CSCs. FA elongation and CL remodelling could therefore represent attractive targets to improve the therapeutic treatments of PDAC.

In summary, these results highlighted the importance of lipid metabolism in PDAC, contributing to elucidate the biology of PDAC. In addition, this investigation may suggest possible targets for the development of new therapeutic strategies against PDAC. The data obtained in this thesis might form the basis for further research aim at the investigation of new strategies against PDAC, for example by performing *in vitro* preclinical evaluation of compounds able to act on CL remodelling and/or FA elongation pathways to reduce PCSCs vitality and to affect PDAC.

6. Annex tables

1. Common identified species in P cells and PCSCs of PaCa3, PaCa44, MiaPaCa2 and PC1J PDAC cell lines about four biological replicas.

Class	Species
CE	14:0, 16:0, 16:1, 18:0, 18:1, 18:2, 18:3, 20:1, 20:3, 20:4, 20:5, 22:6, 24:1
Cer	14:0, 16:0, 18:1, 20:0, 22:0, 22:3, 24:1, 26:1
CH	27:0
CL	66:4, 66:5, 68:2, 68:5, 68:6, 70:6
DG	32:0, 32:1, 34:0, 34:1, 36:1, 38:2, 38:3, 38:4, 38:5, 40:5, 40:6
dhCer	16:0, 18:0, 20:0, 22:0, 24:0, 24:1
dhSM	14:0, 16:0, 18:0, 20:0, 22:0
FA	16:0, 16:1, 18:0, 18:1, 18:2, 20:1, 20:2, 20.3, 20.4, 22:1, 22:6, 24:1, 24:2
LPA	16:0, 18:0, 18:1, 18:2, 20:4
LPC	16:0, 16:1, 18:0, 18:1, 18:2,18:3, 20:0, 20:1, 20:3, 20:4, 22:0, 22:1, 22:2, 22:4, 22:5, 22:6, 24:0, 24:1, 26:0
LPE	16:0, 16:1, 18:0, 18:1, 18:2, 20:4, 20:5
LPG	16:0, 16:1, 18:0, 18:1, 18:2, 18:3, 20:5, 22:6
LPI	16:0, 16:1, 18:0, 18:1, 18:2, 20:4
LPS	16:0, 18:0, 18:1, 18:2, 20:4, 22:0, 22:6, 24:0, 24:1
O-DG	32:0, 34:1, 34:2, 36:2, 40:5
O- LPA	18:0
O-LPC	16:0, 18:0, 20:0
O-LPE	16:0, 16:1, 18:1
O-PC	30:0, 30:1, 32:0, 32:1, 32:2, 32:3, 34:1, 34:2, 34:3, 36:1, 36:2, 36:3, 36:4, 36:5, 36:6, 38:1, 38:2, 38:3, 38:4, 38:5, 38:6, 38:7, 40:2, 40:4, 40:6, 40:7
O-PE	30:1, 30.2, 32:0, 32:1, 32:2, 32:3, 34:0, 34:1, 34:2, 34:3, 34:4, 36:2, 36:3, 36:4, 36:5, 38:2, 38:3, 38:4, 38:5, 38:6, 38:7, 40:2, 40:3, 40:4, 40:5, 40:6, 40:7, 40:8,
O-TG	50:2, 52:4, 52:5, 54:5, 54:6, 56:6, 56:7
PA	32:0, 32:1, 34:0, 34:1, 34:2, 36:1, 36:2, 38:2
PC	28:0, 30:0, 30:1, 32:0, 32:1, 32:2, 34:1, 34:2, 34:3, 34:4, 36:1, 36:2, 36:3, 36:4, 36:6, 38:2, 38:3, 38:5, 38:6, 40:1, 40:2, 40:3, 40:4, 40:7
PE	30:0, 30:1, 32:0, 32:1, 32:2, 34:1, 34:2, 34:3, 36:1, 36:2, 36:3, 36:4, 36:5, 38:1, 38:2, 38:3, 38:4, 38:5, 38:6, 38:7, 40:1, 40:2, 40:3, 40:4, 40:5, 40:6, 40:7
PG	30:0, 30:1, 32:0, 32:1, 32:2, 34:1, 34:2, 34:3, 36:1, 36:2, 36:3, 36:4, 36:5, 38:1, 38:2, 38:4, 38:5, 38:6
PI	32:1, 32:2, 34:1, 34:2, 34:3, 36:1, 36:2, 36:3, 36:4, 36:5, 38:1, 38:2, 38:4, 38:5, 38:6, 40:1, 40:2, 40:3, 40:4, 40:5, 40:6, 40:7
PIP	34:2, 36:1, 36:2, 36:3, 38:2, 38:3, 38:4, 40:5, 40:6
PIP2	34:1, 34:2, 36:1, 36:2, 36:3, 38:2, 38:3, 38:4, 40:5, 40:6
P-LPA	18:0
P-LPC	18:0, 20:0, 20:1
P-PC	30:0, 32:0, 34:0, 36:0, 38:0
P-PE	30:0, 32:0
PS	32:0, 32:1, 34:1, 34:2, 36:1, 36:2, 36:3, 36:4, 36:5, 38:1, 38:2, 38:3, 38:4, 38:5, 38:6, 40:1, 40:2, 40:3, 40:4, 40:5, 40:6, 40:7
SG	18:0, 18:1
SM	14:0, 16:0, 16:1, 18:0, 18:1, 20:0, 20:1, 22:0, 22:1, 22:2, 24:2, 24:3
TG	46:0, 46:1, 46:2, 46:3, 48:0, 48:1, 48:2, 48:3, 50:1, 50:2, 50:3, 50:4, 52:2, 52:3, 52:4, 52:5, 52:6, 54:3, 54:4, 54:5, 54:6, 54:7, 56:4, 56:5, 56:7, 56:8, 58:5, 58:7, 58:8

2. Venn diagram of the genes related to the lipid predicted active reactions in PaCa3, PaCa44, MiaPaCa2 and PC1J CSCs compared to P cells.

Cell lines	Predicted genes
PaCa3, PaCa44, MiaPaCa2, PC1J	*MTMR8, SYNJ2, SYNJ2, MTMR6, MTMR7, PTEN, SACM1L, MTMR9, MTMR14, SYNJ1, MTMR2, MTMR1, MTMR4, MTMR3, ELOVL5*
PaCa3, PaCa44, MiaPaCa2	*TMEM189, SGMS2, SGMS1*
PaCa3, PaCa44, PC1J	*CHPT1, CEPT1, ELOVL6*
PaCa44, MiaPaCa2, PC1J	*PLD1*
PaCa3, MiaPaCa2	*PTDSS1*
PaCa3, PC1J	*ELOVL3*
PaCa44, MiaPaCa2	*CERT1*
PaCa44, PC1J	*FADS2*
MiaPaCa2, PC1J	*PLCD1, PLCE1, INPP5E, FIG4, PLCB1, PLCB4, PLCD4, OCRL, PLCG1, PLCB2*

3. Common predicted genes, encoded phosphoinositide lipid phosphatase enzyme names and their related substrates between diagram of the genes PaCa3, PaCa44, MiaPaCa2 and PC1J CSCs compared to P cells.

Predicted genes	Encoded enzymes name	Substrate of relative catalytic activity
SYNJ1	Synaptojanin 1	PIP2
SYNJ2	Synaptojanin 2	PIP2
SACM1L	SAC1 like phosphatidylinositide phosphatase	PIP
MTMR1	Myotubularin related protein 1	PIP2
MTMR2	Myotubularin related protein 2	PIP2
MTMR3	Myotubularin related protein 3	PIP2
MTMR4	Myotubularin related protein 4	PIP3
MTMR6	Myotubularin related protein 6	PIP3, PIP2
MTMR7	Myotubularin related protein 7	PIP3
MTMR8	Myotubularin related protein 8	PIP3
MTMR9	Myotubularin related protein 9	PIP2
MTMR14	Myotubularin related protein 14	PIP3, PIP2
PTEN	Phosphatase and tensin homolog	PIP3, PIP2

General conclusion

The PhD research project presented here has provided a significant contribution towards the understanding of features of PCSCs, improving the knowledge of the signalling and metabolic changes of these cells.

Since PCSCs are responsible for PDAC chemo- and radio- resistance, tumorigenesis, and metastasis, the in-depth study proved to be extremely important in identifying the dysregulated pathways involved in PDAC and in suggesting possible new therapeutic targets to eradicate this type of tumour.

The first result was to confirm the validity of *in-vitro* generated PCSCs as a suitable cellular model which very well represented this different subpopulation of PDAC cells. In particular, four PDAC cell lines were selected for this project, *i.e.*, PaCa3, PaCa44, MiaPaCa2 and PC1J, obtaining four PCSC lines.

The project was carried out using a multi-omics approach for the analysis of proteomics and lipidomics profile of PCSCs. The proteomics analysis was based on a SWATH label free strategy. A total of 121, 186, 212 and 235 proteins have been identified as differentially expressed in PaCa3, PaCa44, MiaPaCa2 and PC1J CSCs, respectively. Among these dysregulated proteins, the mitochondrial trifunctional enzyme subunit alpha (HADHA) was particularly interesting since it was upregulated in all four PCSCs. The global implications of modulated proteins have also been elucidated, thus finding them mainly involved in different lipid metabolism related pathways, among which FA elongation and biosynthesis of unsaturated FAs were detected.

Accordingly, LC-MS and LC-MS/MS lipidomic analyses of the four PCSC lines were performed, measuring a total of 755 lipid species. Lipidomics revealed a trend towards upregulation of long and very long chain FAs in PCSCs, some of which are the products of the fatty acid elongase-5 (Elovl5) enzymatic activity, a gene related to the lipid reaction predicted as active. In particular, FA 18:1, FA 20:2, FA 20:3 and FA 22:4 species were statistically significantly increased in both MiaPaca2 and PC1J CSCs, while FA 20:4 was up in both Paca3 and MiaPaca2 CSCs.

Moreover, the integration of proteomics and lipidomics data showed the upregulation of HADHA (as above stated) and the induction in MiaPaCa2 and PC1J CSCs of molecular species of cardiolipin with mixed incorporation of FA 16:0, FA 18:1 and FA 18:2 acyl chains. Interestingly, HADHA has a monolysocardiolipin acyltransferase activity, and it uses as substrates the palmitoleoyl-CoA (C16:0-CoA), oleoyl-CoA (C18:1-CoA) as well as linoleoyl-CoA (C18:2-CoA).

In conclusion, the multi-omics analysis suggested a crucial role of cardiolipin remodelling, alpha subunit of the mitochondrial trifunctional protein and long chain FAs in stem cells of pancreatic cancer. Further investigation on dysregulated distinctive pathways of PCSCs will be required into the understanding of the role of these ways on this sub-population of cells, and to identify and to develop promising news therapies against PDAC.

Bibliography

[1] "I NUMERI DEL CANCRO IN ITALIA 2019."

[2] P. Rawla, T. Sunkara, and V. Gaduputi, "Epidemiology of Pancreatic Cancer: Global Trends, Etiology and Risk Factors," *World J Oncol,* vol. 10, no. 1, pp. 10-27, Feb 2019, doi: 10.14740/wjon1166.

[3] D. P. Ryan, T. S. Hong, and N. Bardeesy, "Pancreatic adenocarcinoma," *N Engl J Med,* vol. 371, no. 11, pp. 1039-49, Sep 11 2014, doi: 10.1056/NEJMra1404198.

[4] C. S. Yabar and J. M. Winter, "Pancreatic Cancer: A Review," *Gastroenterol Clin North Am,* vol. 45, no. 3, pp. 429-45, Sep 2016, doi: 10.1016/j.gtc.2016.04.003.

[5] A. Vincent, J. Herman, R. Schulick, R. H. Hruban, and M. Goggins, "Pancreatic cancer," *The Lancet,* vol. 378, no. 9791, pp. 607-620, 2011, doi: 10.1016/s0140-6736(10)62307-0.

[6] C. Di Carlo, J. Brandi, and D. Cecconi, "Pancreatic cancer stem cells: Perspectives on potential therapeutic approaches of pancreatic ductal adenocarcinoma," *World J Stem Cells,* vol. 10, no. 11, pp. 172-182, Nov 26 2018, doi: 10.4252/wjsc.v10.i11.172.

[7] B. W. Stewart and C. P. Wild, Eds. *World Cancer Report 2014* (World Cancer Report). 2014.

[8] C. Bosetti *et al.*, "Cigarette smoking and pancreatic cancer: an analysis from the International Pancreatic Cancer Case-Control Consortium (Panc4)," *Ann Oncol,* vol. 23, no. 7, pp. 1880-8, Jul 2012, doi: 10.1093/annonc/mdr541.

[9] C. L. Wolfgang *et al.*, "Recent progress in pancreatic cancer," *CA Cancer J Clin,* vol. 63, no. 5, pp. 318-48, Sep 2013, doi: 10.3322/caac.21190.

[10] S. Chandana, H. M. Babiker, and D. Mahadevan, "Therapeutic trends in pancreatic ductal adenocarcinoma (PDAC)," *Expert Opin Investig Drugs*, vol. 28, no. 2, pp. 161-177, Feb 2019, doi: 10.1080/13543784.2019.1557145.

[11] "Pancreatic Cancer Treatment (Adult) (PDQ®)–Health Professional Version." National Cancer Institute. http://pancreatic.org/pancreatic-cancer/about-the-pancreas/. (accessed March, 2020).

[12] S. Grover and S. Syngal, "Hereditary Pancreatic Cancer," *Gastroenterology*, vol. 139, no. 4, pp. 1076-1080.e2, 2010, doi: 10.1053/j.gastro.2010.08.012.

[13] "Pancreatic Cancer Risk Factors." https://www.cancer.org/cancer/pancreatic-cancer/causes-risks-prevention/risk-factors.html. (accessed March, 2020).

[14] J. Li, M. J. Poi, and M. D. Tsai, "Regulatory mechanisms of tumor suppressor P16(INK4A) and their relevance to cancer," *Biochemistry,* vol. 50, no. 25, pp. 5566-82, Jun 28 2011, doi: 10.1021/bi200642e.

[15] C. Caulin *et al.*, "An inducible mouse model for skin cancer reveals distinct roles for gain- and loss-of-function p53 mutations," *J Clin Invest,* vol. 117, no. 7, pp. 1893-901, Jul 2007, doi: 10.1172/JCI31721.

[16] E. L. Deer *et al.*, "Phenotype and genotype of pancreatic cancer cell lines," *Pancreas,* vol. 39, no. 4, pp. 425-35, May 2010, doi: 10.1097/MPA.0b013e3181c15963.
[17] N. Santana-Codina *et al.*, "Oncogenic KRAS supports pancreatic cancer through regulation of nucleotide synthesis," *Nat Commun,* vol. 9, no. 1, p. 4945, Nov 23 2018, doi: 10.1038/s41467-018-07472-8.
[18] Z. Fan *et al.*, "Critical role of KRAS mutation in pancreatic ductal adenocarcinoma," *Translational Cancer Research,* vol. 7, no. 6, pp. 1728-1736, 2018, doi: 10.21037/tcr.2018.10.19.
[19] E. Castellano and J. Downward, "RAS Interaction with PI3K: More Than Just Another Effector Pathway," *Genes Cancer,* vol. 2, no. 3, pp. 261-74, Mar 2011, doi: 10.1177/1947601911408079.
[20] S. Ahmed, A. D. Bradshaw, S. Gera, M. Z. Dewan, and R. Xu, "The TGF-beta/Smad4 Signaling Pathway in Pancreatic Carcinogenesis and Its Clinical Significance," *J Clin Med,* vol. 6, no. 1, Jan 5 2017, doi: 10.3390/jcm6010005.
[21] P. T. Fullerton, Jr., C. J. Creighton, and M. M. Matzuk, "Insights Into SMAD4 Loss in Pancreatic Cancer From Inducible Restoration of TGF-beta Signaling," *Mol Endocrinol,* vol. 29, no. 10, pp. 1440-53, Oct 2015, doi: 10.1210/me.2015-1102.
[22] X. X. Feng Wang, Chunying Yang, Jianliang Shen, Junhua Mai, Han-Cheon Kim, Dickson Kirui, Ya'an Kang, Jason B. Fleming, Eugene J. Koay, Sankar Mitra, Mauro Ferrari and Haifa Shen, "SMAD4 Gene Mutation Renders Pancreatic Cancer Resistance to Radiotherapy through Promotion of Autophagy," *Clin Cancer Res,* vol. 24, no. 13, pp. 2979-2980, 2018, doi: 10.1158/1078-0432.CCR-18-0291.
[23] J. Y. Kim and S. M. Hong, "Precursor Lesions of Pancreatic Cancer," *Oncol Res Treat,* vol. 41, no. 10, pp. 603-610, 2018, doi: 10.1159/000493554.
[24] R. H. Hruban *et al.*, "Pancreatic intraepithelial neoplasia: a new nomenclature and classification system for pancreatic duct lesions," *Am J Surg Pathol,* vol. 25, no. 5, pp. 579-86, May 2001, doi: 10.1097/00000478-200105000-00003.
[25] M. A. Lewis and J. C. Yao, "Molecular pathology and genetics of gastrointestinal neuroendocrine tumours," *Curr Opin Endocrinol Diabetes Obes,* vol. 21, no. 1, pp. 22-7, Feb 2014, doi: 10.1097/MED.0000000000000033.
[26] L. C. Fry, K. Monkemuller, and P. Malfertheiner, "Molecular markers of pancreatic cancer: development and clinical relevance," *Langenbecks Arch Surg,* vol. 393, no. 6, pp. 883-90, Nov 2008, doi: 10.1007/s00423-007-0276-0.
[27] T. J. Grant, K. Hua, and A. Singh, "Molecular Pathogenesis of Pancreatic Cancer," *Prog Mol Biol Transl Sci,* vol. 144, pp. 241-275, 2016, doi: 10.1016/bs.pmbts.2016.09.008.
[28] A. R. Moghadam *et al.*, "Ral signaling pathway in health and cancer," *Cancer Med,* vol. 6, no. 12, pp. 2998-3013, Dec 2017, doi: 10.1002/cam4.1105.
[29] L. Brunelli, E. Caiola, M. Marabese, M. Broggini, and R. Pastorelli, "Comparative metabolomics profiling of isogenic KRAS wild type and

mutant NSCLC cells in vitro and in vivo," *Sci Rep,* vol. 6, p. 28398, Jun 22 2016, doi: 10.1038/srep28398.
[30] F. Vogiatzi *et al.*, "Mutant p53 promotes tumor progression and metastasis by the endoplasmic reticulum UDPase ENTPD5," *Proc Natl Acad Sci U S A,* vol. 113, no. 52, pp. E8433-E8442, Dec 27 2016, doi: 10.1073/pnas.1612711114.
[31] W. Wang, B. Cheng, L. Miao, Y. Mei, and M. Wu, "Mutant p53-R273H gains new function in sustained activation of EGFR signaling via suppressing miR-27a expression," *Cell Death Dis,* vol. 4, p. e574, Apr 4 2013, doi: 10.1038/cddis.2013.97.
[32] M. Eriksson *et al.*, "Effect of Mutant p53 Proteins on Glycolysis and Mitochondrial Metabolism," *Mol Cell Biol,* vol. 37, no. 24, Dec 15 2017, doi: 10.1128/MCB.00328-17.
[33] Y. T. I Kogan-Sakin, Y Buganim, A Molchadsky, H Solomon, S Madar, I Kamer, P Stambolsky, A Shelly, N Goldfinger, S Valsesia-Wittmann, A Puisieux, A Zundelevich, E N Gal-Yam, C Avivi, I Barshack, M Brait, D Sidransky, E Domany & V Rotter, "Mutant p53R175H upregulates Twist1 expression and promotes epithelial–mesenchymal transition in immortalized prostate cells," *Cell Death and Differentiation,* vol. 18, pp. 271–281, 2010, doi: 10.1038/cdd.2010.94.
[34] S. Weissmueller *et al.*, "Mutant p53 drives pancreatic cancer metastasis through cell-autonomous PDGF receptor beta signaling," *Cell,* vol. 157, no. 2, pp. 382-394, Apr 10 2014, doi: 10.1016/j.cell.2014.01.066.
[35] X. Zhou, Q. Hao, and H. Lu, "Mutant p53 in cancer therapy-the barrier or the path," *J Mol Cell Biol,* vol. 11, no. 4, pp. 293-305, Apr 1 2019, doi: 10.1093/jmcb/mjy072.
[36] X. Liao *et al.*, "Clinicopathological characterization of SMAD4-mutated intestinal adenocarcinomas: A case-control study," *PLoS One,* vol. 14, no. 2, p. e0212142, 2019, doi: 10.1371/journal.pone.0212142.
[37] G. Bond-Smith, N. Banga, T. M. Hammond, and C. J. Imber, "Pancreatic adenocarcinoma," *Bmj,* vol. 344, no. may16 1, pp. e2476-e2476, 2012, doi: 10.1136/bmj.e2476.
[38] C. Guillén-Ponce, J. Blázquez, I. González, E. de-Madaria, J. Montáns, and A. Carrato, "Diagnosis and staging of pancreatic ductal adenocarcinoma," *Clinical and Translational Oncology,* vol. 19, no. 10, pp. 1205-1216, 2017, doi: 10.1007/s12094-017-1681-7.
[39] K. Okano *et al.*, "18F-fluorodeoxyglucose positron emission tomography to indicate conversion surgery in patients with initially unresectable locally advanced pancreatic cancer," *Japanese Journal of Clinical Oncology,* vol. 48, no. 5, pp. 434-441, 2018, doi: 10.1093/jjco/hyy033.
[40] L. van Manen *et al.*, "Elevated CEA and CA19-9 serum levels independently predict advanced pancreatic cancer at diagnosis," *Biomarkers,* vol. 25, no. 2, pp. 186-193, 2020, doi: 10.1080/1354750x.2020.1725786.
[41] H. Dou, G. Sun, and L. Zhang, "CA242 as a biomarker for pancreatic cancer and other diseases," in *Glycans and Glycosaminoglycans as Clinical Biomarkers and Therapeutics - Part A,* (Progress in Molecular Biology and Translational Science, 2019, pp. 229-239.

[42] X. G. Ni *et al.*, "The clinical value of serum CEA, CA19-9, and CA242 in the diagnosis and prognosis of pancreatic cancer," *European Journal of Surgical Oncology (EJSO)*, vol. 31, no. 2, pp. 164-169, 2005, doi: 10.1016/j.ejso.2004.09.007.

[43] "Clinical manifestations, diagnosis, and staging of exocrine pancreatic cancer - UpToDate." https://www.uptodate.com/contents/clinical-manifestations-diagnosis-and-staging-of-exocrine-pancreatic-cancer#H18017084 (accessed March, 2020).

[44] S. Cascinu, M. Falconi, V. Valentini, S. Jelic, and E. G. W. Group, "Pancreatic cancer: ESMO Clinical Practice Guidelines for diagnosis, treatment and follow-up," *Ann Oncol*, vol. 21 Suppl 5, pp. v55-8, May 2010, doi: 10.1093/annonc/mdq165.

[45] "TNM staging | Pancreatic cancer " https://www.cancerresearchuk.org/about-cancer/pancreatic-cancer/stages-types-grades/tnm-staging (accessed March, 2020).

[46] M. Amrutkar and I. P. Gladhaug, "Pancreatic Cancer Chemoresistance to Gemcitabine," *Cancers (Basel)*, vol. 9, no. 11, Nov 16 2017, doi: 10.3390/cancers9110157.

[47] C. Liang *et al.*, "Complex roles of the stroma in the intrinsic resistance to gemcitabine in pancreatic cancer: where we are and where we are going," *Experimental & Molecular Medicine*, vol. 49, no. 12, pp. e406-e406, 2017, doi: 10.1038/emm.2017.255.

[48] T. Saito *et al.*, "Combination therapy with gemcitabine and nab-paclitaxel for locally advanced unresectable pancreatic cancer," *Molecular and Clinical Oncology*, vol. 6, no. 6, pp. 963-967, 2017, doi: 10.3892/mco.2017.1251.

[49] M. C. Cabrera, "Cancer stem cell plasticity and tumor hierarchy," *World Journal of Stem Cells*, vol. 7, no. 1, p. 27, 2015, doi: 10.4252/wjsc.v7.i1.27.

[50] S. Santamaria, M. Delgado, L. Kremer, and J. A. Garcia-Sanz, "Will a mAb-Based Immunotherapy Directed against Cancer Stem Cells Be Feasible?," *Front Immunol*, vol. 8, p. 1509, 2017, doi: 10.3389/fimmu.2017.01509.

[51] V. Plaks, N. Kong, and Z. Werb, "The cancer stem cell niche: how essential is the niche in regulating stemness of tumor cells?," *Cell Stem Cell*, vol. 16, no. 3, pp. 225-38, Mar 5 2015, doi: 10.1016/j.stem.2015.02.015.

[52] S. M. Dieter *et al.*, "Distinct types of tumor-initiating cells form human colon cancer tumors and metastases," *Cell Stem Cell*, vol. 9, no. 4, pp. 357-65, Oct 4 2011, doi: 10.1016/j.stem.2011.08.010.

[53] S. Valle, L. Martin-Hijano, S. Alcalá, M. Alonso-Nocelo, and B. Sainz Jr, "The Ever-Evolving Concept of the Cancer Stem Cell in Pancreatic Cancer," *Cancers*, vol. 10, no. 2, 2018, doi: 10.3390/cancers10020033.

[54] J. Brandi *et al.*, "Proteomic analysis of pancreatic cancer stem cells: Functional role of fatty acid synthesis and mevalonate pathways," *J Proteomics*, vol. 150, pp. 310-322, Jan 6 2017, doi: 10.1016/j.jprot.2016.10.002.

[55] C. Li *et al.*, "Identification of Pancreatic Cancer Stem Cells," *Cancer Research*, vol. 67, no. 3, pp. 1030-1037, 2007, doi: 10.1158/0008-5472.Can-06-2030.

[56] C. A. O'Brien, A. Kreso, and C. H. M. Jamieson, "Cancer Stem Cells and Self-renewal," *clinical Cancer Research,* vol. 16, no. 12, pp. 3113-20, 2010, doi: 10.1158/1078-0432.CCR-09-2824.

[57] N. Facompre, H. Nakagawa, M. Herlyn, and D. Basu, "Stem-like cells and therapy resistance in squamous cell carcinomas," *Adv Pharmacol,* vol. 65, pp. 235-65, 2012, doi: 10.1016/B978-0-12-397927-8.00008-7.

[58] S. Garcia-Silva, J. Frias-Aldeguer, and C. Heeschen, "Stem cells & pancreatic cancer," *Pancreatology,* vol. 13, no. 2, pp. 110-3, Mar-Apr 2013, doi: 10.1016/j.pan.2012.12.003.

[59] K. N. Plaks V., and Werb Z. , "The cancer stem cell niche: How essential is the niche in regulating stemness of tumor cells?," *Cell Stem Cell,* vol. 16, no. 3, pp. 225–238, 2015, doi: 10.1016/j.stem.2015.02.015.

[60] C. V. Rao and A. Mohammed, "New insights into pancreatic cancer stem cells," *World J Stem Cells,* vol. 7, no. 3, pp. 547-55, Apr 26 2015, doi: 10.4252/wjsc.v7.i3.547.

[61] S. Dawood, L. Austin, and M. Cristofanilli, "Cancer stem cells: implications for cancer therapy," *Oncology (Williston Park),* vol. 28, no. 12, pp. 1101-7, 1110, Dec 2014. [Online]. Available: https://www.ncbi.nlm.nih.gov/pubmed/25510809.

[62] J. F.-A. S. García-Silva, and C. Heeschen, "Stem cells & pancreatic cancer," *Pancreatology,* vol. 13, no. 2, pp. 110–113, 2013, doi: 10.1016/j.pan.2012.12.003.

[63] T. Shibue and R. A. Weinberg, "EMT, CSCs, and drug resistance: the mechanistic link and clinical implications," *Nat Rev Clin Oncol,* vol. 14, no. 10, pp. 611-629, Oct 2017, doi: 10.1038/nrclinonc.2017.44.

[64] S. Meidhof *et al.*, "ZEB1-associated drug resistance in cancer cells is reversed by the class I HDAC inhibitor mocetinostat," *EMBO Mol Med,* vol. 7, no. 6, pp. 831-47, Jun 2015, doi: 10.15252/emmm.201404396.

[65] J. H. Taube *et al.*, "Core epithelial-to-mesenchymal transition interactome gene-expression signature is associated with claudin-low and metaplastic breast cancer subtypes," *Proc Natl Acad Sci U S A,* vol. 107, no. 35, pp. 15449-54, Aug 31 2010, doi: 10.1073/pnas.1004900107.

[66] A. D. Rhim *et al.*, "EMT and dissemination precede pancreatic tumor formation," *Cell,* vol. 148, no. 1-2, pp. 349-61, Jan 20 2012, doi: 10.1016/j.cell.2011.11.025.

[67] A. Mielgo, M. van Driel, A. Bloem, L. Landmann, and U. Gunthert, "A novel antiapoptotic mechanism based on interference of Fas signaling by CD44 variant isoforms," *Cell Death Differ,* vol. 13, no. 3, pp. 465-77, Mar 2006, doi: 10.1038/sj.cdd.4401763.

[68] A. Gzil, I. Zarebska, W. Bursiewicz, P. Antosik, D. Grzanka, and L. Szylberg, "Markers of pancreatic cancer stem cells and their clinical and therapeutic implications," *Mol Biol Rep,* vol. 46, no. 6, pp. 6629-6645, Dec 2019, doi: 10.1007/s11033-019-05058-1.

[69] H. Sun *et al.*, "The Pancreatic Cancer-Initiating Cell Marker CD44v6 Affects Transcription, Translation, and Signaling: Consequences for Exosome Composition and Delivery," *J Oncol,* vol. 2019, p. 3516973, 2019, doi: 10.1155/2019/3516973.

[70] Z. Wang, H. Sun, J. Provaznik, T. Hackert, and M. Zoller, "Pancreatic cancer-initiating cell exosome message transfer into noncancer-initiating cells: the importance of CD44v6 in reprogramming," *J Exp Clin Cancer Res,* vol. 38, no. 1, p. 132, Mar 19 2019, doi: 10.1186/s13046-019-1129-8.
[71] Z. Zhou *et al.*, "The CD24+ cell subset promotes invasion and metastasis in human osteosarcoma," *EBioMedicine,* vol. 51, 2020, doi: 10.1016/j.ebiom.2019.102598.
[72] J. H. Lee, S. H. Kim, E. S. Lee, and Y. S. Kim, "CD24 overexpression in cancer development and progression: a meta-analysis," *Oncol Rep,* vol. 22, no. 5, pp. 1149-56, Nov 2009, doi: 10.3892/or_00000548.
[73] D. Maetzel *et al.*, "Nuclear signalling by tumour-associated antigen EpCAM," *Nat Cell Biol,* vol. 11, no. 2, pp. 162-71, Feb 2009, doi: 10.1038/ncb1824.
[74] P. C. Hermann *et al.*, "Distinct populations of cancer stem cells determine tumor growth and metastatic activity in human pancreatic cancer," *Cell Stem Cell,* vol. 1, no. 3, pp. 313-23, Sep 13 2007, doi: 10.1016/j.stem.2007.06.002.
[75] A. Nomura *et al.*, "CD133 initiates tumors, induces epithelial-mesenchymal transition and increases metastasis in pancreatic cancer," *Oncotarget,* vol. 6, no. 10, pp. 8313–8322, 2015, doi: 10.18632/oncotarget.3228.
[76] R. Marechal *et al.*, "High expression of CXCR4 may predict poor survival in resected pancreatic adenocarcinoma," *Br J Cancer,* vol. 100, no. 9, pp. 1444-51, May 5 2009, doi: 10.1038/sj.bjc.6605020.
[77] G. Vassalli, "Aldehyde Dehydrogenases: Not Just Markers, but Functional Regulators of Stem Cells," *Stem cells international,* 3904645, 2019, doi: 10.1155/2019/3904645.
[78] C. Li *et al.*, "c-Met is a marker of pancreatic cancer stem cells and therapeutic target," *Gastroenterology,* vol. 141, no. 6, pp. 2218-2227 e5, Dec 2011, doi: 10.1053/j.gastro.2011.08.009.
[79] W. Scheper and S. Copray, "The molecular mechanism of induced pluripotency: a two-stage switch," *Stem Cell Rev Rep,* vol. 5, no. 3, pp. 204-23, Sep 2009, doi: 10.1007/s12015-009-9077-x.
[80] H. Lin *et al.*, "Knockdown of OCT4 suppresses the growth and invasion of pancreatic cancer cells through inhibition of the AKT pathway," *Mol Med Rep,* vol. 10, no. 3, pp. 1335-42, Sep 2014, doi: 10.3892/mmr.2014.2367.
[81] M. Herreros-Villanueva *et al.*, "SOX2 promotes dedifferentiation and imparts stem cell-like features to pancreatic cancer cells," *Oncogenesis,* vol. 2, p. e61, Aug 5 2013, doi: 10.1038/oncsis.2013.23.
[82] W. Zhang, Y. Sui, J. Ni, and T. Yang, "Insights into the Nanog gene: A propeller for stemness in primitive stem cells," *Int J Biol Sci,* vol. 12, no. 11, pp. 1372-1381, 2016, doi: 10.7150/ijbs.16349.
[83] E. Pelosi, G. Castelli, and U. Testa, "Pancreatic Cancer: Molecular Characterization, Clonal Evolution and Cancer Stem Cells," *Biomedicines,* vol. 5, no. 4, Nov 18 2017, doi: 10.3390/biomedicines5040065.
[84] H. Clevers and R. Nusse, "Wnt/beta-catenin signaling and disease," *Cell,* vol. 149, no. 6, pp. 1192-205, Jun 8 2012, doi: 10.1016/j.cell.2012.05.012.

[85] H. Aberle, A. Bauer, J. Stappert, A. Kispert, and R. Kemler, "beta-catenin is a target for the ubiquitin-proteasome pathway," *EMBO J,* vol. 16, no. 13, pp. 3797-804, Jul 1 1997, doi: 10.1093/emboj/16.13.3797.

[86] Y. Komiya and R. Habas, "Wnt signal transduction pathways," *Organogenesis,* vol. 4, no. 2, pp. 68-75, Apr 2008, doi: 10.4161/org.4.2.5851.

[87] I. Ackers and R. Malgor, "Interrelationship of canonical and non-canonical Wnt signalling pathways in chronic metabolic diseases," *Diab Vasc Dis Res,* vol. 15, no. 1, pp. 3-13, Jan 2018, doi: 10.1177/1479164117738442.

[88] A. L. Garcia, A. Udeh, K. Kalahasty, and A. S. Hackam, "A growing field: The regulation of axonal regeneration by Wnt signaling," *Neural Regen Res,* vol. 13, no. 1, pp. 43-52, Jan 2018, doi: 10.4103/1673-5374.224359.

[89] I. N. Sari, L. T. H. Phi, N. Jun, Y. T. Wijaya, S. Lee, and H. Y. Kwon, "Hedgehog Signaling in Cancer: A Prospective Therapeutic Target for Eradicating Cancer Stem Cells," *Cells,* vol. 7, no. 11, Nov 10 2018, doi: 10.3390/cells7110208.

[90] K. S. Jeng, C. F. Chang, and S. S. Lin, "Sonic Hedgehog Signaling in Organogenesis, Tumors, and Tumor Microenvironments," *Int J Mol Sci,* vol. 21, no. 3, Jan 23 2020, doi: 10.3390/ijms21030758.

[91] J. Fu *et al.*, "GANT-61 inhibits pancreatic cancer stem cell growth in vitro and in NOD/SCID/IL2R gamma null mice xenograft," *Cancer Lett,* vol. 330, no. 1, pp. 22-32, Mar 1 2013, doi: 10.1016/j.canlet.2012.11.018.

[92] G. B. Carballo, J. R. Honorato, G. P. F. de Lopes, and T. Spohr, "A highlight on Sonic hedgehog pathway," *Cell Commun Signal,* vol. 16, no. 1, p. 11, Mar 20 2018, doi: 10.1186/s12964-018-0220-7.

[93] D. J. Robbins, D. L. Fei, and N. A. Riobo, "The Hedgehog signal transduction network," *Sci Signal,* vol. 5, no. 246, p. re6, Oct 16 2012, doi: 10.1126/scisignal.2002906.

[94] C. Karamboulas and L. Ailles, "Developmental signaling pathways in cancer stem cells of solid tumors," *Biochim Biophys Acta,* vol. 1830, no. 2, pp. 2481-95, Feb 2013, doi: 10.1016/j.bbagen.2012.11.008.

[95] E. V. Abel *et al.*, "The Notch pathway is important in maintaining the cancer stem cell population in pancreatic cancer," *PLoS One,* vol. 9, no. 3, p. e91983, 2014, doi: 10.1371/journal.pone.0091983.

[96] C. K. a. L. Ailles, "Developmental signaling pathways in cancer stem cells of solid tumors," *Biochimica et Biophysica Acta - General Subjects,* vol. 1830, no. 2, pp. 2481–2495, 2013, doi: 10.1016/j.bbagen.2012.11.008.

[97] A. Viale *et al.*, "Oncogene ablation-resistant pancreatic cancer cells depend on mitochondrial function," *Nature,* vol. 514, no. 7524, pp. 628-632, 2014, doi: 10.1038/nature13611.

[98] S. Galavotti *et al.*, "The autophagy-associated factors DRAM1 and p62 regulate cell migration and invasion in glioblastoma stem cells," *Oncogene,* vol. 32, no. 6, pp. 699-712, 2012, doi: 10.1038/onc.2012.111.

[99] N. S. Katheder *et al.*, "Microenvironmental autophagy promotes tumour growth," *Nature,* vol. 541, no. 7637, pp. 417-420, Jan 19 2017, doi: 10.1038/nature20815.

[100] A. Yang *et al.*, "Autophagy Sustains Pancreatic Cancer Growth through Both Cell-Autonomous and Nonautonomous Mechanisms," *Cancer Discov*, vol. 8, no. 3, pp. 276-287, Mar 2018, doi: 10.1158/2159-8290.CD-17-0952.
[101] L. Q. Li, D. Pan, S. W. Zhang, Y. X. D., X. L. Zheng, and H. Chen, "Autophagy regulates chemoresistance of gastric cancer stem cells via the Notch signaling pathway," *Eur Rev Med Pharmacol Sci,* vol. 22, no. 11, pp. 3402-3407, Jun 2018, doi: 10.26355/eurrev_201806_15162.
[102] J. A. Engelman, J. Luo, and L. C. Cantley, "The evolution of phosphatidylinositol 3-kinases as regulators of growth and metabolism," *Nature Reviews Genetics,* vol. 7, no. 8, pp. 606-619, 2006, doi: 10.1038/nrg1879.
[103] N. Chalhoub and S. J. Baker, "PTEN and the PI3-kinase pathway in cancer," *Annu Rev Pathol,* vol. 4, pp. 127-50, 2009, doi: 10.1146/annurev.pathol.4.110807.092311.
[104] S. Matsubara, Q. Ding, Y. Miyazaki, T. Kuwahata, K. Tsukasa, and S. Takao, "mTOR plays critical roles in pancreatic cancer stem cells through specific and stemness-related functions," *Scientific Reports,* vol. 3, no. 1, 2013, doi: 10.1038/srep03230.
[105] E. Giovannetti *et al.*, "MicroRNA-21 in pancreatic cancer: correlation with clinical outcome and pharmacologic aspects underlying its role in the modulation of gemcitabine activity," *Cancer Res,* vol. 70, no. 11, pp. 4528-38, Jun 1 2010, doi: 10.1158/0008-5472.CAN-09-4467.
[106] N. C. a. S. J. Baker, "PTEN and the PI3-Kinase Pathway in Cancer," *Annual Review of Pathology: Mechanisms of Disease,* vol. 4, no. 1, pp. 127–150, 2009, doi: 10.1146/annurev.pathol.4.110807.092311.
[107] A. L. Rinkenbaugh and A. S. Baldwin, "The NF-kappaB Pathway and Cancer Stem Cells," *Cells,* vol. 5, no. 2, Apr 6 2016, doi: 10.3390/cells5020016.
[108] K. Pramanik, M. Makena, K. Bhowmick, and M. Pandey, "Advancement of NF-κB Signaling Pathway: A Novel Target in Pancreatic Cancer," *International Journal of Molecular Sciences,* vol. 19, no. 12, 2018, doi: 10.3390/ijms19123890.
[109] M. Schenk, B. Aykut, C. Teske, N. A. Giese, J. Weitz, and T. Welsch, "Salinomycin inhibits growth of pancreatic cancer and cancer cell migration by disruption of actin stress fiber integrity," *Cancer Lett,* vol. 358, no. 2, pp. 161-169, Mar 28 2015, doi: 10.1016/j.canlet.2014.12.037.
[110] R. Lamb *et al.*, "Antibiotics that target mitochondria effectively eradicate cancer stem cells, across multiple tumor types: treating cancer like an infectious disease," *Oncotarget,* vol. 6, no. 7, pp. 4569-84, Mar 10 2015, doi: 10.18632/oncotarget.3174.
[111] A. Balic *et al.*, "Chloroquine targets pancreatic cancer stem cells via inhibition of CXCR4 and hedgehog signaling," *Mol Cancer Ther,* vol. 13, no. 7, pp. 1758-71, Jul 2014, doi: 10.1158/1535-7163.MCT-13-0948.
[112] M. Fiorillo *et al.*, "Repurposing atovaquone: targeting mitochondrial complex III and OXPHOS to eradicate cancer stem cells," *Oncotarget,* vol. 7, no. 23, pp. 34084-99, Jun 7 2016, doi: 10.18632/oncotarget.9122.
[113] A. Mohammed *et al.*, "Antidiabetic Drug Metformin Prevents Progression of Pancreatic Cancer by Targeting in Part Cancer Stem Cells and mTOR

Signaling," *Transl Oncol,* vol. 6, no. 6, pp. 649-59, Dec 1 2013, doi: 10.1593/tlo.13556.
[114] Y. Zhang *et al.*, "Aspirin counteracts cancer stem cell features, desmoplasia and gemcitabine resistance in pancreatic cancer," *Oncotarget,* vol. 6, no. 12, pp. 9999-10015, Apr 30 2015, doi: 10.18632/oncotarget.3171.
[115] J. Brandi *et al.*, "Secretome protein signature of human pancreatic cancer stem-like cells," *J Proteomics,* vol. 136, pp. 1-12, Mar 16 2016, doi: 10.1016/j.jprot.2016.01.017.
[116] Y. S. Kida *et al.*, "ERRs Mediate a Metabolic Switch Required for Somatic Cell Reprogramming to Pluripotency," *Cell Stem Cell,* vol. 16, no. 5, pp. 547-55, May 7 2015, doi: 10.1016/j.stem.2015.03.001.
[117] F. Yang *et al.*, "Liposome based delivery systems in pancreatic cancer treatment: from bench to bedside," *Cancer Treat Rev,* vol. 37, no. 8, pp. 633-42, Dec 2011, doi: 10.1016/j.ctrv.2011.01.006.
[118] A. Saneja *et al.*, "Development and mechanistic insight into enhanced cytotoxic potential of hyaluronic acid conjugated nanoparticles in CD44 overexpressing cancer cells," *Eur J Pharm Sci,* vol. 97, pp. 79-91, Jan 15 2017, doi: 10.1016/j.ejps.2016.10.028.
[119] E. Dalla Pozza *et al.*, "Pancreatic ductal adenocarcinoma cell lines display a plastic ability to bidirectionally convert into cancer stem cells," *Int J Oncol,* vol. 46, no. 3, pp. 1099-108, Mar 2015, doi: 10.3892/ijo.2014.2796.
[120] P. Huang, C. Y. Wang, S. M. Gou, H. S. Wu, T. Liu, and J. X. Xiong, "Isolation and biological analysis of tumor stem cells from pancreatic adenocarcinoma," *World J Gastroenterol,* vol. 14, no. 24, pp. 3903-7, Jun 28 2008, doi: 10.3748/wjg.14.3903.
[121] G. Yiben, F. Jie, L. Pang-Kuo, S. Wang, W. Qian, and H. Chen, "The effect of B27 supplement on promoting in vitro propagation of Her2/neu-transformed mammary tumorspheres," *Journal of Biotech Research,* vol. 12, 3, pp. 7–18, 2011.
[122] S. O. Min, S. W. Lee, S. Y. Bak, and K. S. Kim, "Ideal sphere-forming culture conditions to maintain pluripotency in a hepatocellular carcinoma cell lines," *Cancer Cell Int,* vol. 15, p. 95, 2015, doi: 10.1186/s12935-015-0240-y.
[123] I. D. Elisa Dalla Pozza, Giulia Biondani, Jessica Brandi, Chiara Costanzo, Elisa Zoratti, Matteo Fassan, Federico Boschi, Davide Melisi, Daniela Cecconi, Maria Teresa Scupoli, Aldo Scarpa, Marta Palmieri, "Pancreatic ductal adenocarcinoma cell lines display a plastic ability to bi-directionally convert into cancer stem cells," *International Journal of Oncology reports,* vol. 46, no. 3, pp. 1099-108, 2014, doi: 10.3892/ijo.2014.2796.
[124] W. J. Griffiths and Y. Wang, "Mass spectrometry: from proteomics to metabolomics and lipidomics," *Chem Soc Rev,* vol. 38, no. 7, pp. 1882-96, Jul 2009, doi: 10.1039/b618553n.
[125] D. J. Stephenson, L. A. Hoeferlin, and C. E. Chalfant, "Lipidomics in translational research and the clinical significance of lipid-based biomarkers," *Transl Res,* vol. 189, pp. 13-29, Nov 2017, doi: 10.1016/j.trsl.2017.06.006.

[126] D. Hu *et al.*, "Proteomic analyses identify prognostic biomarkers for pancreatic ductal adenocarcinoma," *Oncotarget*, vol. 9, no. 11, pp. 9789-9807, Feb 9 2018, doi: 10.18632/oncotarget.23929.
[127] R. A. Moffitt *et al.*, "Virtual microdissection identifies distinct tumor- and stroma-specific subtypes of pancreatic ductal adenocarcinoma," *Nat Genet*, vol. 47, no. 10, pp. 1168-78, Oct 2015, doi: 10.1038/ng.3398.
[128] H. Kim, J. Park, J. I. Wang, and Y. Kim, "Recent advances in proteomic profiling of pancreatic ductal adenocarcinoma and the road ahead," *Expert Rev Proteomics*, vol. 14, no. 11, pp. 963-971, Nov 2017, doi: 10.1080/14789450.2017.1382356.
[129] M. Saison-Ridinger *et al.*, "Reprogramming pancreatic stellate cells via p53 activation: A putative target for pancreatic cancer therapy," *PLoS One*, vol. 12, no. 12, p. e0189051, 2017, doi: 10.1371/journal.pone.0189051.
[130] F. R. Auciello *et al.*, "A Stromal Lysolipid-Autotaxin Signaling Axis Promotes Pancreatic Tumor Progression," *Cancer Discov*, vol. 9, no. 5, pp. 617-627, May 2019, doi: 10.1158/2159-8290.CD-18-1212.
[131] J. M. Urman *et al.*, "Pilot Multi-Omic Analysis of Human Bile from Benign and Malignant Biliary Strictures: A Machine-Learning Approach," *Cancers (Basel)*, vol. 12, no. 6, Jun 21 2020, doi: 10.3390/cancers12061644.
[132] C. L. Lan Dai, Kerby A. Shedden, Cheong J. Lee‖, Chenwei Li‖, HuyVuong Quoc†, Diane M. Simeone‖, and David M. Lubman, "Quantitative Proteomic Profiling Studies of Pancreatic Cancer Stem Cells," *J. Proteom.*, vol. 9, no. 7, pp. 3394–3402, 2010, doi: 10.1021/pr100231m.
[133] J. H. Jianhui Zhu, Yashu Liu, Diane M. Simeone, and David M. Lubman, "Identification of Glycoprotein Markers for Pancreatic Cancer CD24+CD44+ Stem-like Cells Using Nano-LC–MS/MS and Tissue Microarray," *J. Proteom.*, vol. 11, no. 4, pp. 2272–2281, 2012, doi: 10.1021/pr201059g.
[134] S. N. Jianhui Zhu, Jing Wu, and David M. Lubman, "Target Proteomic Profiling of Frozen Pancreatic CD24+ Adenocarcinoma Tissues by Immuno-Laser Capture Microdissection and Nano-LC–MS/MS," *J. Proteom.*, vol. 12, no. 6, pp. 2791–2804, 2013, doi: 10.1021/pr400139c.
[135] K. Y. Satoshi Matsukuma, Tomio Ueno, Atsunori Oga, Moeko Inoue, Yusaku Watanabe, Atsuo Kuramasu, Masanori Fuse, Ryouichi Tsunedomi, Satoshi Nagaoka, Hidetoshi Eguchi, Hiroto Matsui, Yoshitaro Shindo, Noriko Maeda, Yoshihiro Tokuhisa, Reo Kawano, Tomoko Furuya-Kondo, Hiroshi Itoh, Shigefumi Yoshino, Shoichi Hazama, Masaaki Oka, Hiroaki Nagano, "Calreticulin is highly expressed in pancreatic cancer stem-like cells," *Cancer Sci*, vol. 107, no. 11, pp. 1599-1609, 2016, doi: 10.1111/cas.13061.
[136] Y. Y. Choi S, Kim H, Lee H, Chung H, Nam MH, Moon JY, Lee HS, Yoon S, Kim WY, "Clinical and biochemical relevance of monounsaturated fatty acid metabolism targeting strategy for cancer stem cell elimination in colon cancer.," *Biochem. Biophys. Res. Commun.*, vol. 519, no. 1, pp. 100-105, 2019, doi: 10.1016/j.bbrc.2019.08.137.
[137] S. C. Junjie Li, Jessica Thomes-Pepin, Xiaoxiao Ma, Yu Xia, Thomas D Hurley, Daniela Matei, Ji-Xin Cheng "Lipid Desaturation Is a Metabolic

Marker and Therapeutic Target of Ovarian Cancer Stem Cells," *Cell Stem Cell,* vol. 20, no. 3, pp. 303-314.e5., 2016, doi: 10.1016/j.stem.2016.11.004.
[138] Kazuhito Naka *et al.*, "The lysophospholipase D enzyme Gdpd3 is required to maintain chronic myelogenous leukaemia stem cells," *Nat Commun,* vol. 17, no. 11, 2020, doi: 10.1038/s41467-020-18491-9.
[139] Norelle C Wildburger *et al.*, "ESI-MS/MS and MALDI-IMS Localization Reveal Alterations in Phosphatidic Acid, Diacylglycerol, and DHA in Glioma Stem Cell Xenografts," *J Proteome Res,* vol. 14, no. 6, pp. 2511-9, 2015, doi: 10.1021/acs.jproteome.5b00076.
[140] Irma Magaly Rivas Serna *et al.*, "A Lipidomic Signature Complements Stemness Features Acquisition in Liver Cancer Cells," *Int J Mol Sci,* vol. 21, no. 22, 2020, doi: 10.3390/ijms21228452.
[141] Anita Vasudevan *et al.*, "Omega-3 fatty acid is a potential preventive agent for recurrent colon cancer," *Cancer Prev Res,* vol. 7, no. 11, pp. 1138-48, 2015, doi: 10.1158/1940-6207.
[142] M. Herreros-Villanueva, L. Bujanda, D. D. Billadeau, and J. S. Zhang, "Embryonic stem cell factors and pancreatic cancer," *World J Gastroenterol,* vol. 20, no. 9, pp. 2247-54, Mar 7 2014, doi: 10.3748/wjg.v20.i9.2247.
[143] G. Ambrosini *et al.*, "Progressively De-Differentiated Pancreatic Cancer Cells Shift from Glycolysis to Oxidative Metabolism and Gain a Quiescent Stem State," *Cells,* vol. 9, no. 7, Jun 28 2020, doi: 10.3390/cells9071572.
[144] P. Yin *et al.*, "Fzd2 Contributes to Breast Cancer Cell Mesenchymal-Like Stemness and Drug Resistance," *Oncol Res,* vol. 28, no. 3, pp. 273-284, May 29 2020, doi: 10.3727/096504020X15783052025051.
[145] Z. Wang *et al.*, "Cyclin B1/Cdk1 coordinates mitochondrial respiration for cell-cycle G2/M progression," *Dev Cell,* vol. 29, no. 2, pp. 217-32, Apr 28 2014, doi: 10.1016/j.devcel.2014.03.012.
[146] C. C. Linder, "Genetic variables that influence phenotype," *ILAR J,* vol. 47, no. 2, pp. 132-40, 2006, doi: 10.1093/ilar.47.2.132.
[147] K. Ortmayr, S. Dubuis, and M. Zampieri, "Metabolic profiling of cancer cells reveals genome-wide crosstalk between transcriptional regulators and metabolism," *Nat Commun,* vol. 10, no. 1, p. 1841, Apr 23 2019, doi: 10.1038/s41467-019-09695-9.
[148] J. Brandi *et al.*, "Investigating the Proteomic Profile of HT-29 Colon Cancer Cells After Lactobacillus kefiri SGL 13 Exposure Using the SWATH Method," *J Am Soc Mass Spectrom,* vol. 30, no. 9, pp. 1690-1699, Sep 2019, doi: 10.1007/s13361-019-02268-6.
[149] L. B. Weiswald, D. Bellet, and V. Dangles-Marie, "Spherical cancer models in tumor biology," *Neoplasia,* vol. 17, no. 1, pp. 1-15, Jan 2015, doi: 10.1016/j.neo.2014.12.004.
[150] T. Ishiguro, H. Ohata, A. Sato, K. Yamawaki, T. Enomoto, and K. Okamoto, "Tumor-derived spheroids: Relevance to cancer stem cells and clinical applications," *Cancer Sci,* vol. 108, no. 3, pp. 283-289, Mar 2017, doi: 10.1111/cas.13155.
[151] F. Wang *et al.*, "Isolation and characterization of intestinal stem cells based on surface marker combinations and colony-formation assay,"

Gastroenterology, vol. 145, no. 2, pp. 383-95 e1-21, Aug 2013, doi: 10.1053/j.gastro.2013.04.050.
[152] S. Amini, F. Fathi, J. Mobalegi, H. Sofimajidpour, and T. Ghadimi, "The expressions of stem cell markers: Oct4, Nanog, Sox2, nucleostemin, Bmi, Zfx, Tcl1, Tbx3, Dppa4, and Esrrb in bladder, colon, and prostate cancer, and certain cancer cell lines," *Anat Cell Biol,* vol. 47, no. 1, pp. 1-11, Mar 2014, doi: 10.5115/acb.2014.47.1.1.
[153] J. Organista-Nava *et al.*, "The HPV16 E7 oncoprotein increases the expression of Oct3/4 and stemness-related genes and augments cell self-renewal," *Virology,* vol. 499, pp. 230-242, Dec 2016, doi: 10.1016/j.virol.2016.09.020.
[154] C. C. Chang, G. S. Shieh, P. Wu, C. C. Lin, A. L. Shiau, and C. L. Wu, "Oct-3/4 expression reflects tumor progression and regulates motility of bladder cancer cells," *Cancer Res,* vol. 68, no. 15, pp. 6281-91, Aug 1 2008, doi: 10.1158/0008-5472.CAN-08-0094.
[155] M. Nishimoto *et al.*, "Oct-3/4 maintains the proliferative embryonic stem cell state via specific binding to a variant octamer sequence in the regulatory region of the UTF1 locus," *Mol Cell Biol,* vol. 25, no. 12, pp. 5084-94, Jun 2005, doi: 10.1128/MCB.25.12.5084-5094.2005.
[156] N. Moore and S. Lyle, "Quiescent, slow-cycling stem cell populations in cancer: a review of the evidence and discussion of significance," *J Oncol,* vol. 2011, 2011, doi: 10.1155/2011/396076.
[157] A. Pasto *et al.*, "Cancer stem cells from epithelial ovarian cancer patients privilege oxidative phosphorylation, and resist glucose deprivation," *Oncotarget,* vol. 5, no. 12, pp. 4305-19, Jun 30 2014, doi: 10.18632/oncotarget.2010.
[158] D. Nantajit, M. Fan, N. Duru, Y. Wen, J. C. Reed, and J. J. Li, "Cyclin B1/Cdk1 phosphorylation of mitochondrial p53 induces anti-apoptotic response," *PLoS One,* vol. 5, no. 8, p. e12341, Aug 23 2010, doi: 10.1371/journal.pone.0012341.
[159] M. Kahn, "Wnt Signaling in Stem Cells and Cancer Stem Cells: A Tale of Two Coactivators," *Prog Mol Biol Transl Sci,* vol. 153, pp. 209-244, 2017, doi: 10.1016/bs.pmbts.2017.11.007.
[160] M. Tomizawa, F. Shinozaki, T. Sugiyama, S. Yamamoto, M. Sueishi, and T. Yoshida, "Frizzled-2: A potential novel target for molecular pancreatic cancer therapy," *Oncol Lett,* vol. 7, no. 1, pp. 74-78, Jan 2014, doi: 10.3892/ol.2013.1681.
[161] H. Ou *et al.*, "Frizzled 2-induced epithelial-mesenchymal transition correlates with vasculogenic mimicry, stemness, and Hippo signaling in hepatocellular carcinoma," *Cancer Sci,* vol. 110, no. 4, pp. 1169-1182, Apr 2019, doi: 10.1111/cas.13949.
[162] D. Szklarczyk *et al.*, "STRING v11: protein-protein association networks with increased coverage, supporting functional discovery in genome-wide experimental datasets," *Nucleic Acids Res,* vol. 47, no. D1, pp. D607-D613, Jan 8 2019, doi: 10.1093/nar/gky1131.
[163] B. Snel, G. Lehmann, P. Bork, and M. A. Huynen, "STRING: a web-server to retrieve and display the repeatedly occurring neighbourhood of a gene,"

Nucleic Acids Res, vol. 28, no. 18, pp. 3442-4, Sep 15 2000, doi: 10.1093/nar/28.18.3442.
[164] W. Shi *et al.*, "Unravel the molecular mechanism of XBP1 in regulating the biology of cancer cells," *J Cancer,* vol. 10, no. 9, pp. 2035-2046, 2019, doi: 10.7150/jca.29421.
[165] R. R. Madsen, "PI3K in stemness regulation: from development to cancer," *Biochem Soc Trans.,* vol. 48, no. 1, pp. 301-315, 2020, doi: 10.1042/BST20190778.
[166] W. G. Jiang, A. Douglas-Jones, and R. E. Mansel, "Expression of peroxisome-proliferator activated receptor-gamma (PPARgamma) and the PPARgamma co-activator, PGC-1, in human breast cancer correlates with clinical outcomes," *Int J Cancer,* vol. 106, no. 5, pp. 752-7, Sep 20 2003, doi: 10.1002/ijc.11302.
[167] C. F. Teng, L. B. Jeng, and W. C. Shyu, "Role of Insulin-like Growth Factor 1 Receptor Signaling in Stem Cell Stemness and Therapeutic Efficacy," *Cell Transplant,* vol. 27, no. 9, pp. 1313-1319, Sep 2018, doi: 10.1177/0963689718779777.
[168] Y. Fang *et al.*, "Rictor has a pivotal role in maintaining quiescence as well as stemness of leukemia stem cells in MLL-driven leukemia," *Leukemia,* vol. 31, no. 2, pp. 414-422, Feb 2017, doi: 10.1038/leu.2016.223.
[169] L. Jin *et al.*, "Phosphorylation-mediated activation of LDHA promotes cancer cell invasion and tumour metastasis," *Oncogene,* vol. 36, no. 27, pp. 3797-3806, Jul 6 2017, doi: 10.1038/onc.2017.6.
[170] J. Fan *et al.*, "Tyrosine phosphorylation of lactate dehydrogenase A is important for NADH/NAD(+) redox homeostasis in cancer cells," *Mol Cell Biol,* vol. 31, no. 24, pp. 4938-50, Dec 2011, doi: 10.1128/MCB.06120-11.
[171] P. Sancho *et al.*, "MYC/PGC-1α Balance Determines the Metabolic Phenotype and Plasticity of Pancreatic Cancer Stem Cells," *Cell Metab.*, vol. 22, no. 4, pp. 590-605, 2015, doi: 10.1016/j.cmet.2015.08.015.
[172] P. P. Liu *et al.*, "Metabolic regulation of cancer cell side population by glucose through activation of the Akt pathway," *Cell Death Differ,* vol. 21, no. 1, pp. 124-35, Jan 2014, doi: 10.1038/cdd.2013.131.
[173] S. Valle *et al.*, "Exploiting oxidative phosphorylation to promote the stem and immunoevasive properties of pancreatic cancer stem cells," *Nat Commun,* vol. 11, no. 1, p. 5265, Oct 16 2020, doi: 10.1038/s41467-020-18954-z.
[174] C. Wang *et al.*, "Elevated level of mitochondrial reactive oxygen species via fatty acid beta-oxidation in cancer stem cells promotes cancer metastasis by inducing epithelial-mesenchymal transition," *Stem Cell Res Ther,* vol. 10, no. 1, p. 175, Jun 13 2019, doi: 10.1186/s13287-019-1265-2.
[175] M. Visweswaran, F. Arfuso, S. Warrier, and A. Dharmarajan, "Aberrant lipid metabolism as an emerging therapeutic strategy to target cancer stem cells," *Stem Cells,* vol. 38, no. 1, pp. 6-14, Jan 2020, doi: 10.1002/stem.3101.
[176] C. M. Metallo *et al.*, "Reductive glutamine metabolism by IDH1 mediates lipogenesis under hypoxia," *Nature,* vol. 481, no. 7381, pp. 380-4, Nov 20 2011, doi: 10.1038/nature10602.

[177] J. H. Lee *et al.*, "Branched-chain amino acids sustain pancreatic cancer growth by regulating lipid metabolism," *Exp Mol Med*, vol. 51, no. 11, pp. 1-11, Nov 29 2019, doi: 10.1038/s12276-019-0350-z.
[178] L. Tirinato *et al.*, "Lipid Droplets: A New Player in Colorectal Cancer Stem Cells Unveiled by Spectroscopic Imaging," *Stem Cells*, vol. 33, no. 1, pp. 35-44, 2014, doi: 10.1002/stem.1837.
[179] J. W. Miklas *et al.*, "TFPa/HADHA is required for fatty acid beta-oxidation and cardiolipin re-modeling in human cardiomyocytes," *Nat Commun*, vol. 10, no. 1, p. 4671, Oct 11 2019, doi: 10.1038/s41467-019-12482-1.
[180] C. Ye, Z. Shen, and M. L. Greenberg, "Cardiolipin remodeling: a regulatory hub for modulating cardiolipin metabolism and function," *J Bioenerg Biomembr*, vol. 48, no. 2, pp. 113-23, Apr 2016, doi: 10.1007/s10863-014-9591-7.
[181] M. El-Hafidi, F. Correa, and C. Zazueta, "Mitochondrial dysfunction in metabolic and cardiovascular diseases associated with cardiolipin remodeling," *Biochim Biophys Acta Mol Basis Dis*, vol. 1866, no. 6, p. 165744, Jun 1 2020, doi: 10.1016/j.bbadis.2020.165744.
[182] K. Pfeiffer *et al.*, "Cardiolipin stabilizes respiratory chain supercomplexes," *J Biol Chem*, vol. 278, no. 52, pp. 52873-80, Dec 26 2003, doi: 10.1074/jbc.M308366200.
[183] D. Nolfi-Donegan, A. Braganza, and S. Shiva, "Mitochondrial electron transport chain: Oxidative phosphorylation, oxidant production, and methods of measurement," *Redox Biol*, vol. 37, p. 101674, Oct 2020, doi: 10.1016/j.redox.2020.101674.
[184] T. H. Haines and N. A. Dencher, "Cardiolipin: a proton trap for oxidative phosphorylation," *FEBS Lett*, vol. 528, no. 1-3, pp. 35-9, Sep 25 2002, doi: 10.1016/s0014-5793(02)03292-1.
[185] S. E. Gasanov, A. A. Kim, L. S. Yaguzhinsky, and R. K. Dagda, "Non-bilayer structures in mitochondrial membranes regulate ATP synthase activity," *Biochim Biophys Acta Biomembr*, vol. 1860, no. 2, pp. 586-599, Feb 2018, doi: 10.1016/j.bbamem.2017.11.014.
[186] D. Acehan, A. Malhotra, Y. Xu, M. Ren, D. L. Stokes, and M. Schlame, "Cardiolipin affects the supramolecular organization of ATP synthase in mitochondria," *Biophys J*, vol. 100, no. 9, pp. 2184-92, May 4 2011, doi: 10.1016/j.bpj.2011.03.031.
[187] A. K. Seneviratne *et al.*, "The Mitochondrial Transacylase, Tafazzin, Regulates for AML Stemness by Modulating Intracellular Levels of Phospholipids," *Cell Stem Cell*, vol. 24, no. 4, pp. 621-636 e16, Apr 4 2019, doi: 10.1016/j.stem.2019.02.020.
[188] A. K. Seneviratne, M. Xu, and A. D. Schimmer, "Tafazzin modulates cellular phospholipid composition to regulate AML stemness," *Mol Cell Oncol*, vol. 6, no. 5, p. e1620051, 2019, doi: 10.1080/23723556.2019.1620051.
[189] E. M. De Francesco, F. Sotgia, and M. P. Lisanti, "Cancer stem cells (CSCs): metabolic strategies for their identification and eradication," *Biochem J*, vol. 475, no. 9, pp. 1611-1634, May 9 2018, doi: 10.1042/BCJ20170164.

[190] R. K. Tyagi, A. Azrad, H. Degani, and Y. Salomon, "Simultaneous extraction of cellular lipids and water-soluble metabolites: evaluation by NMR spectroscopy," *Magn Reson Med*, vol. 35, no. 2, pp. 194-200, Feb 1996, doi: 10.1002/mrm.1910350210.
[191] A. Kielkowska *et al.*, "A new approach to measuring phosphoinositides in cells by mass spectrometry," *Adv Biol Regul*, vol. 54, pp. 131-41, Jan 2014, doi: 10.1016/j.jbior.2013.09.001.
[192] J. Hartler *et al.*, "Deciphering lipid structures based on platform-independent decision rules," *Nat Methods*, vol. 14, no. 12, pp. 1171-1174, Dec 2017, doi: 10.1038/nmeth.4470.
[193] A. Nguyen, S. A. Rudge, Q. Zhang, and M. J. Wakelam, "Using lipidomics analysis to determine signalling and metabolic changes in cells," *Curr Opin Biotechnol*, vol. 43, pp. 96-103, Feb 2017, doi: 10.1016/j.copbio.2016.10.003.
[194] E. Fahy, M. Sud, D. Cotter, and S. Subramaniam, "LIPID MAPS online tools for lipid research," *Nucleic Acids Res*, vol. 35, no. Web Server issue, pp. W606-12, Jul 2007, doi: 10.1093/nar/gkm324.
[195] M. Sud *et al.*, "LMSD: LIPID MAPS structure database," *Nucleic Acids Res*, vol. 35, no. Database issue, pp. D527-32, Jan 2007, doi: 10.1093/nar/gkl838.
[196] C. Gaud *et al.*, "BioPAN: a web-based tool to explore mammalian lipidome metabolic pathways on LIPID MAPS," *F1000Research*, vol. 10, no. 4, 2021. [Online]. Available: https://doi.org/10.12688/f1000research.28022.1.
[197] V. W. Daniels, K. Smans, I. Royaux, M. Chypre, J. V. Swinnen, and N. Zaidi, "Cancer cells differentially activate and thrive on de novo lipid synthesis pathways in a low-lipid environment," *PLoS One*, vol. 9, no. 9, p. e106913, 2014, doi: 10.1371/journal.pone.0106913.
[198] A. K. Cotte, V. Aires, F. Ghiringhelli, and D. Delmas, "LPCAT2 controls chemoresistance in colorectal cancer," *Mol Cell Oncol*, vol. 5, no. 3, p. e1448245, 2018, doi: 10.1080/23723556.2018.1448245.
[199] A. Meyers, T. M. Weiskittel, and P. Dalhaimer, "Lipid Droplets: Formation to Breakdown," *Lipids*, vol. 52, no. 6, pp. 465-475, Jun 2017, doi: 10.1007/s11745-017-4263-0.
[200] T. Petan, E. Jarc, and M. Jusovic, "Lipid Droplets in Cancer: Guardians of Fat in a Stressful World," *Molecules*, vol. 23, no. 8, Aug 3 2018, doi: 10.3390/molecules23081941.
[201] A. R. Thiam and M. Beller, "The why, when and how of lipid droplet diversity," *J Cell Sci*, vol. 130, no. 2, pp. 315-324, Jan 15 2017, doi: 10.1242/jcs.192021.
[202] K. Bensaad *et al.*, "Fatty acid uptake and lipid storage induced by HIF-1alpha contribute to cell growth and survival after hypoxia-reoxygenation," *Cell Rep*, vol. 9, no. 1, pp. 349-365, Oct 9 2014, doi: 10.1016/j.celrep.2014.08.056.
[203] S. Rak, T. De Zan, J. Stefulj, M. Kosovic, O. Gamulin, and M. Osmak, "FTIR spectroscopy reveals lipid droplets in drug resistant laryngeal carcinoma cells through detection of increased ester vibrational bands intensity," *Analyst*, vol. 139, no. 13, pp. 3407-15, Jul 7 2014, doi: 10.1039/c4an00412d.

[204] S. Beloribi-Djefaflia, S. Vasseur, and F. Guillaumond, "Lipid metabolic reprogramming in cancer cells," *Oncogenesis,* vol. 5, p. e189, Jan 25 2016, doi: 10.1038/oncsis.2015.49.
[205] A. Pol, S. P. Gross, and R. G. Parton, "Review: biogenesis of the multifunctional lipid droplet: lipids, proteins, and sites," *J Cell Biol,* vol. 204, no. 5, pp. 635-46, Mar 3 2014, doi: 10.1083/jcb.201311051.
[206] R. Haselgrubler *et al.*, "Hypolipidemic effects of herbal extracts by reduction of adipocyte differentiation, intracellular neutral lipid content, lipolysis, fatty acid exchange and lipid droplet motility," *Sci Rep,* vol. 9, no. 1, p. 10492, Jul 19 2019, doi: 10.1038/s41598-019-47060-4.
[207] S. Zhang *et al.*, "Morphologically and Functionally Distinct Lipid Droplet Subpopulations," *Sci Rep,* vol. 6, p. 29539, Jul 8 2016, doi: 10.1038/srep29539.
[208] H. A. Costa *et al.*, "Discovery and functional characterization of a neomorphic PTEN mutation," *Proc Natl Acad Sci U S A,* vol. 112, no. 45, pp. 13976-81, Nov 10 2015, doi: 10.1073/pnas.1422504112.
[209] F. Vandeput, K. Backers, V. Villeret, X. Pesesse, and C. Erneux, "The influence of anionic lipids on SHIP2 phosphatidylinositol 3,4,5-trisphosphate 5-phosphatase activity," *Cell Signal,* vol. 18, no. 12, pp. 2193-9, Dec 2006, doi: 10.1016/j.cellsig.2006.05.010.
[210] J. Swierczynski, A. Hebanowska, and T. Sledzinski, "Role of abnormal lipid metabolism in development, progression, diagnosis and therapy of pancreatic cancer," *World J Gastroenterol,* vol. 20, no. 9, pp. 2279-303, Mar 7 2014, doi: 10.3748/wjg.v20.i9.2279.
[211] T. D. Bunney and M. Katan, "Phosphoinositide signalling in cancer: beyond PI3K and PTEN," *Nat Rev Cancer,* vol. 10, no. 5, pp. 342-52, May 2010, doi: 10.1038/nrc2842.
[212] G. Ramazzotti *et al.*, "Phosphoinositide 3 Kinase Signaling in Human Stem Cells from Reprogramming to Differentiation: A Tale in Cytoplasmic and Nuclear Compartments," *Int J Mol Sci,* vol. 20, no. 8, Apr 24 2019, doi: 10.3390/ijms20082026.
[213] C. Birtolo, V. L. Go, A. Ptasznik, G. Eibl, and S. J. Pandol, "Phosphatidylinositol 3-Kinase: A Link Between Inflammation and Pancreatic Cancer," *Pancreas,* vol. 45, no. 1, pp. 21-31, Jan 2016, doi: 10.1097/MPA.0000000000000531.
[214] S. Shakya *et al.*, "Altered lipid metabolism marks glioblastoma stem and non-stem cells in separate tumor niches," *bioRxiv,* p. 2020.09.20.304964, 2020, doi: 10.1101/2020.09.20.304964.
[215] F. Luongo, F. Colonna, F. Calapa, S. Vitale, M. E. Fiori, and R. De Maria, "PTEN Tumor-Suppressor: The Dam of Stemness in Cancer," *Cancers (Basel),* vol. 11, no. 8, Jul 30 2019, doi: 10.3390/cancers11081076.
[216] J. A. Engelman, J. Luo, and L. C. Cantley, "The evolution of phosphatidylinositol 3-kinases as regulators of growth and metabolism," *Nat Rev Genet,* vol. 7, no. 8, pp. 606-19, Aug 2006, doi: 10.1038/nrg1879.
[217] O. F. Kuzu, M. A. Noory, and G. P. Robertson, "The Role of Cholesterol in Cancer," *Cancer Res,* vol. 76, no. 8, pp. 2063-70, Apr 15 2016, doi: 10.1158/0008-5472.CAN-15-2613.

[218] C. D. Green, C. G. Ozguden-Akkoc, Y. Wang, D. B. Jump, and L. K. Olson, "Role of fatty acid elongases in determination of de novo synthesized monounsaturated fatty acid species," *J Lipid Res,* vol. 51, no. 7, pp. 1871-7, Jul 2010, doi: 10.1194/jlr.M004747.

[219] A. E. Leonard *et al.*, "Cloning of a human cDNA encoding a novel enzyme involved in the elongation of long-chain polyunsaturated fatty acids," *Biochem J,* vol. 350 Pt 3, pp. 765-70, Sep 15 2000. [Online]. Available: https://www.ncbi.nlm.nih.gov/pubmed/10970790.

[220] Y. Ohno *et al.*, "ELOVL1 production of C24 acyl-CoAs is linked to C24 sphingolipid synthesis," *Proc Natl Acad Sci U S A,* vol. 107, no. 43, pp. 18439-44, Oct 26 2010, doi: 10.1073/pnas.1005572107.

[221] W. A. Taylor, E. M. Mejia, R. W. Mitchell, P. C. Choy, G. C. Sparagna, and G. M. Hatch, "Human trifunctional protein alpha links cardiolipin remodeling to beta-oxidation," *PLoS One,* vol. 7, no. 11, p. e48628, 2012, doi: 10.1371/journal.pone.0048628.

[222] Ayesh K Seneviratne *et al.*, "The Mitochondrial Transacylase, Tafazzin, Regulates for AML Stemness by Modulating Intracellular Levels of Phospholipids," *Cell Stem Cell,* vol. 24, no. 4, pp. 621-636, 2019, doi: 10.1016/j.stem.2019.02.020.

[223] Ayesh K. Seneviratne, Mingjing Xu, and A. D. Schimmer, "Tafazzin modulates cellular phospholipid composition to regulate AML stemness," *MCO,* vol. 6, no. 5, 2019, doi: 10.1080/23723556.2019.1620051.

[224] G. A. Patwardhan and Y. Y. Liu, "Sphingolipids and expression regulation of genes in cancer," *Prog Lipid Res,* vol. 50, no. 1, pp. 104-14, Jan 2011, doi: 10.1016/j.plipres.2010.10.003.

[225] K. Kitatani, M. Taniguchi, and T. Okazaki, "Role of Sphingolipids and Metabolizing Enzymes in Hematological Malignancies," *Mol Cells,* vol. 38, no. 6, pp. 482-95, Jun 2015, doi: 10.14348/molcells.2015.0118.

[226] S. Ghosh, S. K. Juin, and S. Majumdar, "Cancer stem cells and ceramide signaling: the cutting edges of immunotherapy," *Mol Biol Rep,* vol. 47, no. 10, pp. 8101-8111, Oct 2020, doi: 10.1007/s11033-020-05790-z.

[227] T. Shah, B. Krishnamachary, F. Wildes, J. P. Wijnen, K. Glunde, and Z. M. Bhujwalla, "Molecular causes of elevated phosphoethanolamine in breast and pancreatic cancer cells," *NMR Biomed,* vol. 31, no. 8, p. e3936, Aug 2018, doi: 10.1002/nbm.3936.

[228] F. Elvas, S. Stroobants, and L. Wyffels, "Phosphatidylethanolamine targeting for cell death imaging in early treatment response evaluation and disease diagnosis," *Apoptosis,* vol. 22, no. 8, pp. 971-987, Aug 2017, doi: 10.1007/s10495-017-1384-0.

[229] J. H. Stafford and P. E. Thorpe, "Increased exposure of phosphatidylethanolamine on the surface of tumor vascular endothelium," *Neoplasia,* vol. 13, no. 4, pp. 299-308, Apr 2011, doi: 10.1593/neo.101366.

[230] L. T. Tan *et al.*, "Targeting Membrane Lipid a Potential Cancer Cure?," *Front Pharmacol,* vol. 8, p. 12, 2017, doi: 10.3389/fphar.2017.00012.

[231] H. W. Davis *et al.*, "Enhanced phosphatidylserine-selective cancer therapy with irradiation and SapC-DOPS nanovesicles," *Oncotarget,* vol. 10, no. 8, pp. 856-868, Jan 25 2019, doi: 10.18632/oncotarget.26615.

Acknowledgments

I would like to thank my supervisor Prof. Daniela Cecconi. She gave me the opportunity to work with her and her team, to publish high-quality scientific papers and to go abroad to learn about lipidomics and to grow as a scientist. Thank you, Daniela, for all your support and your teaching; I have learned a lot from you.

I am very grateful to Giuliana and Jessica for their friendship that made my three years in the lab very pleasant. Giuliana, I will never forget our lab days with dozens of cell culture flasks. I hope all your dreams will come true. Jessica, thank you for your helpfulness and your willingness to share your knowledge with me, for listening to and supporting me.

Thanks to Prof. Marta Palmieri and Prof. Emilio Marengo and to all the members of their research groups (Ilaria, Elisa, Giulia and Christian; and Marcello). Without them I would never have done my PhD so well. I am very grateful for the valuable time that each of you dedicated to me.

I would also like to thank Prof. Michael Wakelam and Dr Andrea F. Lopez-Clavijo, and their group (especially to Bebiana and Greg), to give me the opportunity to spend three months at the Lipidomics facility of Babraham Institute in Cambridge (UK). It was an honour to meet you. Andrea, it was a pleasure to work side by side with you at literally any time of the day and night. Thank you also for all the precious time you dedicated to me for my thesis. You are an amazing woman, so strong and determined. I have a great deal of respect for you. My only regret is that I could never personally say goodbye to Michael, who died prematurely in March 2020. He strongly believed in me and my potential, he made me feel a capable and special scientist. You would be proud of our paper, which will be dedicated to you.

I would like to dedicate this thesis to my family: dad, mum, Chiara and Gianluca. Thank you, everything that I am today is because of your love, your perseverance, dedication and support. Love you all, a lot.

Another special dedication is to my partner Stefano. Thank you for being so understanding, for making me laugh, as well as for all your help, especially during the painful periods of these three years. You believe in me more than I do, you are so special.

Finally, I want to thank all the friends I made during my PhD, especially Laura and Jessica. Our chats, our laughs, our mental breakdowns, our walks, and our affection are the best part of my period in Verona. You have been my substitute family and you made me feel at home.